EVALUATION OF AAV TRAFFICKING AND TRANSDUCTION IN THE RETINA

Kenton Tyler Woodard

A dissertation submitted to the faculty of the University of North Carolina at Chapel Hill in partial fulfillment of the requirements for the degree of Doctor of Philosophy in the Graduate Curriculum in Neurobiology in the School of Medicine

Chapel Hill
2016

Approved by:

Aravind Asokan

Donald Budenz

Patricia Maness

R. Jude Samulski

Ellen Weiss

ABSTRACT

Kenton Tyler Woodard: Evaluation of AAV trafficking and transduction in the retina
(Under the direction of R. Jude Samulski)

Gene delivery by viruses, specifically AAV, offers an efficient way to safely supply exogenous DNA to cells long term *in vivo*. The ability of AAV to infect post-mitotic neurons makes it a great vector for neuroscience applications. The small, accessible, and compartmentalized nature of the eye have made it an ideal organ for gene therapy research. The route of delivery into the eye largely dictates the tropism and distribution of AAV, but never has the numerous routes been compared using a single vector and titer. We injected scAAV2 containing CMV-GFP transgenes into the various compartments (IS, IC, IVIT, SR, SC) within the eyes of mice. Anterior chamber injections lead to fluorescence mainly in the anterior portion while the posterior injections lead to transduction of the ciliary body and retina. Transduction of the retina is of interest to potentially treat retinal degenerative disorders. IC and IVIT injections led to transduction of the inner retina and SR and SC injections transduced the outer retina, with the best fluorescence detected by either SR or IVIT delivery. Many AAV serotypes are known to efficiently transduce the retina when delivered to the SR space, but show limited success when delivered to the vitreous due to the inner limiting membrane (ILM). Therefore, a collection of capsid mutants was used to understand the trafficking patterns of AAV in the retina. Transduction of AAV by SR delivery occurred by a heparan sulfate (HS) independent mechanism whereas IVIT transduction was highly dependent on HS binding. This was due to the accumulation of vector at the ILM where HS proteoglycan (HSPG) was abundantly found. For clinical relevance, this mechanism was tested in human *ex vivo* retinas and determined to

be conserved. The HS-binding motif enhanced the transduction of other AAV serotypes (AAV1, AAV8) by the same mechanism. To determine the extent of HS-binding on tropism, capsid motifs from other AAV serotypes were used to create chimeric AAV2 capsids. A motif from AAV1 enhanced the transduction along the retinal vessels whereas the galactose motif from AAV9 lead to Müller glial specific transduction. Together, the double chimera showed characteristics of both motifs that completely ablated native AAV2 transduction. Through rational engineering of AAV using various capsid motifs, we have identified motifs involved in retinal trafficking and generated a novel capsid variant for targeted and enhanced transduction within the retina by IVIT delivery.

Dedicated to my close friends and family for their love, friendship, and support throughout the years. To my parents for helping to develop my curiosity in science and encouraging the pursuit my goals. And to Gustavo for his love and inspiration.

ACKNOWLEDGEMENTS

First, I would like to thank my mentors at Ursinus College for everything they had done to help me get to this point. To Dr. Ellen Dawley for showing me how interesting biology research can be, for guiding me as I completed my Honor thesis, and for opening her home. To Dr. Becky Kohn for helping me mature as a scientist, researcher, and mentor. Second, I am so thankful for all the support and advice of my graduate mentor, Dr. R. Jude Samulski, throughout the years as I carried out the work presented herein. These mentors continue to inspire me to try my best and enjoy the work that I do. Specifically, I extend my thanks to Drs. Katharine Liang, Thomas Lentz, Matthew Hirsch for their friendship, encouragement, and advice. To Dr. Chengwen Li for his guidance and advice throughout graduate school. To William Bennett for help assistance during intraocular injections. To Drs. Jean Bennett, Peter Campochiaro, and Brian Gilger for their assistance in carrying out injections in large animal models and for their advice. I am grateful to the UNC Histology Core, Vector Core, and In Situ Hybridization Core for teaching techniques needed to carry out this work. Finally, I appreciate all the friendships, assistance, and hospitality of the UNC GTC which has been my home for the last several years.

PREFACE

Growing up, I had the desire to help people by using science. As a high schooler, the obvious choice seemed to be a physician. But in my first semester of college, I realized that I wanted to do more than just treat patients, I wanted to develop the medicine that would cure them. My interest in neuroscience led me to do research in two laboratories in undergraduate at Ursinus College and fueled my passion to teach others about science. I worked to develop my skills in my pursuit to be a great scientist. I came to graduate school at University of North Carolina at Chapel Hill with the desire to be a developmental neurobiologist but open to new experiences. By allowing myself to explore new ideas in science, I found an avenue to truly cure people affected by diseases. The journey challenged me, but through this struggle, I have learned the most valuable of lessons. As I come to the end of graduate school, I am humbled and thankful for my experiences, excited to explore, and looking forward to the future.

TABLE OF CONTENTS

LIST OF TABLES

LIST OF FIGURES

LIST OF ABBREVIATIONS

AAV	Adeno-associated virus
AMD	Age-related macular degeneration
CBA	Chicken beta actin
CBh	Mini chicken beta actin
CMV	Cytomegalovirus
CNS	Central nervous system
CRISPR	Cluster regularly-interspaced short palindromic repeats
CsCl	Cesium chloride
DAPI	4', 6-diamindino-2-phenylindole
DNA	Deoxyribonucleic acid
ECL	*Erythrina cristagalli* lectin
EDTA	Ethylenediaminetetraacetic acid
EGFR	Epidermal growth factor receptor
Endo	Endothelium
Epi	Epithelium
ERG	Electroretinogram
FISH	Fluorescence *in situ* hybridization
FGFR	Fibroblast growth factor receptor
fMRI	Functional magnetic resonance imaging
GAL	Galactose
GCL	Ganglion cell layer
GFP	Green fluorescent protein
HGFR	Hepatocyte growth factor receptor
HS	Heparan sulfate

HSPG	Heparan sulfate proteoglycan
HNPP	2-hydroxy-3-naphtoic acid-2’-phenylanilide phosphate
IC	Intracameral
IHC	Immunohistochemistry
ILM	Inner limiting membrane
INL	Inner nuclear layer
IPL	Inner plexiform layer
IS	Intrastromal
ITR	Inverted terminal repeat
IVIT	Intravitreal
LCA	Leber Congenital Amaurosis
$MgCl_2$	Magnesium chloride
MOI	Multiplicity of infection
mRNA	Messenger ribonucleic acid
MUC	Mucin
NaCl	Sodium chloride
NHP	Non-human primate
OCT	Optical coherence tomography
ORF	Open reading frame
ONL	Outer nuclear layer
OPL	Outer plexiform layer
PDGFR	Platelet-derived growth factor receptor
PNS	Peripheral nervous system
PR	Photoreceptors
qPCR	Quantitative polymerase chain reaction

rAAV	Recombinant Adeno-associated virus
RGC	Retinal ganglion cells
RNA	Ribonucleic acid
RPE	Retinal pigment epithelium
SIA	Sialic acid
SC	Suprachoroidal
scAAV	Self-complementary Adeno-associated virus
SR	Subretinal
ssAAV	Single-stranded Adeno-associated virus
SSC	Saline-sodium citrate
TBS	Tris buffered saline
vg	Viral genomes

CHAPTER 1: Introduction to AAV and its use in gene delivery

1.1 The benefits of using AAV

The ability to express exogenous DNA within a cell allows researchers or clinicians to study ectopic gene expression or provide healthy genetic copies to genetically-diseased cells. The phosphate groups on the DNA backbone provide a polarity to the DNA molecule that allow it to be moved by applying a magnetic field, commonly done during electroporation. *In vitro*, this method is commonly used to transform bacterial and eukaryotic cells, but its use *in vivo* is limited to dividing cells and is not a viable delivery method for human trials [1]. To circumvent these shortfalls, viruses offer a natural vector that can efficiently deliver DNA to cells. Numerous virus types have been domesticated and tested for their ability to transduce tissues or cells of interest. Viruses like lentivirus led the way for early viral gene delivery and opened the door to the use of other viral vectors, like adenovirus [2]. Typically, these viral vectors were based off a pathogenic virus that were well characterized. Although efforts have been made to improve the safety of these vectors by removing much of the viral genome [3, 4], the viral components still can evoke a pathogenic response within the host. Therefore, the majority of the gene therapy field has flocked to viruses with inherently better safety profiles. One such viral vector is Adeno-associated virus (AAV) due to its ability for site-specific integration [5], non-pathogenic [6] and non-immunogenic nature which is a huge benefit in terms of safety for trials. The benign nature of AAV is evidenced by the large human population that has been previously exposed to AAV without any complications [7]. In addition, the replication of AAV is dependent on the co-infection of specific viruses (*e.g.* adenovirus (Ad), herpes simplex virus [8, 9]), which reduces

the risk of vector mobilization. Together, these attributes make AAV a good vector for gene delivery and have led to research on much of the AAV biology.

1.2 The AAV life cycle and biology

AAV consists of a linear, single-stranded DNA genome surrounded by a viral protein capsid. The capsid topography and motifs promote the interaction with glycans and receptors on the cell surface needed for viral entry (Figure 1.1). These glycan and receptor interactions are discussed in greater detail below. Through receptor-mediated endocytosis, AAV virions enter the cell surrounded by a clathrin-coated vesicle. The vesicle is trafficked along microtubules toward the perinuclear region using dynein motor proteins [10] as the endosome begins to acidify. The acidification exposes the phospholipase A2 domain tucked inside the capsid for the virion to escape [11]. Once out of the endosome, AAV uses actin filaments [12] and nuclear pore complexes, like importin-β [13], to enter the nucleus. Inside in the nucleus, the viral genome becomes exposed for second-strand synthesis [14]. Virions that fail to escape endosomes become degraded by proteasomes.

The AAV genome is protected inside the viral capsid until it reaches the nucleus (Figure 1.2). Once inside the nucleus, the capsid breaks down to expose the genome to the cellular machinery [14]. The ~4.7kb genome is a single-stranded DNA molecule [15] capped at each end by an inverted terminal repeat (ITR). The single-stranded molecule is first converted to a double-stranded molecule through second-strand synthesis. The ITRs are important in forming a secondary structure that aides in the initiation of second-strand synthesis. After the second DNA strand has been synthesized, and with the co-infection with one of the viruses stated above, transcription of the two ORFs (*rep* and *cap*) generates various products via three internal promoters: p5, p19, p40. The translation of those products yields the eight proteins needed for AAV replication and assembly [16]. The *rep* gene is translated into four Rep proteins needed for nearly every aspect of AAV genome replication and packaging. The *cap* gene is involved in the

production of proteins needed to compose the AAV capsid structure. The *cap* gene produces one AAP protein and three capsid viral proteins (VP1, VP2, and VP3) from the p40 promoter (Figure 1.2). The VP1 protein contains the sequences of VP2 and VP3, and VP2 contains the sequence of VP3. The three proteins come together, via the AAP protein, in a ratio of approximately one VP1 and one VP2 to 10 VP3 which form the 60-subunits needed to make the T = 1 icosahedral structure [17].

When these proteins come together, VP3 is surface exposed with the remaining VPs predicted to be tucked into the internal part of the capsid [17]. The VP3 has eight β-barrels which twist around in the monomer of the AAV capsid (Figure 1.3). The twists in the monomer form loops, known as variable regions, that are important to the capsid monomers assembly. When the subunits come together to form the viral capsid, the topography of the capsid form protrusions (threefold axis of symmetry), valleys (twofold axis of symmetry), and pores (fivefold axis of symmetry). Important to this topography is the threefold axis of symmetry protrusions (shown in blue, Figure 1.3). The regions around the protrusions are responsible for the interaction of AAV virion with the cell glycans. Various AAV serotypes exist which differ in their variable regions and mediate interaction with various glycans on the cell surface.

1.3 AAV capsid motifs for glycan binding

Glycans and receptors have been elucidated for the transductions several of the AAV serotypes (Table 1.1). Heparan sulfate (HS) proteoglycan (HSPG) is used by both rAAV2 and rAAV3 [18]. rAAV6 displays a dual glycan interaction with HSPG and sialic acid (SIA); however, HSPG binding alone is insufficient for cellular entry [19]. Various linkages of sialic acid are important for the transduction of rAAV1, rAAV4, and rAAV5 serotypes [19, 20]. N-linked galactose (GAL) is used for the transduction of rAAV9 serotype [21]. These binding motifs tend to involve the base of the protrusion at the threefold axis of symmetry (Figure 1.4). For example, rAAV2 HS-binding motif is a patch of basic residues at the base of the threefold axis

of symmetry protrusions. Glycans expressed on the cell surface, in part, dictate the tissue and cellular tropism observed with the various AAV capsids. By altering these motifs, the transduction profile can be modified. (*e.g.* ablating the HS-binding motif in rAAV2 alters the transduction of away from the HSPG-rich liver tissue [22]). In addition to the attachment to these glycans, AAV serotypes interact secondarily with cell receptors (Table 1.1). These co-receptors include growth factor receptor (FGFR, HGFR, PDGFR, EGFR), integrins, and laminin receptors [18, 23, 24].

1.4 Recombinant AAV (rAAV) as a vector for gene delivery

rAAV can be domesticated for the purposes of DNA gene transfer through the removal of the two genes replacing them with a desired transgene. Because only the ~145bp ITRs are necessary to produce rAAV, the 4.7kb genomes can be almost entirely removed to effectively package a transgene of a similar size. To produce rAAV, three plasmids are supplied to cells through transfection methods [25]. The *rep* and *cap* genes are supplied *in trans* to the plasmid containing the transgene flanked by ITRs. The 3' ITR is used to package the genome into the preformed capsids [16], and the lack of ITRs on the *rep*/*cap* plasmid prevents the formation of wild-type AAV in the production of rAAV. The ITR isolated from AAV2 allow the transgenes to be packaged into multiple AAV capsids through a process known as pseudotyping [26]. This allows transgene expression to be accurately assessed among the different AAV serotypes. The third plasmid supplies Ad genes (*i.e.* E1a, E2a, E1b, E4) needed to start AAV production [27]. Using biochemical purification methods (*e.g.* density gradient, column chromatography), rAAV can be then purified from these plasmids and other cellular proteins to yield concentrated, pure viral reagent that can infect mitotic and post-mitotic cells for long-term gene expression on the order of years [25].

1.5 Self-complementary rAAV transgene cassette

rAAV particles that successfully traffic to the nucleus and uncoat must then convert the single-stranded genome to a double-stranded DNA molecule. This second-strand synthesis is said to be rate-limiting in the expression of the transgene [28]. To circumvent this bottleneck, a self-complementary (scAAV) construct [29] can be used. To produce the scAAV, the TRS at the 5' end ITR (Figure 1.2) is mutated to no longer promote the nicking of the double-stranded DNA molecule. The self-complementary DNA is packaged into the capsid to form scAAV [30]. The total amount of DNA packaged into the rAAV capsid remains constant at <5kb; therefore, scAAV package approximately half the size (~2.5 kb) of the native single-stranded AAV (ssAAV). scAAV shows increased transduction efficacy that is faster and more stable than the classic ssAAV construct [29-32]. In addition to the increased transduction efficacy, scAAV can lead to transgene expression of cells not seen with ssAAV, indicating that some cell populations may not possess the molecular machinery needed for second-strand synthesis [33]. scAAV is becoming more popular in the use of gene therapy to assess capsid transduction and for transgenes small enough to fit its size constraint.

1.6 Gene transfer in the nervous system

The post-mitotic nature of most of the nervous system limits the viral vectors capable of being used for *in vivo* gene transfer [34]. The ability of rAAV to transduce both post-mitotic and mitotic cells makes it of particular interest to the neuroscience community. Not only is rAAV capable of transducing nervous tissue, the various capsids display differences in their transduction profile based on the serotype [35]. These differences are advantageous when looking for targeted transduction of specific cell types or regions within the nervous system. There are two major groups that comprise the nervous tissue: central nervous system (CNS) and peripheral nervous system (PNS). The CNS consists of the brain and spinal cord which are protected by the skull and vertebrate, respectively. The PNS is the remaining neurons and

supporting cells that innervate the internal organs and muscles. Although the PNS is more accessible than the CNS, the compact nature of the CNS and the numerous disorders that affect this part of nervous system have made it the focus for gene therapy applications. Specifically, sensory organs of the CNS, like the eyes, are of particular interest because they lie outside the skull, are small, and easily accessible.

1.7 Retinal gene therapy

Vision relies on a healthy retina, a visual pathway from the eyes to the brain, and brain structures needed for visual processing. While there are some disorders that affect the latter structures of vision, the retina has a large variety of heritable diseases. The retina is particularly interesting because of its laminar structure (Figure 1.5) and the majority of diseases that affect the outer retina. The term outer retina here is defined as the photoreceptors (PR) in the outer nuclear layer (ONL) and retinal pigment epithelium (RPE). Because the cells of the ONL are intimately responsible for the generation of the vision, treatment of these cells can provide a subjective readout of therapeutic success. In addition to this subjective analysis, several objective assessments can be done to measure retinal structure using optical coherence tomography (OCT), function using electroretinogram (ERG) and connectivity using functional magnetic resonance imaging (fMRI). Together, these attributes make retinal gene therapy a popular topic for clinicians and researchers.

The conversion of light into a neuronal signal is accomplished in the retina, specifically by the PR. Light must be able to pass through the structures in the anterior eye (*i.e.* cornea and lens), through the vitreous, and through the retina before reaching the PR. These specialized structures must work in concert to focus light onto the retina. Two general types of PR exist in mammals: rods and cones. Rods are the PRs capable of sensing very low levels and are the most abundant cell type, capable of providing contrast although still a rough, black-and-white view of the world. Cones are active in high levels of light and are involved in color perception.

These cells are most abundant in the fovea in primates which provide high visual acuity. Although absent in mice, the cone-rich fovea in non-human primates make these animals important in the study of eyes similar in size and structure to humans. However, the structure and function of the retina is similar among mammals, making mice the preferred animal model to study genetic ocular pathologies. PR connect to a number of bipolar cells in the INL. The signal is then propagated to the RGC which have its soma in the GCL. The RGCs send their axons along the inner surface of the retina to exit the eye through the optic nerve head. This is also the exit site for the inner retinal vessels. The optic nerve then tracks from the eyes to the brain for visual processing.

The focused efforts in retinal gene therapy have led to several clinical trials around the world, all showing promising safety results [36-39]. These trials come at the heels of large sets of preclinical data collected in multiple animal models [40-42]. To date, there are over a dozen clinical trials initiated using rAAV to treat the RPE of patients with an RPE65 protein deficiency [Clincialtirals.gov] known as Leber congenital amaurosis (LCA). LCA causes patients to become blind very early in life. Gene therapy treatment to these patients shows modest success mitigating visual loss and confirms that the virus is safe for human use [43, 44]. The clinical injections were performed surgically by subretinal delivery of vector because LCA2 involves pathology of the RPE. The treatment used rAAV2 to carry a hRPE65 gene to replace the defective endogenous *rpe65* gene in the RPE cells. Initially, only the worse eye of each patient was treated to assess safety and tolerance. Studies have now moved forward to treat the contralateral eye [45], which yielded a synergic enhancement in self-reporting visual tests.

1.8 Intraocular injection routes influence transduction

The transduction profile in the retina can depend on the route of administration. A diagram of the eye shows the layers and the site of various injection routes (Figure 1.6). Currently, the standard delivery for retinal gene therapy is through the SR injection between the

ONL and RPE, which generally results in transduction of these two cell layers. The SR injection procedure takes advantage of the loose association between the ONL and RPE to detach the retina and cause a “bleb” where most the viral volume is located. The bleb typically resolves on its own after a day. The restructuring that the SR injection causes is tolerated in young, or mildly-pathogenic, cases, but in cases of severe pathology, SR injections may not be a viable option. For one, PRs that are dying may not survive being separated from their supporting RPE cells. Therefore, advanced retinal pathology can exclude cases of severe retinal degenerative from receiving treatment. Because retinal degeneration is non-uniformly distributed, it can be difficult to determine what area to treat. Because the bleb created by the injection causes an accumulation of vector in that area, leading to focal treatment of the retina. The ability to provide a larger area of treatment to the retina would hopefully save more retinal cells and retain a larger field of vision. Therefore, alternative delivery sites need to be identified and their transduction properties tested for *in vivo* retinal gene transfer.

To circumvent these SR-delivery issues, rAAV is delivered to the vitreous. By delivering to the vitreal space, the vector spreads over a greater area of the retina while offering a less invasive and easier method. Although the IVIT injection is said to be less traumatic for the retina than the SR injection, IVIT delivery of rAAV can cause activation of Müller glia. Much of transduction observed with IVIT delivery is typically in the inner retina.

More recently, injections into the SC space have been studied to take advantage of this space and its proximity to pathological cells of the outer retina. In large animals, the spread of SC injections can be greater than SR injections without retinal detachment. The tight junctions of the RPE and the OLM and may limit the spread of vector though the retina. The SC injection is difficult in the small mouse eye so only large animals have been used to study this injection. We attempted these injections and validated by fundoscopy, OCT, histology. Furthermore, we compared the transduction pattern of several ocular injection routes: IS, IC, IVIT, SR, and SC.

1.9 Results

1.9.1 Transduction from anterior ocular injection routes

Anterior eye injections consist of IS and IC delivery routes. The IS injection showed a hazy fluorescence in the corneal where the injection occurred (Figure 1.7a). The cataract that formed during the injection procedure had cleared prior to evaluation for GFP (data not shown). No other GFP fluorescence was detected by fundoscopy in either the anterior segment or within the retina. IHC on IS-injected eyes showed no transduction of either the cornea, iris, ciliary body, or retina (Figure 1.7b-d)

The transduction by the IC injection route was minimal in the anterior segment of the eye (Figure 1.8a). The retina showed transduction of RGCs by the GFP positive axons leading to the ONH in approximately half of the eyes injected for the study (arrowhead, Figure 1.8b). The transduced RGC somas not seen at the posterior retina by fundoscopy suggest transduced RGCs emanate from the peripheral retina. IHC performed on tissue revealed RGC transduction along the retina periphery and prominent ciliary body transduction (Figure 1.8c). Transduction observed in RGCs (arrow), and INL cells (arrowhead), could be seen in some retinas (Figure 1.8d). The endothelium layer of cornea had faint GFP expression, but not in the other corneal layers (Figure 1.8e). Iris showed some GFP cells by IHC which were not detected by fundoscopy (data not shown).

1.9.2 Transduction by posterior ocular injection route

IVIT delivery exposes rAAV to the inner retinal surface leading to transduction of RGC as seen by the GFP axons visible by fundoscopy (arrowhead, Figure 1.9a). There was no observable transduction in the anterior chamber or cornea by fundoscopy (data not shown). IHC showed predominant RGCs transduction (arrow, Figure 1.9b). Some RPE and INL cells were positive for GFP expression near the optic nerve (arrowhead). The transduced INL cells could

be Müller glia, bipolar, or horizontal cells (Figure 1.9c). No transduction was observed in the iris, cornea, or ciliary body (Figure 1.9d).

SR injections resulted in detachment typically ~60% of the retina. GFP expression was most intense in the area of detachment, but transduction outside this area was also observed which looked like RPE cells (Figure 1.10a). Histology of these injected eyes confirmed RPE transduction along with transduction in the ONL and INL and few instances of RGC transduction (Figure 1.10b). There was very low GFP expression in ciliary body or cornea (Figure 1.10c, d). SR delivery leads to outer retinal transduction without much other expression.

Delivery of vector to the SC space in mice was marked by spread of fluorescein by fundoscopy and lack of detachment seen with OCT (data not shown). Despite injection volume spread the GFP expression was not widely distributed (Figure 1.11a) and was RPE transduction in appearance. Histology of these SC-injected eyes revealed transduction mainly in the RPE and RGC layers (Figure 1.11b-d). Transduction of ciliary body was visible (Figure 1.11d), but not in the cornea (Figure 1.11e).

1.10 Discussion

From the various intraocular injection routes, we show the dramatic difference in rAAV2 transduction of the retina (Table 1.2). In general, transduction was greatest in cells closest to the site of injection, as would be expected. Very little transduction was observed in tissue more distal from the site of injection, indicating that vector does not readily spread throughout the entire eye from a single injection route. Therefore, to sufficiently transduce the entire eye, multiple injections throughout the eye may be needed. Thankfully, there are few disorders which affect multiple structures within the eye. Many disorders affect the retina or RPE, which are sufficiently transduced by posterior intraocular injections: IVIT, SR, and SC.

The SC injection lead to transduction mainly within the RPE. In some areas of the eye, transduction of all retinal layers was observed. The caveat of the SC data is the potential that

they were non-detaching SR injections. This multi-layer transduction may be due to the anterograde transport of rAAV2 [35]. Along with OCT and fundus imaging, histology of various regions of the eye were used to confirm that SR damage was not present. Since the retina is populated by post-mitotic cells, damage caused by the injection is visible in histology and prevents false-identified SC injections for analysis. The transduction of the SC injections showed distribution only over part of the mouse retina. This distribution phenomenon is like that of fluorescent particles in rabbit and *ex vivo* human eyes [46]. The small size of the mouse eye and lack of ultra-high resolution OCT make it difficult to perform a SC injection with confidence. The limited transduction and the difficulty of SC injection makes IVIT and SR the preferred routes from retinal transduction in the mouse.

The IS injections resulted in a fluorescence that appeared confined to the general area where the vector was injected. Again, the injection into the stromal layer could not be validated by OCT; however, the opacity that was created by the injection was most likely within the thick stromal layer rather than the thin other layers (i.e. epithelium and endothelium). We were unable to determine the precise location of fluorescence within the cornea by fundoscopy, and the lack of GFP labelling on corneal sections by IHC did not indicate stromal transduction. Hippert *et al.* (2012) showed similar GFP corneal fluorescence with rAAV2 but did not explore further. The localized transduction of stromal layer makes sense given the two membranes which flank the stromal layers: Bowman's layer and Descement's membrane. These two layers may help to keep the vector confined to the stromal layer and; therefore, additional treatment of the cornea may be needed to help the vector spread over the multiple corneal layers. Various ssAAV vectors carrying the CMV-GFP transgene showed little stromal transduction by rAAV2, but other serotypes were better (rAAV8>rAAV1>rAAV2>rAAV5).

The transduction of only the endothelial layer of the cornea by IC injection may be related to the Descement's membrane. This membrane is found between the endothelial and

stromal layers and likely prevents the spread of vector into deeper layers of the cornea. To determine if this membrane prevents penetration, rAAV trafficking studies would need to be done. The structure of the cornea may not lend well to the penetration of vector and may encourage vector to travel through less resistive routes (*i.e*. through the trabecular meshwork or through the pupil/iris). By fundoscopy, the observed transduction of RGCs indicated vector can flow into the posterior portion of the eye. The volume of the anterior chamber is perhaps too small to accommodate the 1 µl of vector delivered to it, thereby encouraging the flow of vector into the vitreous chamber. The transduction of RGCs were only observed in about half of the eyes that received IC injection and could be related to the various amount of efflux in some injections. To reduce this leakage (both out of the injection site and into the vitreous) half of the volume was used to deliver the same amount of vector to the anterior chamber. Less leakage was observed out of the cornea and reduce the transduction of RGCs (data not shown). This indicates volume may be an important factor in determining the spread of vector throughout the eye. Other researchers have recently published showing IC injection without leakage by leaving an air bubble to sit at the injection site and prevent efflux out [47]. Using similar injection parameters testing a shortened CBA promoter (smCBA) showed robust expression in the trabecular meshwork and ciliary body by proteasome-resistant rAAV2 capsids [47].

Delivery of vector to the vitreous resulted in transduction of the inner retina, but on occasion transduction of the RPE was observed usually near the ONH. The ONH may represent a weak spot in the retina where penetration is easiest. Regardless, the ability to transduce the RPE means that virus can reach all the retina layers from IVIT delivery and warrants further study to understand IVIT trafficking of rAAV.

1.11 Experimental procedures

1.11.1 Virus production and purification

scAAV2 carrying the GFP gene under the control of the ubiquitous CMV promoter were provided by the University of North Carolina Vector Core. Briefly, virus was purified by iodixanol gradient, ion-exchange chromatography, and dialyzed against 350mM NaCl, 5% sorbitol in 1xPBS before being aliquoted and frozen at -80°C. Viral titer was determined by qPCR against wild-type ITR of DNase-resistant vector genomes relative to a virus standard (data not shown).

1.11.2 Animal injections

Adult C57BL/6 mice were used for this study. All animals were housed under 12/12-hour light/dark cycle in the University of North Carolina Division of Laboratory Animal Medicine facilities and were handled in accordance within the guidelines of the Institutional Animal Care and Use Committee at the University of North Carolina. Prior to vector delivery, animals were anesthetized with ketamine (75 mg/kg), xylazine (10 mg/kg), acepromazine (1.5 mg/kg), and dilated with 1% tropicamide and 2.5% phenylephrine. Proparacaine-HCl was applied to eyes as a local anesthetic. Intraocular needles were constructed using 32-gauge cannula connected to a Hamilton syringe via tubing filled with water. An air bubble separated the water from the viral suspension. Freshly thawed viruses were diluted to working stock and incubated in the intraocular needle at room temperature for 10 minutes prior to injection. Needles were evacuated and loaded with fresh suspension. Viral suspension was mixed with fluorescein sodium salt (Sigma) to confirm successful injection as previously described [48].

For IS injections, a small entry point was made with the tip of a beveled 30-gauge needle in the apex of the cornea. The 32-gauge intraocular needle was gently inserted into the hole and then the bevel was turned inward to seal the injection hole. The 1 µl of vector was delivered immediately to result in clouding of the cornea. OCT did not provide a clear picture to observe stromal separation. For IC injections, 1 µl of vector was delivered through a pilot hole made just

off the apex of the cornea. The injection occurred over a period of 30 seconds with just the tip of the needle in the anterior chamber and then held in place for 20 seconds for equilibration. For IVIT injections, a pilot hole was made with the tip of a beveled 30-gauge needle in the superior portion of the eye approximately 0.5 mm posterior to the limbus. The intraocular needle was inserted through this hole into the vitreous over the top of the ONH under direct observation through the microscope. A volume of 1 µl was delivered at a constant rate over 30 seconds using a syringe pump. The needle was pulled back to just the tip and held in place for 20 seconds to allow for intraocular pressure equilibration before removal. For SR or SC injection, the intraocular needle was inserted tangential to the eye and inserted to a depth respective of each injection route. Delivery of fluid was immediate and characterized for success by OCT and fundoscopy of fluorescein distribution using the Micron IV (Phoenix Research Laboratories). Genteal (Novartis) was applied to eyes to prevent corneal drying, and mice could recover on heating pads. Fundus imaging was done at six weeks post-injection to observe *in vivo* GFP fluorescence by sedating animals as described above using the Micron IV.

1.11.3 Enucleation and histology

Animals were sedated prior to enucleation. Eyes were placed immediately in formalin overnight at room temperature. Next, eyes were placed in 70% ethanol and provided to the University of North Carolina Center for Gastrointestinal Biology and Disease Histology Core for paraffin embedding and sectioning. Transverse sections were taken from five regions along the globe and placed on Superfrost slides (Fisher). Standard antibody labeling for paraffin embedded tissue was carried out. Briefly, slides were rehydrated and deparaffinized before antigen retrieval was carried out. Slides were blocked and then labeled with primary antibody overnight at 4°C. After washing, slides were exposed to secondary antibody. Slides were stained for DAPI and coverslipped for imaging. Images were taken on a LeicaSP2 AOBS

Upright Laser Scanning Confocal microscope or Olympus IX83 fluorescent microscope using cellScen software. Images were manipulated minimally with Adobe Photoshop and Illustrator. All images were taken with the same microscope settings to compare fluorescence across samples.

Figures

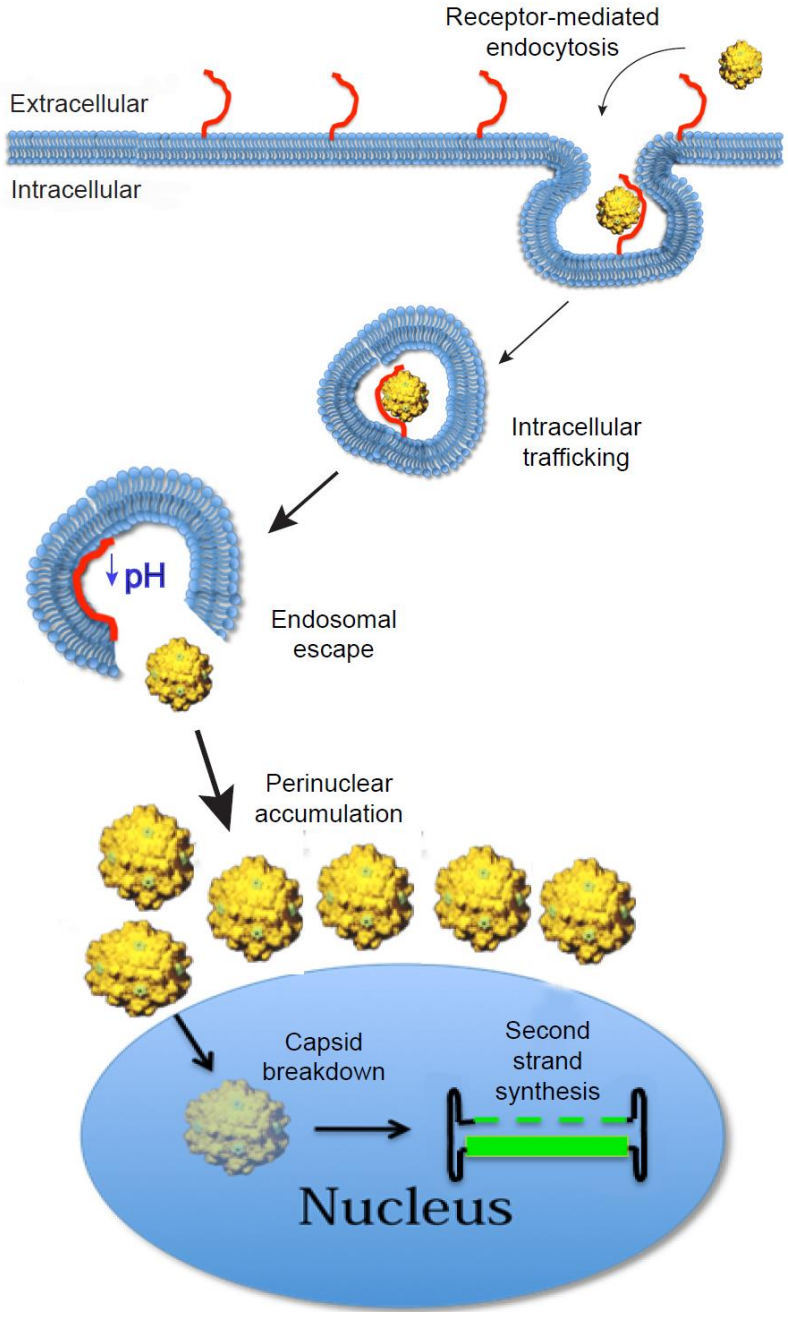

Figure 1.1 Schematic of AAV entry into the cell

AAV capsid interacts with receptors (red) on the cell surface for entry into the cell via receptor-mediated endocytosis. Once in the cell, the acidification of the endosome causes conformational changes in the capsid and escape the vesicle. The virus further traffics to accumulate on the perinuclear membrane before entering the nucleus. Once in the nucleus, the capsid breaks down to expose the viral genome.

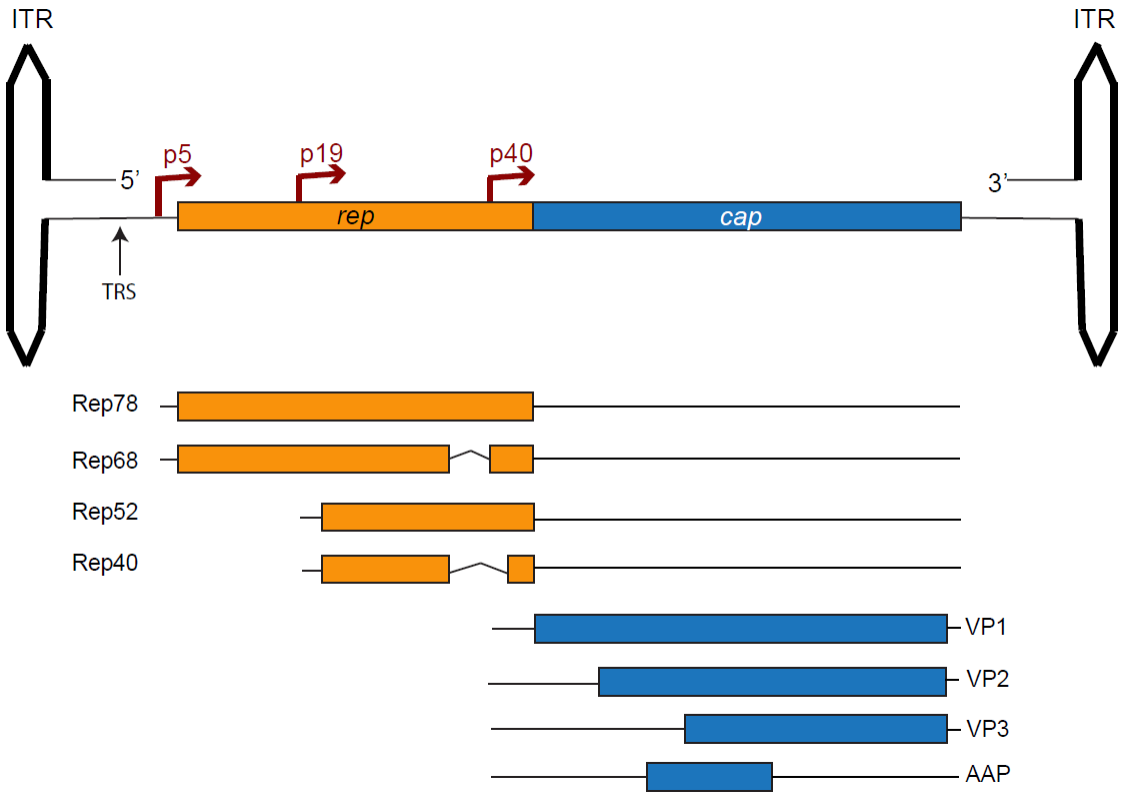

Figure 1.2 AAV genome

AAV2 genome is a linear, single-stranded DNA and consists of two ORF (*rep* and *cap*) flanked by the ITRs. The rep gene encodes four non-structural proteins namely Rep78, Rep68, Rep52, and Rep40 which are required for viral replication. The p5 internal promoter facilities Rep78 and Rep68 transcription while the p19 promoter facilities Rep52 and Rep40 transcription. The cap gene encodes three capsid viral proteins- VP1, VP2, and VP3 that constitute the capsid. The cap gene is transcribed from the internal p40 promoter. An alternate ORF that encoding a protein called assembly activating protein (AAP) is present upstream of the VP3 coding sequence, whose expression is through an unconventional translational initiation codon.

Table 1.1 Glycans and co-receptors used by the various AAV serotypes

Serotypes	Primary receptor (glycan)	Secondary receptor
rAAV1	α2,3/2,6 N-linked SIA	
rAAV2	HSPG	Integrin, FGFR, HGFR, LamR
rAAV3	HSPG	HGFR, LamR
rAAV4	α2,3 O-linked SIA	
rAAV5	α2,3 N-linked SIA	PDGFR
rAAV6	α2,3/2,6 N-linked SIA HSPG	EGFR
rAAV7		
rAAV8		LamR
rAAV9	N-linked GAL	LamR
rAAV10		
rAAV11		
rAAV12		

SIA, sialic acid; HSPG, heparan sulfate proteoglycan; GAL, galactose; FGFR, fibroblast growth factor receptor; HGFR, hepatocyte growth factor receptor; LamR, laminin receptor; PDGFR, platelet-derived growth factor receptor; EGFR, epidermal growth factor receptor.

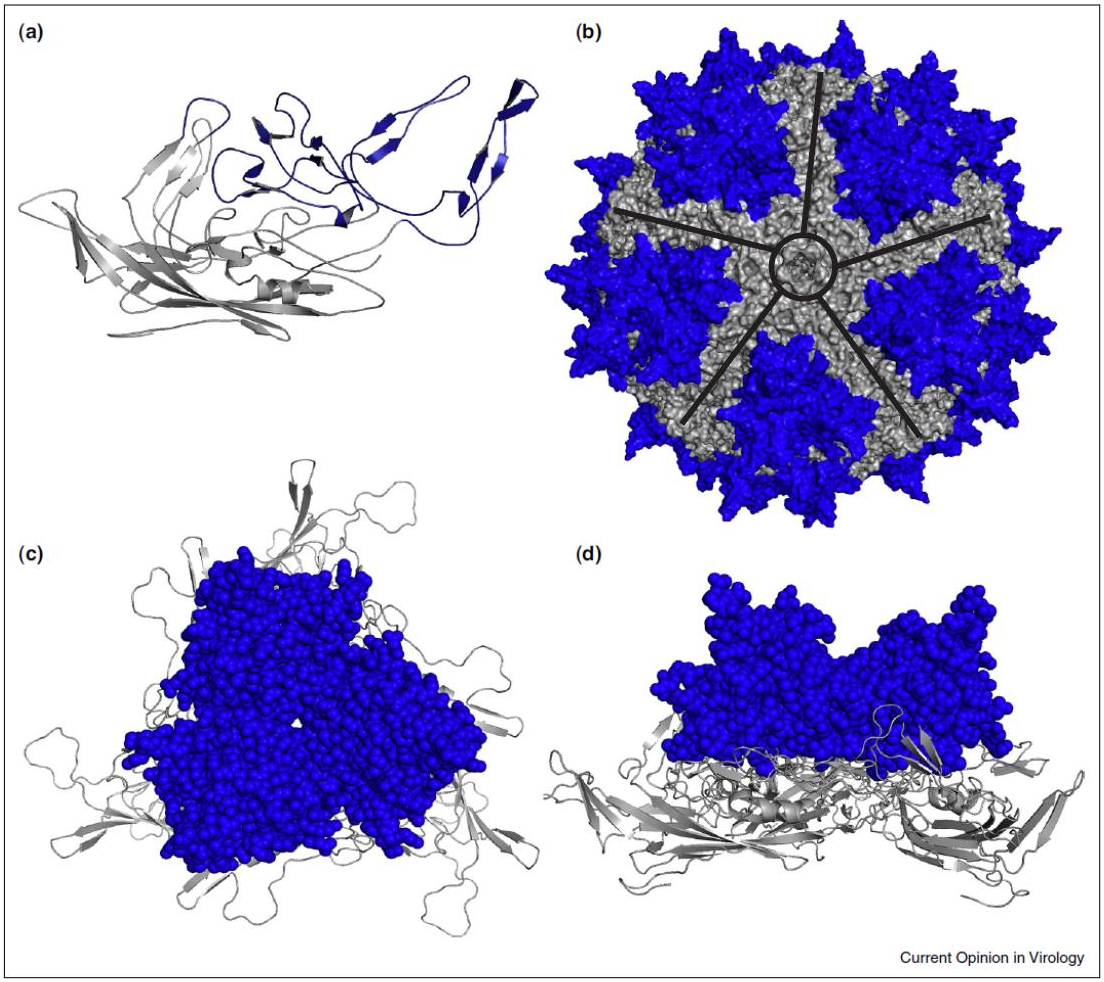

Figure 1.3 Structural analysis of Adeno-associated virus serotype 2 (AAV2) residues targeted for modification
(a) Cartoon representation of the AAV2 VP3 subunit monomer obtained using SWISS-MODEL, with regions subject to receptor footprint modifications highlighted in blue. (b) Surface rendering of an AAV2 capsid model, with 60 VP3 subunits generated using *T* = 1 icosahedral symmetry coordinates with VIPERdb. Regions subject to receptor footprint modifications are shown in blue which also corresponds to the threefold axis of symmetry. The fivefold pore is shown in the black circle with the twofold axis of symmetry in black line. (c) Cartoon of AAV2 VP3 subunit trimer created on VIPERdb, with modified regions highlighted in blue. (d) Side view of AAV with surface modified regions highlighted in blue. Reprinted from *Current Opinion in Virology, Vol 18, V.J. Madigan and A. Asokan, Engineering AAV receptor footprints for gene therapy, 89-96, 2016* with permission from Elsevier

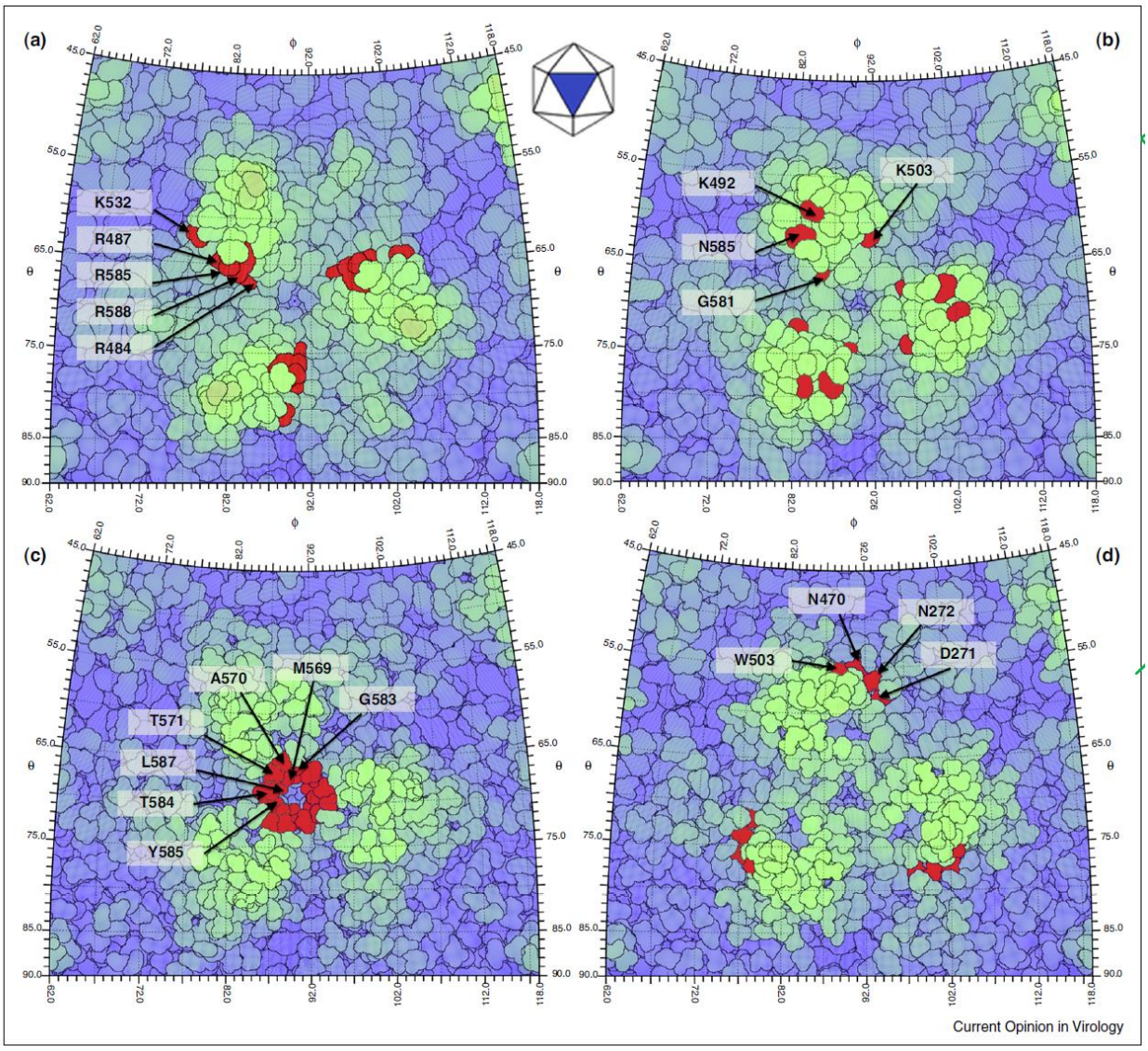

Figure 1.4 Stereographic Roadmap projections of glycan receptor footprints as viewed down the threefold symmetry axis on different naturally occurring AAV serotype capsids

The threefold symmetry axis is shown in the cartoon inset. Only surface exposed amino acids are shown, with each residue boundary depicted in black. The green regions depict the protrusion on the threefold surface, while the blue regions represent the surrounding depressions. Residues colored in red show the different glycan footprints for (a) AAV2- HS; (b) AAV4- MUC; (c) AAV5- SIA; and (d) AAV9-GAL. Reprinted from *Current Opinion in Virology, Vol 18, V.J. Madigan and A. Asokan, Engineering AAV receptor footprints for gene therapy, 89-96, 2016* with permission from Elsevier

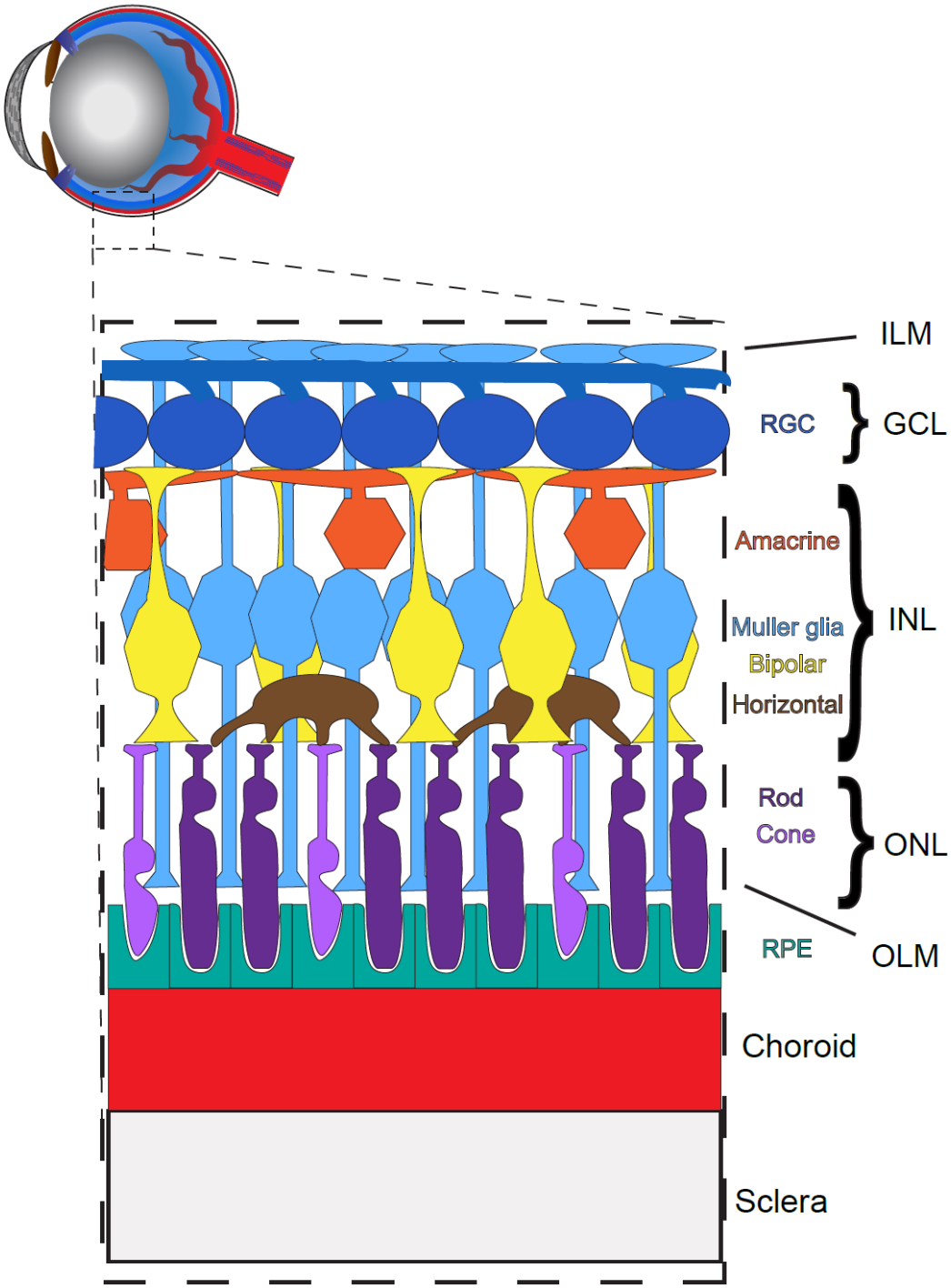

Figure 1.5 Schematic of the eye with a close-up of the posterior segment

RGC (dark blue), amacrine cells (orange), Muller glia (light blue), bipolar cells (yellow), horizontal cells (brown), rods (dark purple), cones (light purple), RPE (teal), choroid (red), sclera (white). ILM, inner limiting membrane; GCL; ganglion cell layer; INL, inner nuclear layer; ONL, outer nuclear layer; RPE, retinal pigment epithelium; RGC, retinal ganglion cells

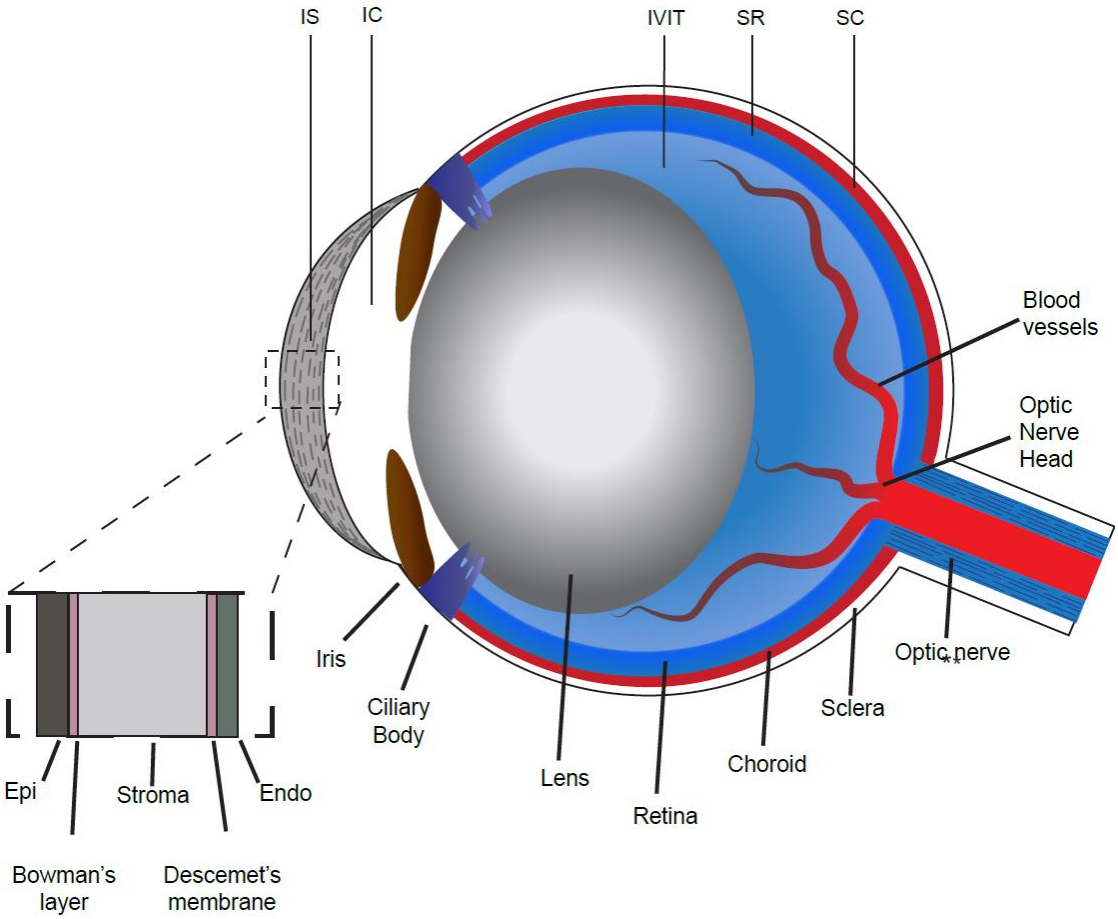

Figure 1.6 Schematic of the mouse eye with routes and close-up of corneal layers

Various structures of the eye are shown as iris (brown), ciliary body (purple), lens (gray). The layers of the posterior eye are displayed with a blood (red) and retinal (blue) layers inside the sclera (white). The layers of the cornea are depicted on inset. Epi, epithelium; Endo, endothelium; IS, intrastromal; IC, Intracameral; IVIT, intravitreal; SR, subretinal; SC, suprachoroidal

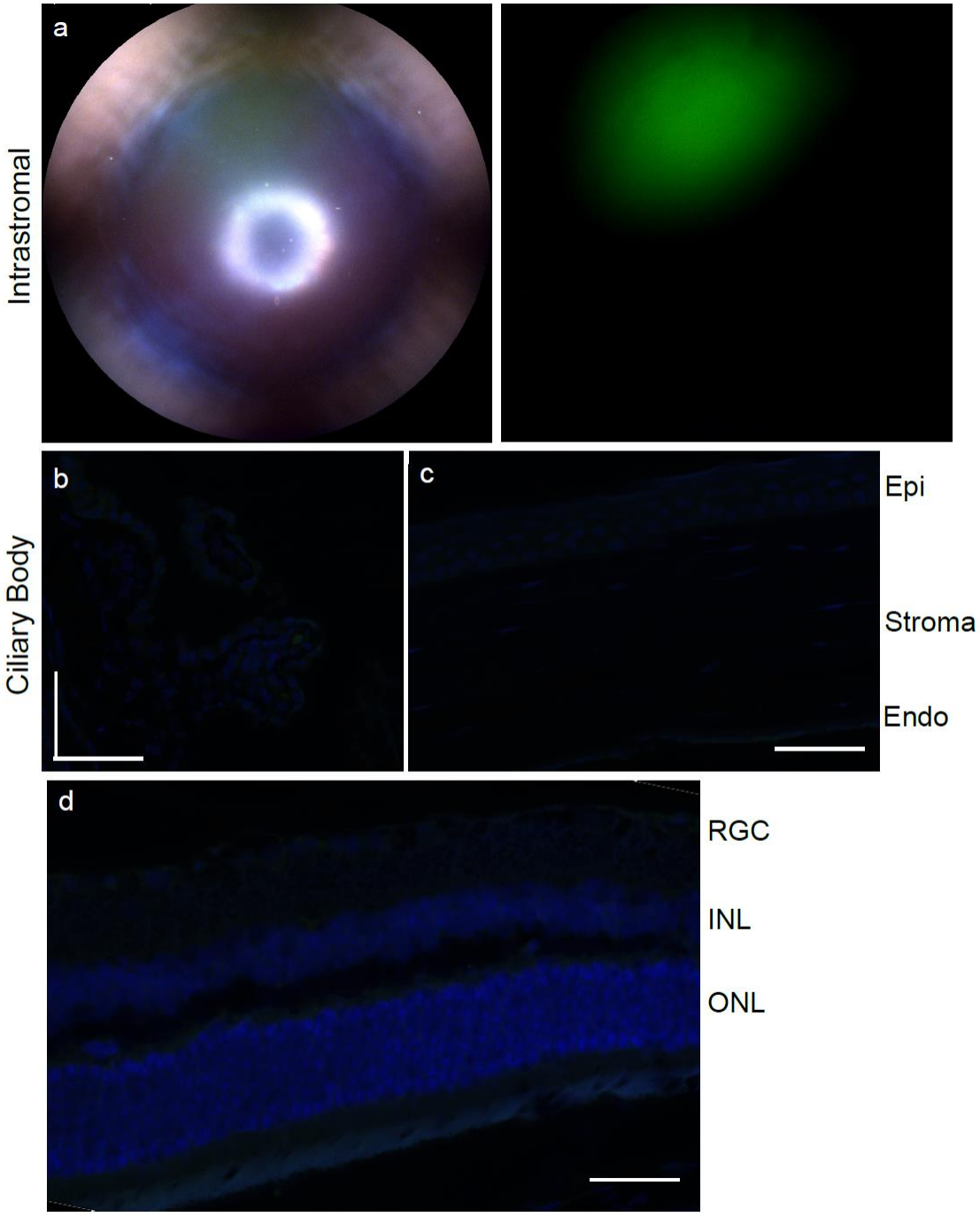

Figure 1.7 Transduction by IS injection

(a) Fundus image of the cornea in bright field (left) and GFP filter (right). (b) Ciliary body, (c) cornea, and (d) retina histology shows no fluorescence. Epi, epithelium; Endo, endothelium; RGC, retinal ganglion cells; INL, inner nuclear layer; ONL, outer nuclear layer; RPE, retinal pigmented epithelium. Scale bar: 50 µm.

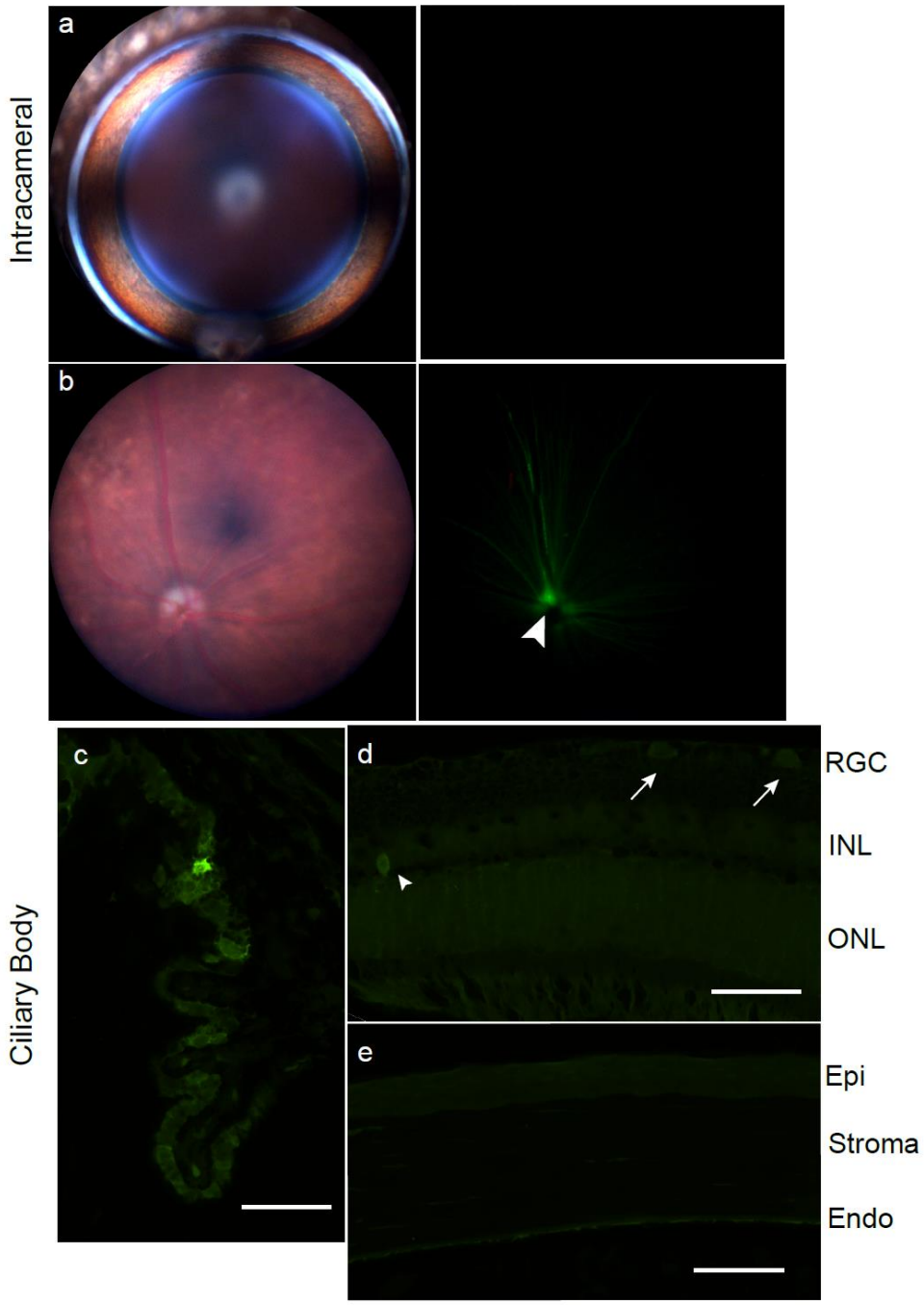

Figure 1.8 Transduction following an IC injection

Fundus images of (a) cornea or (b) retina in bright field (left) or GFP filter (right). Arrowhead indicated GFP-positive RGC axons. (c) Ciliary body, (d) retina, and (e) cornea histology is shown with RGC (arrows) and INL (arrowhead) transduction indicated. Scale bar: 50 µm. Epi, epithelium; Endo, endothelium; ILM, inner limiting membrane; RGC, retinal ganglion cells; INL, inner nuclear layer; ONL, outer nuclear layer; RPE, retinal pigmented epithelium

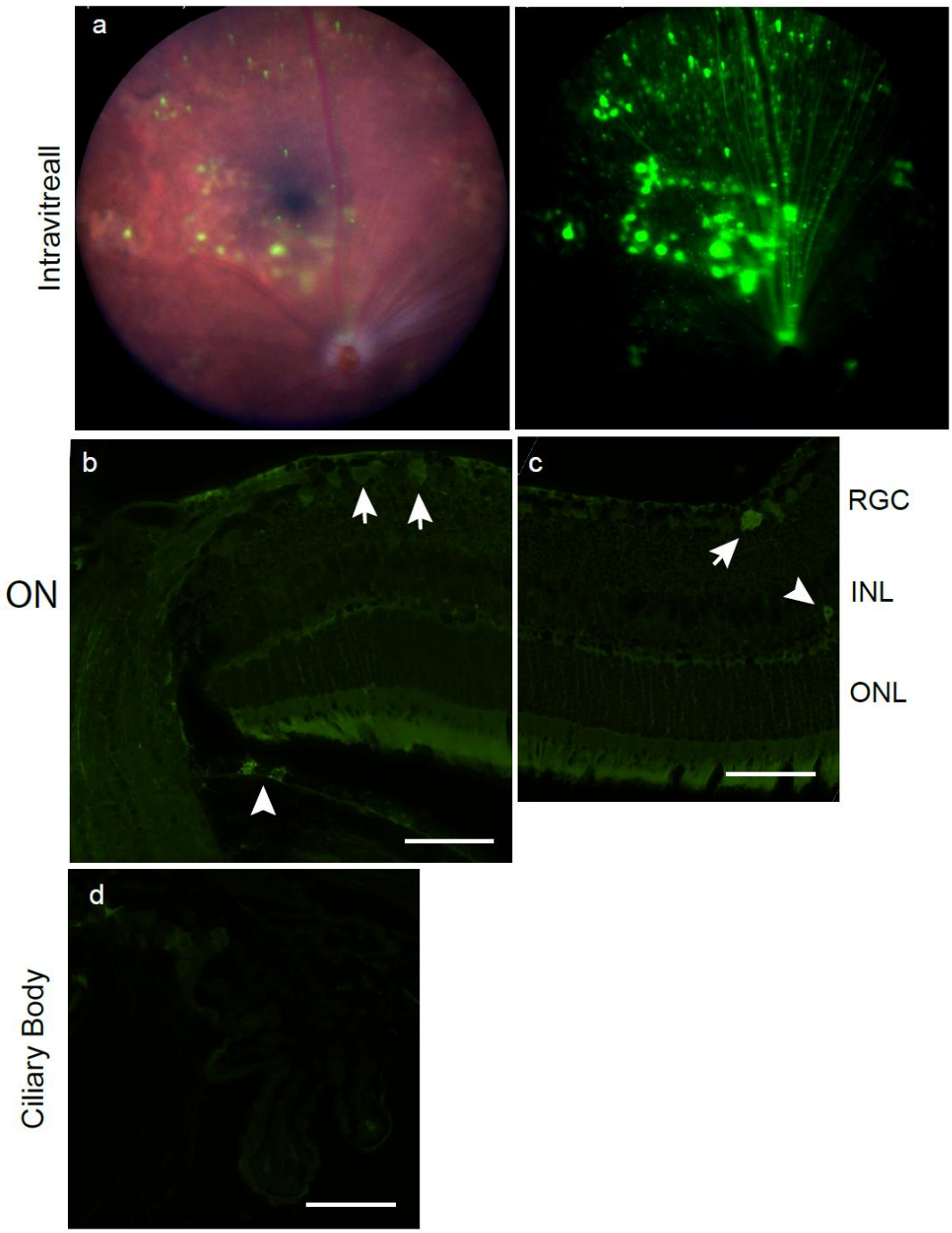

Figure 1.9 Transduction of the mouse retina following IVIT injection

(a) Fundus image of retina in bright field (left) or GFP filter (right). (b) Retinal IHC indicate RGC (arrows) and RPE (arrowhead) fluorescence. (c) Retinal IHC show RGC (arrow) and INL (arrowhead) transduction. (d) Ciliary body shows no transduction. Scale bar: 50 µm. Epi, epithelium; Endo, endothelium; ON, optic nerve; RGC, retinal ganglion cells; INL, inner nuclear layer; ONL, outer nuclear layer; RPE, retinal pigmented epithelium

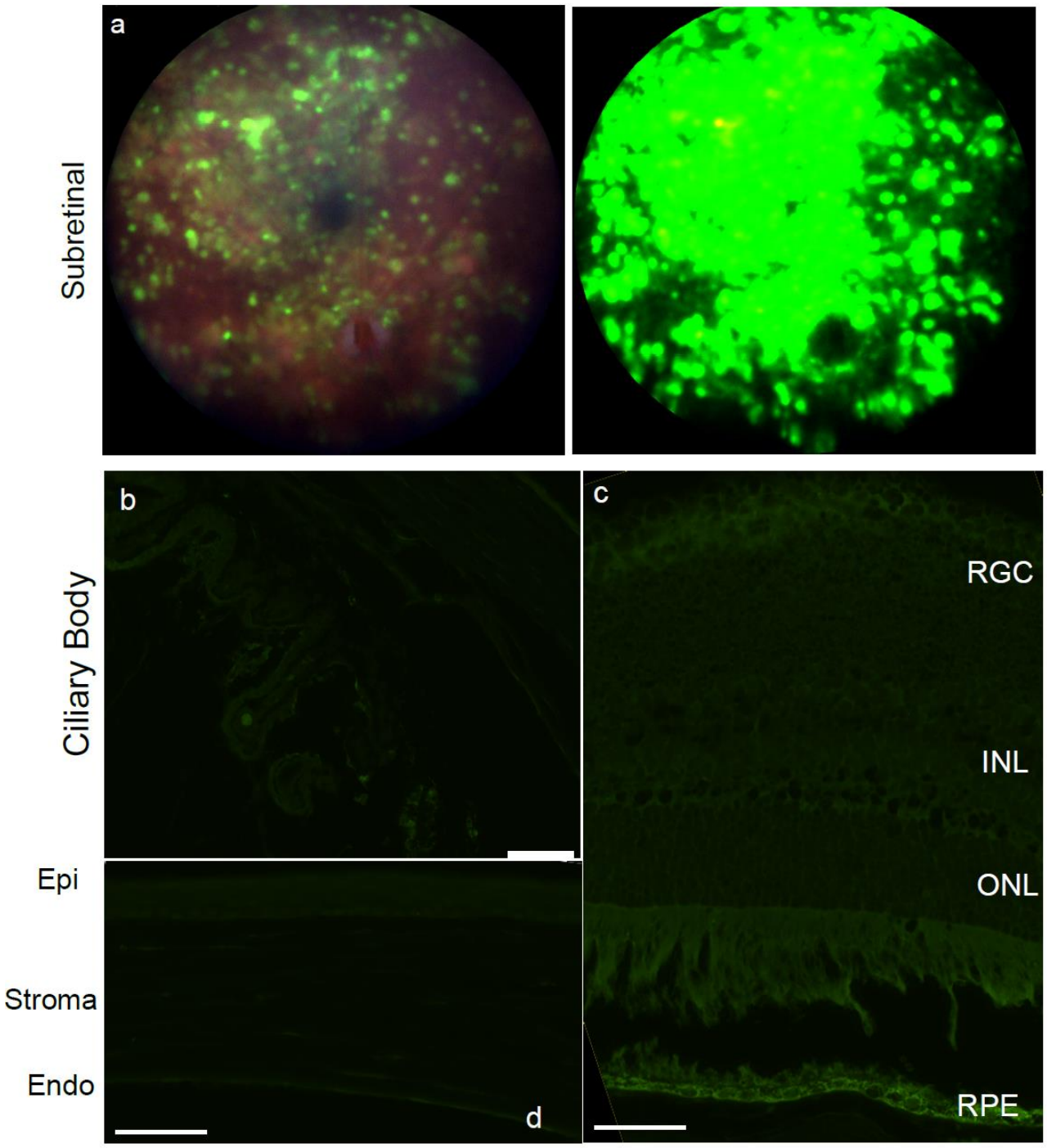

Figure 1.10 Images of GFP expression after SR transduction

(a) Fundus image of GFP fluorescence in bright field (left) and GFP filter (right). (b) Ciliary body, (c) retina, and (d) cornea histology. Scale bars: 50 µm. Epi, epithelium; Endo, endothelium; RGC, retinal ganglion cells; INL, inner nuclear layer; ONL, outer nuclear layer; RPE, retinal pigmented epithelium

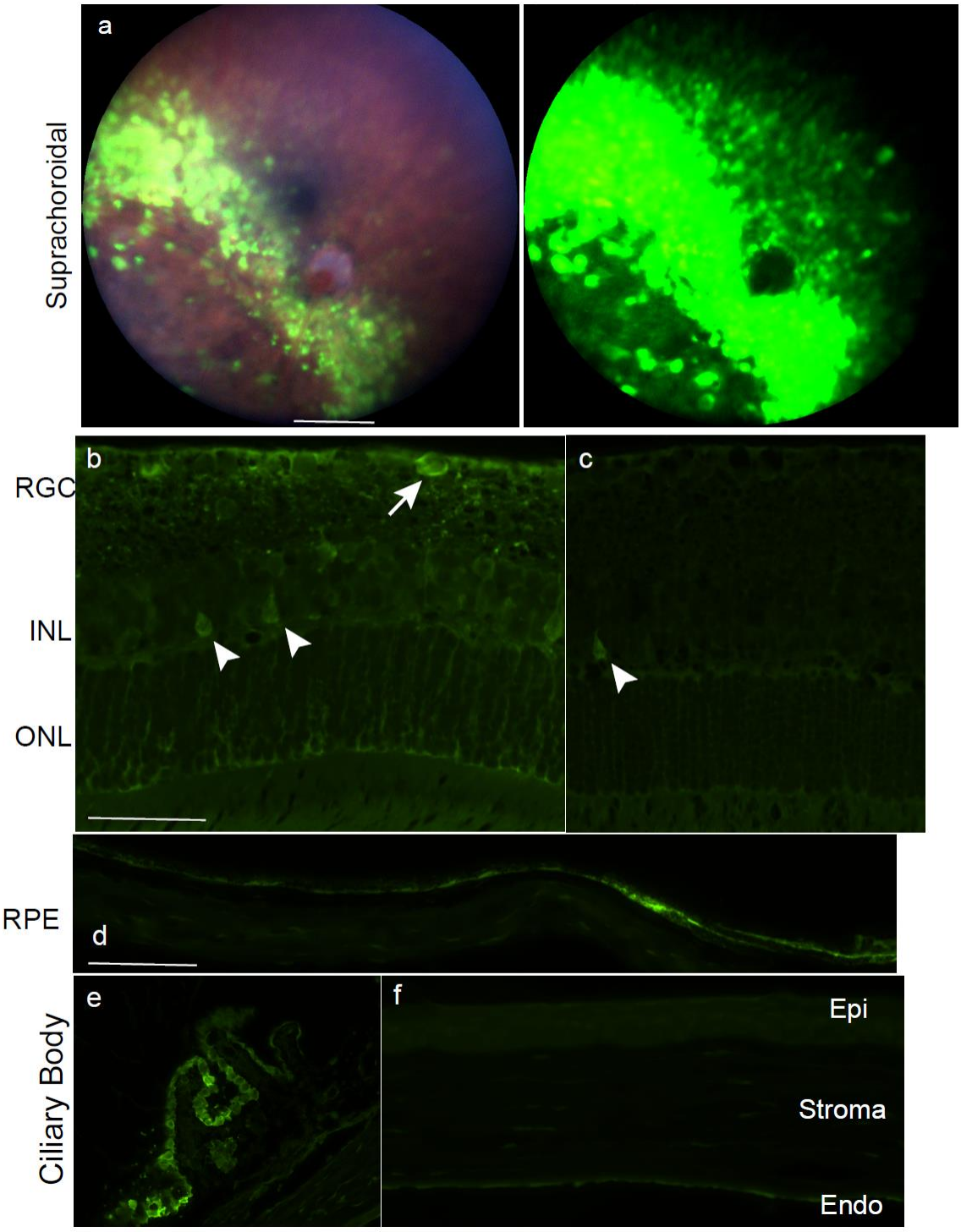

Figure 1.11 Transduction of mouse retinal following SC injection

(a) Fundus images shown in bright field (left) and GFP filter (right). (b-c) Retina, (d) RPE, (e) ciliary body, and (f) cornea are shown in GFP IHC. Arrows: RGC, Arrowhead: INL. Scale bar: 50 µm. Epi, epithelium; Endo, endothelium; RGC, retinal ganglion cells; INL, inner nuclear layer; ONL, outer nuclear layer; RPE, retinal pigmented epithelium

Table 1.2 Transduction profile of scAAV2-CMV-GFP following various intraocular injection routes

	Layer	IS	IC	IVIT	SR	SC
Cornea	Epi	-	-	-	-	-
	Stroma	+	-	-	-	-
	Endo	-	+	-	-	-
Ciliary body		-	++	-	-	++
Retina	RGC	-	+	++	-	+
	INL	-	-	+	+	+
	ONL	-	-	-	-	-
	RPE	-	-	+	++	++

CHAPTER 2: HS binding promotes the accumulation of IVIT-delivered AAV on the retina for enhanced transduction but weakly influences tropism

2.1 Introduction

IVIT delivery of rAAV vectors has become the preferred route to SR for several reasons, including i) technical ease of injection, ii) the potential to deliver vector to a greater area of the retina, and iii) less damage to the retina. For clinical applications, IVIT delivery can be performed as an outpatient procedure and circumvent the retinal disruption that may exclude patients with severe retinal degeneration. However, few serotypes exhibit efficient transduction by IVIT delivery [49] which limits its use in the clinic. rAAV2 is one of the few serotypes that transduce the RGC by IVIT [49-52]. In rodent models, transduction by rAAV2 has been seen in occasional Müller glia, amacrine, and horizontal cells. In addition, rAAV6 expression in the RGC and INL has been seen in rodent models [53-55]. The transduction of the other serotypes has been minimal, if present at all. Understanding viral trafficking and barriers to efficient IVIT transduction provide opportunities to rationally design capsids to overcome the current limitations.

At the vitreoretinal junction, the ILM has been implicated as the barrier responsible for the inefficiency of most rAAV vectors to transduce the retina. Despite the limited transduction, several AAV serotypes are capable of accumulating at the vitreoretinal junction following IVIT delivery [49, 50]. Injections of fluorescently-labeled capsids (rAAV1, 2, 5, 8, and 9) into the vitreous of adult rodents showed rAAV2, rAAV8, and rAAV9 accumulated at the ILM, but only rAAV2 resulted in transduction [49]. With a degenerated ILM, all five rAAV serotypes were capable of transducing the retina [49, 50]. The ILM is composed of the extracellular matrix of the

Müller glial end feet which displays an array of glycans similar to other basement membranes [56, 57] and may prevent access to cells needed for AAV transduction. The binding of rAAV2, rAAV8, and rAAV9 is hypothesized to be due to interaction with the laminin receptor (LamR) at the ILM. However, accumulation by LamR alone is insufficient for the transduction of rAAV8 and rAAV9. The difference in the three viruses is the HS-binding of rAAV2 and may explain why rAAV2 lends to IVIT transduction. Enzymatic digestion of HSPG at the ILM can increase the transduction and penetration of rAAV2 in the retina [58]. Therefore, HS-binding on rAAV2 seems to be both inhibitory and supportive of retinal transduction. rAAV2 shows HSPG-independent transduction in other tissue [22, 59]. It is possible that rAAV2 does not need HSPG binding for retinal transduction and that HSPG may prevent the spread of rAAV2 particles to the outer retina. To this end, rAAV2 capsid interactions with HSPG at the ILM may pose the rate-limiting step to efficient IVIT transduction of the retina. Understanding these interactions will guide rational design of vectors for more efficient IVIT transduction.

To study rAAV interactions at the ILM, a collection of capsids with altered glycan usage was used with a scAAV-CBh-GFP cassette for optimized transgene performance. The CBh promoter is a shortened form of the CBA promoter with the addition of CMV enhancer elements and its small size is beneficial for maximizing the limited transgene capacity of rAAV. The CBh promoter has shown exceptional activity in other neuronal tissue compared to CMV or CBA promoter activity [60] without potential silencing issues. The scAAV form of the transgene facilitates faster expression that is more robust than the classic ssAAV form [33, 61, 62]. In addition to optimizing GFP production, ISH was used to track vector following IVIT. Genetic capsid mutants were used to understand the role of HS-binding to rAAV transduction of the mouse retina without modifying the ILM structure. We used known capsids mutations in the HS-binding footprint of rAAV2 to carry out this analysis. The motif on the rAAV2 capsid consists of a basic patch of residues (R484, R487, K532, R585, and R588) at the base of the threefold axis

of symmetry protrusion [59] and capsid mutants like rAAV2i8 replace residues R585Q and R588T to ablate HS binding and alter tropism away from HS-rich liver tissue to become more systemic when delivered intravenously [22]. Using these capsid mutants, the use of the HS-binding motif was investigated for rAAV IVIT transduction.

2.2 Results

2.2.1 HS binding on rAAV2 is not required for SR transduction

A variety of AAV serotypes, both HS-binding and non-HS-binding, work effectively in retinal transduction when delivered subretinally, suggesting that HS binding is not needed for outer retinal transduction. To determine if rAAV2 requires HS binding in the SR transduction of the outer retina, HS-binding was ablated using the rAAV2i8 capsid. Transduction between rAAV2 and rAAV2i8 were similar by fundoscopy (Figure 2.1). The strongest signal of GFP fluorescence could be seen within the detached area (dotted line), but additional expression could be seen outside the bleb area for both vectors. The transduction outside the detachment appeared to be RPE. Within the detachment, transduction of multiple layers was observed as evident by the fluorescent RGC axons leading to the optic head from the site of injection (arrowhead). IHC was used to evaluate the cell tropism between the two vectors (Figure 2.1b). The RPE and ONL were the major cell layers transduced by both vectors. Areas could be seen where high RPE transduction but low ONL transduction occurred, indicating that RPE is the predominant cell type to be transduced. Transduction of the ONL occurred predominately in rods for both rAAV2 and rAAV2i8 capsids (Figure 2.2a). Similar to the transduction of rAAV2, rAAV2i8 transduction of cells in the INL were identified as rod bipolar cells and Müller glia (arrowhead, Figure 2.2b, c). These results confirm that the rAAV2i8 capsid is infectious in retinal tissue by SR delivery.

2.2.2 HS binding of rAAV2 is required for IVIT transduction in mice

Then HS-binding was assessed for IVIT transduction of rAAV2. Both rAAV2 and rAAV2i8 capsids were delivered intravitreally to adult mice at 10^8 vg. rAAV2-injected eyes were fluorescent at the first imaging time point of two weeks whereas rAAV2i8 showed no expression (data not shown). Eyes were evaluated for up to twelve weeks for the possibility of slower expression kinetics. During that time, rAAV2 fluorescence continued to increase, but no fluorescence was detected with rAAV2i8. By twelve weeks, rAAV2 capsid leads to a diffuse pattern of fluorescence over the neural retina as seen by fundus imaging (Figure 2.3). This diffuse pattern can be explained by the HSPG staining along the entire inner retinal surface (Figure 2.4). The rAAV2i8 capsid did not yield observable GFP fluorescence by fundoscopy which resulted in a 300-fold reduction in GFP fluorescence. We tried a higher titer of $2x\ 10^9$ vg for both rAAV2 and its HS-binding mutant to maximize the chance to observe expression (Figure 2.5). Of course, the expression was much greater with higher titered rAAV2 virus compared to what was observed with the lower titer-injected eyes. To confirm that the vitreous did not specifically inhibit the transduction capsid, virus was mixed with vitreous and delivered subretinally. Both rAAV2 and rAAV2i8 shared intense expression throughout most of the retina (Figure 2.6) that was similar to no vitreous controls.

The eyes injected intravitreally with low titer rAAV were further evaluated by IHC and FISH. rAAV2 transduction was detected in the RGC and INL, with some transduction of photoreceptors observed (arrow, Figure 2.3b). The IHC of HS-ablated rAAV2 capsids revealed a lack of transduction except for few GFP-positive rods. This phenotype has several mechanisms which could be responsible to this phenotype, including changes in the tropism or distribution of the rAAV2i8 capsid. Further analysis using FISH determined the distribution of transgenes following IVIT delivery. This is a better alternative to IHC using antibodies against the capsid have dissociated to release the transgene. Similar to the IHC expression, FISH

signal for rAAV2-delivered transgenes was detected in the RGC and INL (Figure 2.3c). rAAV2i8-injected eyes showed few transgenes present in the ONL, but no signal was detected in either the RGC or INL. These transgenes most likely represent episomes that are stable in the retina. These few transgenes in the ONL may represent a HS-independent way for rAAV2 to enter the retina.

2.2.3 HS binding is necessary for the vitreal accumulation of rAAV2 at the ILM in mice

To obtain a better understand of the trafficking differences between the rAAV2 capsid and its HS-binding mutants following IVIT delivery, eyes were enucleated soon after injection for FISH analysis. FISH was used as an alternative to modifying the capsid with fluorescent particles for visualizing the trafficking. Previous reports have shown AAV particles accumulate at the ILM 24 hours post-injection [49] which was confirmed using our FISH protocol and indicated the detection of transgenes carried in capsids that may still be intact (data not shown). The time point was extended to three days post-injection to allow sufficient time for trafficking differences. A range of vector amount was used to capture any concentration effect in accumulation. In addition, the enzymatic time for FISH signal detection was shortened to provide a more dynamic range. PBS-injected eyes served as the negative control which had minimal background labeling (Figure 2.7). With the shortened detection time, a dose of $1x10^8$ vg had only weak signal in retinas for both rAAV2 and HS-deficient rAAV2-R585E capsids. At a dose of $5x10^8$ vg, transgenes delivered by rAAV2 showed an accumulation at the ILM (black arrow), as well as being present in the ONL (arrowhead). Without HS binding, rAAV2-R585E had only minimal signal in the ONL. At the highest dose tested of $2x10^9$ vg, rAAV2 resulted in even greater signal intensity at the ILM (black arrow) showing increased accumulation of the vector. Additional aggregation of transgenes was seen in the ONL (arrowhead). At the same dose, few rAAV2-R585E-delivered transgenes were detected in the ONL of the retina (arrowhead) but did not result in any accumulation at the ILM. Taken together, these results indicate i) that HS binding

on rAAV2 helps to accumulate vectors at the ILM, ii) that this accumulation increases the number of transgenes residing in the retina, and iii) that capsids can penetrate the retina from the vitreous without binding to HS but to a far less extent (Figure 2.8). Once capsids pass through the ILM barrier, they seem capable of trafficking rapidly to the outer retina. This highlights that rAAV's rate-limiting step to efficient intravitreal transduction of the retina lies with the interaction between capsid and ILM, and enhancing this bottleneck step of trafficking will likely impact transduction in the retina.

2.2.4 HS binding is necessary for the vitreal accumulation of rAAV2 in human retinas

The abundant HSPG staining at the ILM in many animal models, including humans (Figure 2.9), suggests this mechanism may translate across species for clinical applications. To evaluate this hypothesis, a viral binding assay was done on human retinas *ex vivo* and quantified by qPCR. Vectors were applied into the vitreous a couple of hours before being harvested. Transgenes carried by rAAV2 were bound to the retina, unlike those of the rAAV2i8 capsid (Figure 2.10). The HS-deficient rAAV2i8 had relatively low vector binding in any of the collected tissue, but did show a significant increase in binding to the choroid and sclera compared to rAAV2. Together with the mouse data, these results corroborate the mechanism that HS binding promotes the accumulation of AAV vector out of the vitreous and onto the ILM for greater retinal penetration and transduction.

2.2.5 HS binding increases the IVIT transduction of other AAV serotypes

Other serotypes may benefit from the addition of the HS-binding motif and add to the diversity of vectors that could be used for IVIT transduction. The rAAV1 and rAAV6 serotypes differ by only six amino acids, with a single residue responsible for their difference in HSPG binding [19, 63]. To evaluate the influence of HS-binding between rAAV1 and rAAV6 retinal transduction for IVIT transduction, the single residue mutant capsids were tested intravitreally in mice. Although rAAV1 and the HS binding rAAV1-E531K had similar patterns of expression,

rAAV1-E531K had 3-fold greater GFP fluorescence compared to rAAV1 (Figure 2.11a). The removal of HS-binding in rAAV6 using the rAAV6-K531E capsid lead to a reduction in retinal fluorescence by fundoscopy (Figure 2.12). Both rAAV1 and rAAV6 capsids displayed a punctate expression pattern that clustered around the retinal vessels and has been documented in other reports [53, 54]. Because of the homology between rAAV1 and rAAV6, only rAAV1 and rAAV1-E531K were further evaluated for possible differences in cell tropism. IHC performed on these retinas showed the transduction of mainly Müller glia for both capsids by the co-localization of GFP and glutamine synthetase (arrowhead, Figure 2.11b). Additional cells of the INL appear to be transduced (arrow). Both rAAV1 and rAAV1-E531K showed transduction of a few RGC and photoreceptors. The similar transduction patterns of rAAV1 and rAAV1-E531K indicated that HS-binding does not alter the tropism of rAAV1. To confirm that rAAV1-E531K does not use HSPG for transduction, soluble heparin was mixed with capsids and applied to cells for an *in vitro* competition assay. rAAV2 requires HSPG for *in vitro* transduction [18] and showed a dose dependent decrease in transduction (Figure 2.13). Neither rAAV1 nor rAAV1-E531K transduction were affected at any heparin dose, indicating that the rAAV1-E531K capsid does not depend on HS binding for transduction. Transduction with rAAV1-E531K lead to fewer GFP-positive cells compared to rAAV1, indicating that the single amino acid change alone does not provide an enhancement in transduction.

In the same manuscript outlining the amino acid involved in rAAV1/rAAV6 transduction, a single amino acid mutant was identified on rAAV8 which provided HS-binding capability rAAV8-E533K [19]. At eight weeks post-IVIT administration, fundus images revealed low GFP fluorescence for rAAV8 with slightly higher GFP fluorescence that was hazy with rAAV8-E533K (Figure 2.14). FISH analysis to observe trafficking differences soon after injection and found HS-binding promoted the accumulation of vector at the ILM and within the retina (Figure 2.15).

These results suggest that HS binding alone is sufficient to enhance the transduction of IVIT-delivered AAV capsids by increasing the amount of vector that accumulate onto the retina**.**

2.2.6 Motif of rAAV1 lead to transduction along retinal vessels in mouse retinas

One way to design for new capsid variants is to build from a known serotype by adding mutations or motifs. This is the method used when adding the HS-binding motif to the various rAAV capsids. The addition of the HS-binding motif helped to increase the vector accumulation on the retina, but did not alter the transduction pattern of rAAV1 indicating other capsid motifs are responsible for tropism. To determine if a capsid motif from rAAV1 could influence the transduction of rAAV2, the previously described chimeric rAAV2.5 capsid [64] was used for IVIT transduction. While distinct from either parental serotype, the rAAV2.5 capsid revealed an expression pattern surrounding the retinal vessels (Figure 2.16). IHC of these eyes did not reveal any major tropism differences compared to rAAV2, in that RGC, Müller glia, and other cells of the INL were transduced by the chimeric rAAV2.5 capsid but some eyes showed a skewing of transduction to Müller glia. A more recent paper has shown that the amino acid at position 265 on the rAAV2.5 capsid to be solely responsible [65]. Therefore, a rAAV2-265D point mutant was tested IVIT and revealed similar expression to the rAAV2.5 parent (Figure 2.17).

2.2.7 rAAV2.5 testing in large animal models

To determine if the rAAV2.5 was conserved across animal models, CBh-GFP vector was IVIT-delivered to rabbits. Both rAAV2 and 2.5 transduced the vessels, but only rAAV2.5 transduction was specific to the vessels (Figure 2.18). rAAV2.5 was further tested in non-human primate (NHP) by both SR and IVIT deliveries (Figure 2.19). Intense SR transduction resulted in the transduction of PRs whereas IVIT transduction was minimal and restricted to the fovea (Figure 2.20). To determine if inhibitory factors were responsible for the lack of IVIT transduction, ocular fluid samples were collected pre- and post-injection were mixed with virus

or applied to cell culture alone. No inhibition of transduction was seen with any fluid (Figure 2.21). Surprisingly, the post-injection vitreal fluid had rAAV2.5 infectious particles as noted by the GFP-positive cells when vitreous only was delivered as a negative control. To assess if any rAAV2.5 vector made it to the retina, ISH was carried out on SR and IVIT injected retinas. SR shows transgenes in the ONL while IVIT transgenes were only at the ILM (Figure 2.22).

2.2.8 Motif from rAAV9 lead to transduction of Muller glia in mouse retinas

An additional chimeric rAAV2 capsid, rAAV2G9, has been shown to use HS and GAL binding interchangeably for cell transduction [66] since each motif is non-overlapping (Figure 2.23). The rAAV2G9 vector has been tested for transduction within the brain by two routes of injections [67] and further highlights the importance of injection site to the transduction of CNS cells. The dual glycan vector remained in the CNS rather than disseminating to peripheral tissues [67]. Although the IVIT and SR injections remain confined to the eye, this dual glycan has never been tested in the eye and therefore could yield a vector with preferable transgene expression. The use of rAAV2G9 by IVIT delivery resulted in a punctate expression across the retina, which correlated to specific transduction of Müller glia (Figure 2.24). The galactose motif was structured from the rAAV9 capsid so both rAAV9 and a HS-ablated rAAV2i8G9 capsids were tested, but showed no expression following IVIT delivery (Figure 2.25). This indicated that galactose binding alone was insufficient to lead to transduction within the retina. Lectin antibody to identify the presence of galactose in the retina indicated much of the staining occurred around the ONL but was not very abundantly expressed (Figure 2.26).

2.2.9 Combination of motifs in the rAAV2.5G9 can result in enhanced, targeted transduction

To determine which motif was dominant, a double chimera rAAV2.5G9 was created and tested. The intravitreal delivery of rAAV2.5G9 lead to expression similar to the rAAV2.5 parent when imaged by fundoscopy (Figure 2.27). Quantification of the expression comparing all

capsids showed rAAV2.5 and rAAV2.5G9 to have the highest transduction and non-HS-binding capsids to have the lowest transduction (Figure 2.28). The fluorescence around the retinal vessels was very evident with punctate expression found around the vessels. IHC of the rAAV2.5G9-injected eyes revealed a Müller glia specific transduction profile (Figure 2.27). Therefore, the addition of either the rAAV1 or rAAV9 motif appear to have equal ability to control tropism, but dominate over the tropism provided by the HS-binding motif.

2.3 Discussion

The experiments conducted herein provide a greater understand for the early trafficking of rAAV following intravitreal delivery and how to exploit this trafficking to enhance transduction. As virus is injected into the vitreous, it travels through the vitreous humor, resulting in a dilution of the vector concentration. Once the virus reaches the retina, the capsid interacts with the glycans present on the ILM to concentrate the virus out of the vitreous. Days following delivery. After concentration of the virus, vectors penetrate through the retinal layers where they transduce the various retinal cells. In the weeks after delivery, transgene expression is detectable and remains so for months. Not all AAV serotypes aggregate sufficiently to promote penetration into the retina and lead to transgene expression. This issue can be circumvented through the application of HS-binding motif on the capsid, thereby allowing the capsid to interact with the ILM, without causing a change a tropism. The interaction of rAAV capsids with the ILM poses the rate-limiting step to retinal trafficking [49, 50]. Therefore, interaction with this membrane should be increased to maximize the number of capsids entering the retina. Pores present in the ILM may explain why few HS-binding deficient capsids could pass through the ILM and traffic rapidly to the outer retina. Relatively similar amount of rAAV2 capsids were found rapidly in the outer retina, supporting the idea of a non-glycan-mediated entry like through a pore. These deep-penetrating vectors may represent the few capsids whose trajectory was align to allow them to quickly pass through the pores and through the retinal interior. However, most

vectors must interact with the ILM before they can penetrate the retina. If capsids cannot interact with the ILM, they remained diluted in the vitreous, unable to transduce the retina. Even if a higher concentration of vector is used, lack of interaction with the ILM is insufficient to aggregate capsids onto the retina surface and lead to further retinal transduction. We could increase the amount of vector in the retina by adding a HS-binding motif to the non-HS-binding capsids. This may be an alternative strategy to current methods of getting high titer vector into the retina using to either ILM digestion or a sub-ILM injection [49-51, 68]. It is easy to see how development of better capsids that are capable of transducing without these invasive aides would be of interest for researchers and clinicians alike.

The ILM structure is found across multiple species and could serve to attract and concentrate rAAV capsids out of the vitreous for not just mice, but also human. As hypothesized, we found the same accumulation on the retina with only the HS-binding rAAV2 using human *ex vivo* retinas. The kinetics of vector dispersion through the vitreous humor are likely to be slower due to the volume, which will also mean longer times until interaction with the ILM and penetration into the retina. Although these kinetic studies must be worked out further for primate intravitreal delivery, the mechanism that HS-binding motifs positively influence vector accumulation on the retina will make vectors more effective. It is important to remember that the transduction observed in a mouse model may not be indicative to other animal models. While the mouse has become a standard model for retinal gene transfer, certain size and anatomical differences exist between them and larger animal models. In addition, the thickness differences of the ILM between mouse and primates may lead to selection of capsids that are not as efficient across species. The addition of the HS-binding motif, mechanism of vector accumulation was conserve in both mouse and human retinas. The phenotype of rAAV2.5 was confirmed in a rabbit model and validates translation of this work.

The interaction between the AAV capsid and HS binding is mediated by a static charge. The negative charge of the sulfate groups on the heparan chain, which are found on the proteoglycan core of HSPG, serves to attract the basic patch of residues on the rAAV2 capsid. Through this sulfate interaction, the heparin chain falls along the inner surface of the 3-fold protrusion of the capsid surface. We used capsid mutants to change this charge interaction to no longer attract the sulfate group and obstructs the heparan chain interaction with the capsid. It could be argued that this charge interaction is the most important interaction between rAAV and ILM; therefore, the capsid is really drawn to any highly-charged molecule. We used dextran sulfate to act as a surrogate for heparan sulfate. We mixed rAAV2 capsids with dextran sulfate or heparan sulfate (heparin) or un-sulfated heparan sulfate (heparosan) before IVit delivery. We found heparin and heparosan dramatically decreased transduction of rAAV2 while dextran sulfate resulted in no change (Figure 2.29). This data indicates that rAAV2 specifically interacts with HSPG and not through electrostatic charge alone. Therefore, random changes to make the capsid more charged may have little influence.

Indeed, HS binding lead to a greater presence of transgenes in the retina compared to the parent capsid when assessed by FISH soon after injection. Transgenes of non-HS-binding rAAV1 and rAAV8 could still be detected in the retina, but to a lesser extent. The lack of expression with HS-binding rAAV3 when injected intravitreally (data not shown) was expected because this serotype is inefficient in the transduction of most cell types [69] and may encounter additional barriers for efficient transduction of cells. rAAV6 is a serotype of interest for retinal transduction and has been modified to increase the specific transduction of Müller glia using the ShH10 capsid [70]. Without HS binding, the ShH10 vector may reveal a much weaker fluorescence. From our model, any capsid that had an HS-binding motif would can accumulate at the ILM. The recent publication by Boye *et al.* used HSPG-binding rAAV5 and rAAV8 but was unsuccessful to enhance their GFP fluorescence, indicating this HS-binding enhancement is not

universal to all capsids [71]. This may be related to their shortened CBA promoter and that use of a different promoter may revealed expression. We would predict that rAAV5 capsid should have enhanced transduction with the HSPG binding mutation. In addition, other labs have tested rAAV5 and rAAV8 using a CAG promoter and have shown expression [72] and serves as reason to reevaluate all rAAV capsids transduction following intravitreal delivery by FISH. By using GFP expression as the only way of analyzing where capsids have trafficked in the retina, there is an incomplete picture formed by the activity of the promoter. FISH analysis provides a simple way to detect the location of viral transgenes as a surrogate for the location of capsids. FISH is better alternative to modifying the capsid surface with fluorescent Cy3 dye which binds to the Lys residues on the capsid. Modifying residues on the rAAV1 capsid can alter expression levels (*i.e.* rAAV1-E531K vs rAAV1), so it could be argued that the Cy dye could be masking the expression of serotypes in earlier studies [49, 50].

Increasing the viral concentration could increase the vector interaction with ILM and in the retina, but is more likely to evoke an immune response as the vitreal space is not immune privileged like the subretinal space [73]. Therefore, it is optimal to use lower concentrations of vector to avoid this response. Therefore, we chose to work with a low concentration of vector was used to maximize expression rather than using high titers of vector. Other labs sought to maximize expression in other ways. A recent manuscript lead to a selection of a peptide incorporated onto the rAAV2 capsid has enhanced IVIT transduction in both mouse and non-human primates [74]. While this peptide is located near the HS binding footprint, this capsid shows a dependency on HSPG for transduction and may still exploit the same HS-mediated accumulation mechanism outlined above. This hypothesis was tested using the peptide in the context of HS binding. As predicted with our model, GFP expression was only detected when the Arg (R) residues involved in the HS-binding motif were present (Figure 2.30). We found the peptide insertion to reduce rAAV2 transduction, suggesting that a reduction in HSPG binding

may be met with a reduction in IVIT transduction. Other attempts to enhance transduction use capsids modified to avoid proteasomal degradation [75], thereby enhancing intracellular trafficking to help increase the transgene expression of intravitreally-delivered capsids. However, a recent publication suggests that these vectors may not benefit from late-stage traffic enhancement [71] that are downstream of ILM binding. To take advantage of the retinal structure, binding to the ILM can be used to accumulate vectors at the retina for transduction.

Although HSPG is abundant at the ILM, other receptors can play a role in the transduction of the retina from the vitreous. The transduction by rAAV1 and rAAV6 suggest the presence of 2,3 and 2,6 N-linked SIA at the ILM. The pattern of transduction observed by fundus may indicate a distinct pattern of sialic acid in the retina that is visible by flat mount staining. It would be beneficial to perform FISH on whole mount retinas soon after injection to observe accumulation of vector. Laminin receptor (LamR) is known to interact with rAAV2, rAAV3, rAAV8, and rAAV9 serotypes [24] and laminin staining is at the ILM restricted to the blood vessels. Although these capsids can interact with laminin receptors at the vitreoretinal junction, this interaction seems insufficient to promote efficient intravitreal retinal transduction. Again, a re-evaluation of all rAAV serotypes using FISH as the detection method would provide a greater understanding to virus trafficking and transduction in the retina.

The similar transduction profiles of SR-delivered rAAV2 and rAAV2i8 indicate that rAAV2 does not require HS binding for retinal transduction. It may be that the SR delivery effectively concentrates the vector, thereby skewing capsids towards expression. In addition to transduction by receptor-mediated endocytosis, SR provides abundant rAAV vectors to the phagocytic RPE and may explain why the RPE appears to be the primary cell target by both rAAV2 and rAAV2i8. It would be of interest to see if the RGC transduction of subretinally-delivered rAAV2 is due to the HSPG on the ILM pulling on the vector. FISH could be used to map the trafficking of SR-delivered vector to better understand this phenomenon.

Amino acids transplanted from AAV1 capsid onto AAV2 capsid were sufficient to alter the transduction pattern to mimic the pattern closer to that observed with AAV1. It is unclear how the difference in residues between rAAV2 and rAAV2.5 promote this vascular tropism. The rAAV2.5 capsid has been shown to bind HS with the same efficiency as rAAV2[64] and no evidence of additional cellular receptor usage has been identified. The transduction of the retina along the vasculature with rAAV2.5 may be a result of the tropism shift towards Muller glia. Muller glia are known to wrap around the vasculature in the retina and may account for this phenotype. However, the transduction shift to favor Muller glia may indicate the addition of a receptor used by rAAV2.5 that is found on the Muller glia cells. Although transduction of the vasculature endothelial cells has been previously shown with rAAV2.5 after cardiac injection [76], histology of rAAV2.5-injected retinas did not reveal co-localization of GFP and an endothelial cell marker (data not shown). The use of the rAAV2.5 capsid also displayed greater fluorescence than the rAAV2 capsid. The higher transduction by rAAV2.5 has been shown in multiple tissues, including brain[60] and muscle[64]. Similar to previously published results, the phenotype of rAAV2.5 in the eye could be recapitulated by a single point mutant at position 265.

Finally, galactose binding alone was insufficient to transduce the retina, but in conjunction with HS binding provided a tropism shift to specific transduction of Müller glia. The results of the immunostaining did not provide a clear mechanism to the Muller glial tropism of rAAV2G9. Galactose was detected only in the outer retina. If capsids are modified to enhancement of intracellular trafficking, rAAV8 and rAAV9 capsids result in GFP expression in retinas with normal ILM [77]. This suggests capsids can penetrate the retina, but face additional intracellular barriers to efficient transduction.

To ensure that the phenotype observed with rAAV2.5G9 was reproducible, rAAV2- and rAAV2.5G9-CBh-GFP vectors were provided independently to two established retinal gene therapy labs (Drs. Robin Ali and Alberto Aurrichio) to perform intraocular injections. All injections

resulted in the fluorescence pattern described above and the similar tropism for Muller glia (data not shown). Increase in fluorescence could be observed with increased doses of vector.

As more of the capsid biology of AAV becomes available, we will have better insight into which capsid motifs can be modified to produce a desired outcome. Taken together, the collection of capsids show that HS binding is beneficial to vector transduction, but that other capsid motifs have a greater influence on the transduction profile of the capsid in the retina. These capsid motifs are important for the targeting of vectors to specific cells of the retina and capsid motifs can enhance the transduction levels of currently available vectors with few capsid changes needed. While retinal gene therapy has been met with success in the past, long-term data is beginning to reveal that treatment of patients is more complicated than previously thought. The disappointing results of AVA-101 trial for wet AMD and the weakening therapeutic response seen in LCA patients indicate that there are additional mechanisms that must be understood to effectively treat patients. It may be that current therapies only work to delay the pathology, but do not work to reverse the damage already done by the time the patient seeks help. If this is the case, early intervention in the treatment of retinal degenerative diseases will yield the greatest therapeutic response. While most of the patients enrolled in retinal gene therapy trials are adults, some children have been enrolled and could provide evidence to support the use of early intervention.

2.4 Experimental procedures

2.4.1 Virus production and purification

scAAV carrying the GFP gene under the control of the ubiquitous CBh promoter [78] were produced by triple transfection method using polyethylenimine [25]. Viruses were harvested as previously described [66]. Lysate was clarified by centrifugation at 6200x*g* and purified by iodixanol gradient ultracentrifugation at 402,000x*g* for 1 hour. Viruses were pulled from the 40%/60% interface, purified by ion-exchange chromatography on a 1-ml Q HyperD F

column (Pall) and eluted with 200 mM NaCl, 25 mM Tris [pH 9.0]. AAV8-E533K vector was difficult to produce a significant yield by iodixanol. Therefore, AAV8 and AAV8-E533K were purified by CsCl and then by sucrose to obtain pure vector. Viruses were dialyzed against 350mM NaCl, 5% sorbitol in 1xPBS before being aliquoted and frozen at -80°C. Viral titer was determined by qPCR against wild-type ITR of DNase-resistant vector genomes relative to a virus standard (data not shown). Viruses underwent electrophoresis on a 1% Bis-Tris gel (Novex) and silver stain (Life Technologies) to assess purity (data not shown).

2.4.2 Animal injections

Adult C57BL/6 mice were used for this study. All animals were housed under 12/12-hour light/dark cycle in the University of North Carolina Division of Laboratory Animal Medicine facilities and were handled in accordance within the guidelines of the Institutional Animal Care and Use Committee at the University of North Carolina. Prior to vector delivery, animals were anesthetized with ketamine (75 mg/kg), xylazine (10 mg/kg), acepromazine (1.5 mg/kg), and dilated with 1% tropicamide and 2.5% phenylephrine. Proparacaine-HCl was applied to eyes as a local anesthetic. Intraocular needles were constructed using 32-gauge cannula connected to a Hamilton syringe via tubing filled with water. An air bubble separated the water from the viral suspension. Freshly thawed viruses were diluted to working stock and incubated in the intraocular needle at room temperature for 10 minutes prior to injection. Needles were evacuated and loaded with fresh suspension. Viral suspension was mixed with fluorescein sodium salt (Sigma) to confirm successful injection as previously described [48]. All injections were carried out by the same surgeon. For IVIT injections, a pilot hole was made with the tip of a beveled 30-gauge needle in the superior portion of the eye approximately 0.5 mm posterior to the limbus. The intraocular needle was inserted through this hole into the vitreous under direct observation through the microscope. A volume of 1 µl as delivered at a constant rate over 30 seconds using a syringe pump. The needle was held in place for 20 seconds to allow for

intraocular pressure equilibration before removal. For SR injection, the intraocular needle was inserted tangential to the eye. Delivery of fluid was immediate and characterized for success by OCT and fundoscopy of fluorescein distribution using the Micron IV (Phoenix Research Laboratories). Genteal (Novartis) was applied to eyes to prevent corneal drying, and mice could recover on heating pads.

2.4.3 *In vivo* imaging

Fundus images and OCT were carried out by dilating and sedating animals as described above. All fluorescent images were taken under the same settings and similar retinal position using the Micron IV. The green channel of the fluorescent fundus image was isolated, converted to grayscale, and quantified by integrated density measurements using ImageJ (National Institutes of Health).

2.4.4 Enucleation and histology

Animals were sedated and perfused with PBS containing 1 unit heparin per ml, followed by 4% PFA in PBS. Eyes were enucleated and a puncture was made anterior to the limbus using an 18G needle before incubating in 4% PFA for 10 minutes. The anterior segment, musculature, and lens were removed and eyecups were placed in 10% sucrose at 4°C overnight followed by 20% and 30% sucrose incubations. Eyecups were embedded in OCT cutting media (Sakura), frozen at -20°C, and stored at -80°C. Ten-micron transverse sections were collected on pre-cleaned Superfrost Plus slides (Fisher) and stored at -80°C until further processing.

2.4.5 IHC of retinal sections

Sections were washed in TBS containing 0.3% Tween-20 (TBS-T) and incubated in blocking buffer (10% normal goat serum, 0.1% Triton-x 100 in PBS) for 1 hour in a humid chamber. Slides were incubated in antibody solution (3% NGS, 0.1% Triton x-100 in PBS) with primary antibodies in a humid chamber overnight at room temperature. Primary antibodies used

were rabbit anti-GFP (1:500; Millipore), mouse anti-glutamine synthetase (1:100; Abcam), mouse anti-heparan sulfate 10E4 epitope (1:70; Amsbio), mouse anti-rhodopsin (1:100; Rockland), and mouse anti-PKC alpha [H-7] (1:250; Santa Cruz). After three washes with TBS-T, secondary fluorescent antibodies were applied in antibody solution for 2 hours in a humid chamber. Secondary antibodies were Alexa-Fluor 488 goat anti-rabbit (1:1000; Molecular Probes), Alexa-Fluor 568 goat anti-mouse (1:1000; Molecular Probes), or Alexa Fluor 568 rabbit anti-goat (1:1000; Molecular Probes). Slides were mounted in Prolong Gold Antifade with DAPI (Molecular Probes) as stated by manufacturer's protocol. Images were taken on a LeicaSP2 AOBS Upright Laser Scanning Confocal microscope or Olympus IX83 fluorescent microscope using cellScen software. Images were manipulated minimally with Adobe Photoshop and Illustrator.

2.4.6 Soluble HS analog assay

For *in vitro* studies, HEK293 cells were plated in a 24-well dish at a density of 10^5 cells per well and allowed to adhere overnight at 37°C, 5% CO_2. Viruses were pre-incubated with soluble heparin at the specified concentrations for 1 hour prior to the addition to cells at a concentration of 10,000 vg per cell. Cells were harvested 48 hours later and quantified by flow cytometry.

2.4.7 Fluorescence *in situ* hybridization

The GFP gene was cloned into the pSPT18 vector (Roche RNA in vitro transcription kit) at the HindIII and EcoRI sites and sequenced for confirmation. Plasmids were linearized with these restriction enzymes and purified by phenol-chloroform extraction/ethanol precipitation and re-suspended in water. Linearized plasmids were quantified by spectrophometry and verified by DNA sequencing before *in vitro* transcription of antisense and sense riboprobes were carried as described by the manufacturer (Roche). Aliquots of riboprobes were frozen in water and were quantified as described by the manufacturer and analyzed by gel electrophoresis and SYBR

Gold staining (Invitrogen). Riboprobe functionality was assayed for sensitivity and selectivity by dot blot of virus controls to a positively-charged nitrocellulose membrane (Roche). Both sense and antisense probe could detect viral GFP transgene equally (data not shown).

Frozen slides were heated to 55°C for 10 minutes and pre-treated as previously described [79]. Slides were then incubated in hybridization buffer (50% formamide, 10 mM Tris [pH 7.6], 200 μg/ml yeast tRNA, 1x Denhardt's solution, 10% dextran sulfate, 600mM NaCl, 0.25% SDS, 1mM EDTA [pH 8]) without probe at hybridization temperature of 65°C for 2 to 4 hours. Slides were transferred to pre-hybridization buffer containing 50 ng/ml of sense riboprobe to specifically detect DNA and not mRNA transcripts. Slides were heated to 80°C for 20 minutes, snap chilled on ice, and incubated overnight at 65°C. Slides were washed in 50% formamide/2x SSC at 65°C for 30 minutes, 2x SSC at 55°C for 20 minutes, and two washes of 0.2x SSC at 55°C for 20 minutes. Slides were washed in 1x Washing Buffer (Roche) followed by incubation of 10% sheep serum in 1x Blocking Buffer for 1 hour in a humid chamber. Sheep anti-DIG-AP antibody (1:1000; Roche) was applied and incubated 2 to 3 hours in a humid chamber. Slides were washed three times in Washing Buffer with gentle agitation for 10 minutes followed by two incubations in Detection Buffer (100 mM Tris, 100 mM NaCl, 10 mM $MgCl_2$ [pH 8.0]) for 10 minutes. HNPP/Fast Red detection substrate was prepared and applied as directed by the manufacturer (Roche) for two to three applications. Following the detection reaction, slides were rinsed in distilled water and coverslipped using Prolong Gold antifade reagent with DAPI. Images were taken on a LeicaSP2 AOBS Upright Laser Scanning Confocal microscope or an Olympus IX83 fluorescent microscope.

2.4.8 *Ex vivo* human retinal binding assay

Human whole globes were procured immediately after death and placed in a moist chamber on ice for 4 days. The anterior chamber, iris, and lens were removed and the globe was quartered with some vitreous remaining attached to the retina. Ten μl of vector was applied

to the vitreous at a titer of $2x10^9$ vg/μl and allowed to bind to the retina for 2 hours at 4°C. The quartered retinas were kept out of media to prevent the vector solution from spilling over the sides of the retinal slice. Following the incubation, PBS was washed over the tissue, collected, and stored at -80°C. Vitreous, retina, choroid, and sclera were collected separately and stored at -80°C. Tissue samples were digested and purified using the DNeasy Blood & Tissue kit (Qiagen). Virus in the collected samples was quantified by qPCR using primers against GFP and hGAPDH housekeeping genes.

2.4.9 NHP injections

Two female cynomolgus primates (age: #313- ~3.5 years, #309- ~1.5 years) were housed at the University of Pennsylvania. Primates were tested for neutralizing antibodies to rAAV2 prior to injection. A total of 1E11 vg scAAV2.5-CBh-GFP were delivered in 150 µl volume either SR or IVIT, imaged one month later, and sacrifice at 2 month timepoint. Injection assessment, *in vivo* fundus imaging, histology and IHC were provided by Dr. Jean Bennett. ISH was carried out as described above.

2.5 Figures

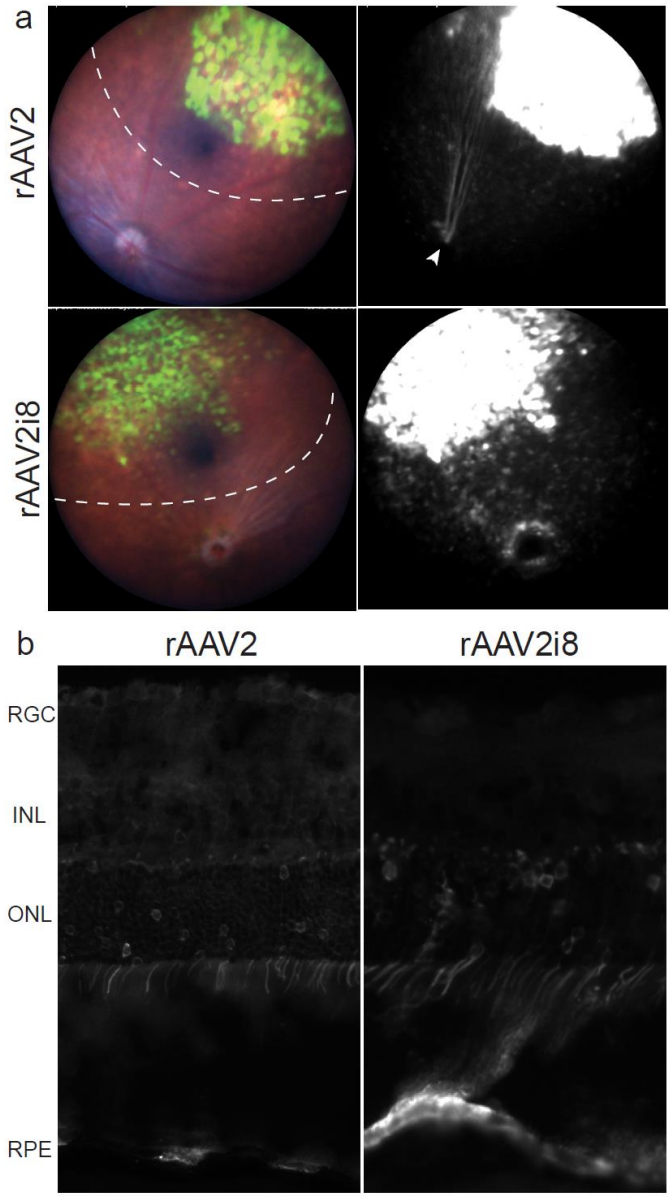

Figure 2.1 GFP fluorescence following subretinal delivery of rAAV2 and HS-deficient rAAV2i8 vector eight weeks post-injection

(a) Images show representative fundus and fluorescence of eyes treated with rAAV2i8 capsid and rAAV2 capsid. Dotted lines indicated detached area of injection. Transduction of ganglion cells can be observed by the GFP axons leading from the injection site to the optic disc in rAAV2-injected eyes (arrowhead). (b) Histology of eyes indicated similar transduction of RPE and ONL between the rAAV2 and its HS deficient rAAV2i8 vector. Scale bar = 20 μm. RGC, retinal ganglion cell layer; INL, inner nuclear layer; ONL, outer nuclear layer.

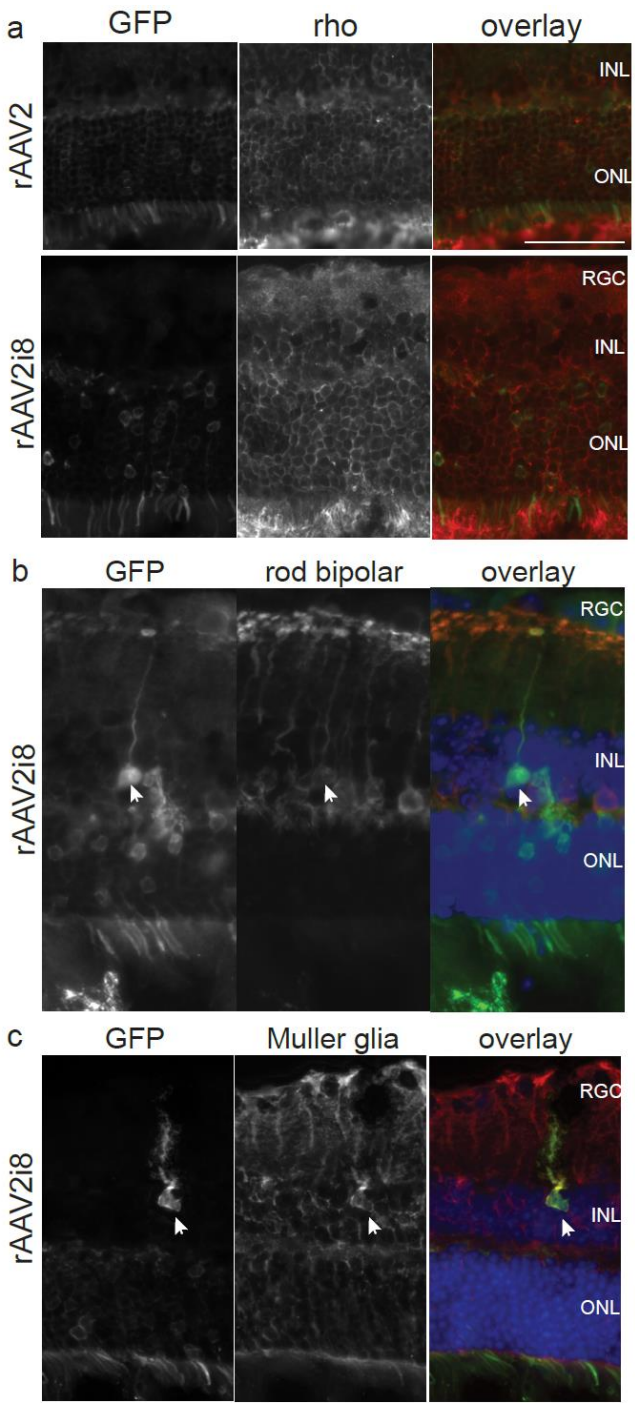

Figure 2.2 IHC of subretinally injected rAAV2i8 and rAAV2 capsids

Both capsids showed most transduction in the ONL and RPE, with fewer transduced cells of the INL and RGC. Staining for rhodopsin indicated that transduction occurred in rods for both rAAV2 and rAAV2i8 capsids. Transduction of rAAV2i8 lead to transduction of (b) rod bipolar cells and (c) Muller glia. Scale bar = 50 um. RGC, retinal ganglion cell layer; INL, inner nuclear layer; ONL, outer nuclear layer.

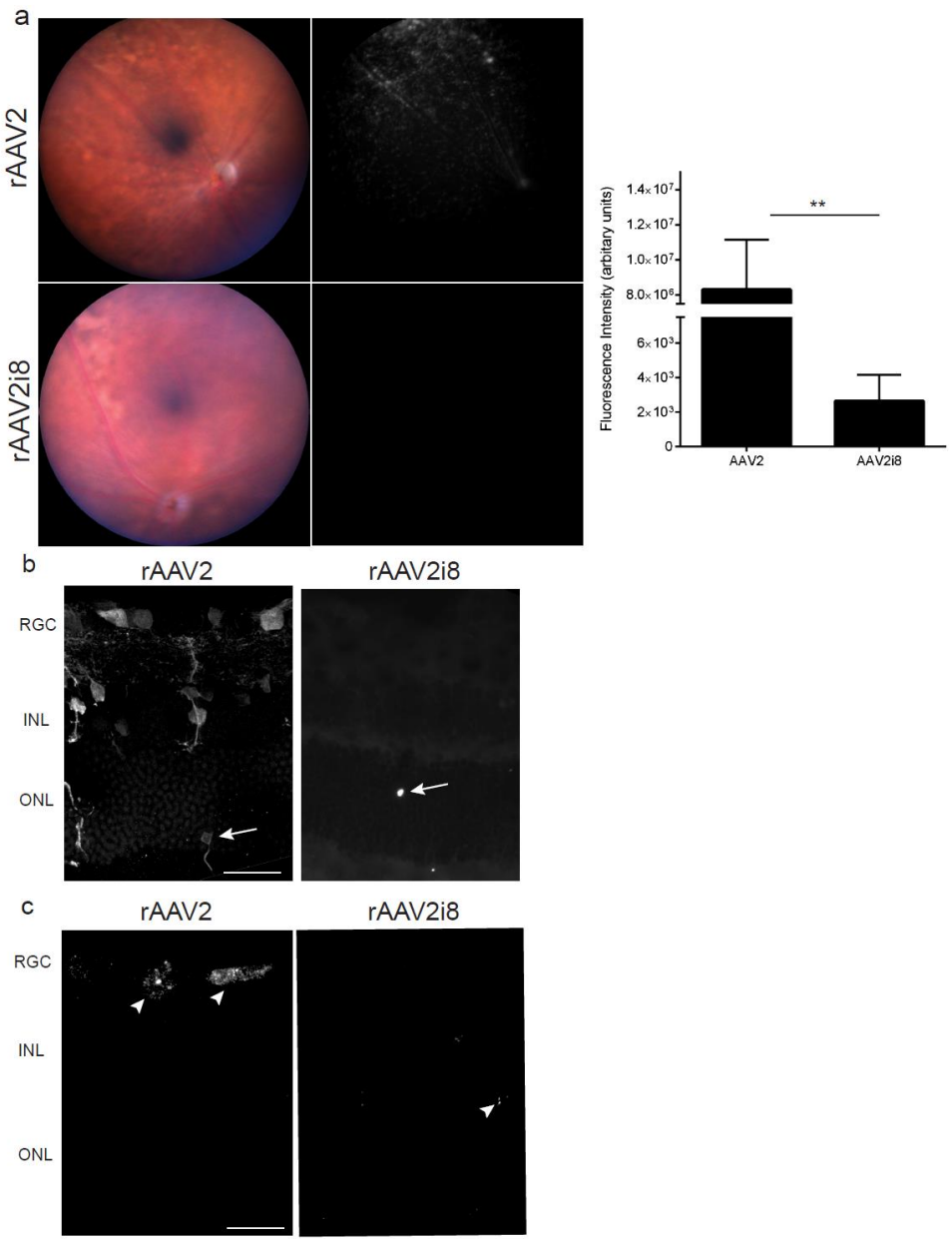

Figure 2.3 GFP fluorescence following intravitreal delivery of rAAV2 vector and its HS-binding deficient variants twelve weeks post-injection

(a) Images show representative fundus and fluorescence of eyes treated with rAAV2 capsid or rAAV2i8 capsid. Quantification of fundus images showed a 300-fold decrease in expression between rAAV2 and rAAV2i8. (b) IHC of rAAV2-injected retinas show fluorescence mainly in the RGC with fewer GFP-positive somas in the INL. Rare transduction of photoreceptors could be observed (arrow). (c) FISH substrate was applied three times to maximize sensitivity and detected the location of transgenes within the retina. Arrowheads highlight GFP transgenes in the retina. Scale bar = 20 μm. RGC, retinal ganglion cell layer; INL, inner nuclear layer; ONL, outer nuclear layer. Graph is shown with error bars indicating the standard error mean (SEM) and significance is detected by a non-parametric t-test (**p<0.01).

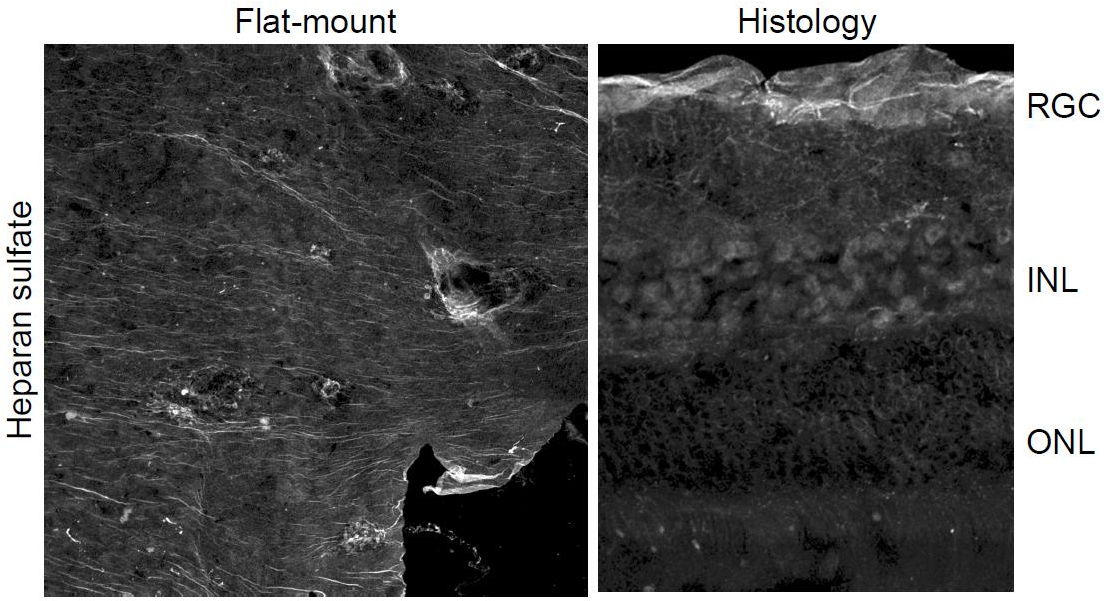

Figure 2.4 HSPG staining of mouse retina viewed by flat-mount and histology.

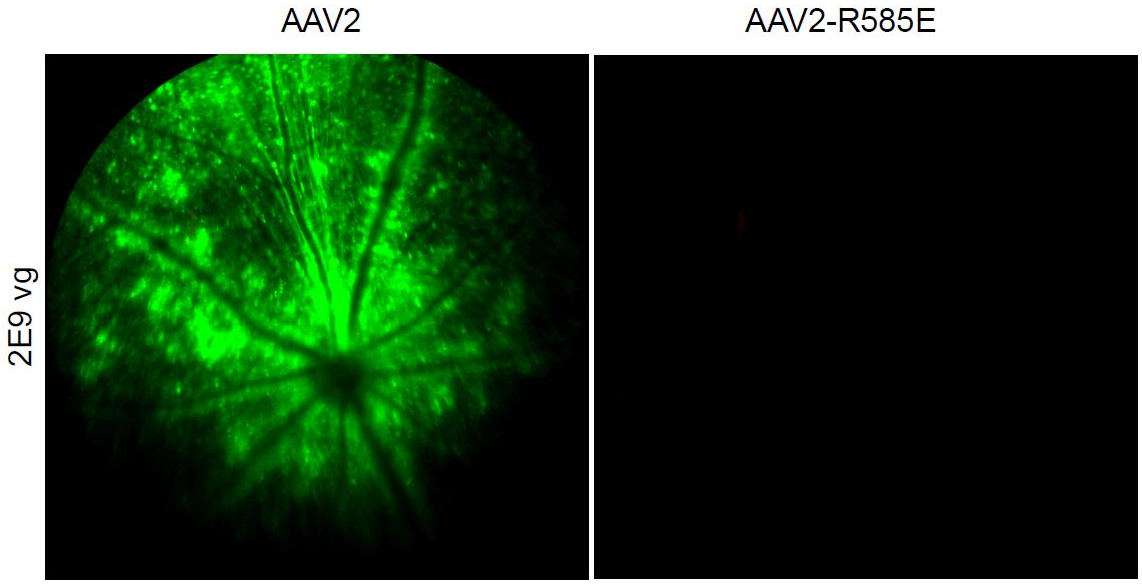

Figure 2.5 Intravitreal delivery of high-titer rAAV2 capsids resulted in transduction only in the presence of HS binding

Fundus images of eyes injected with $2x10^9$ vg rAAV2 or rAAV2-R585E vector were collected at 8 weeks following delivery. Transduction with rAAV2-R58E is absent, but rAAV2 shows a diffuse pattern that does not accumulate in any particular pattern.

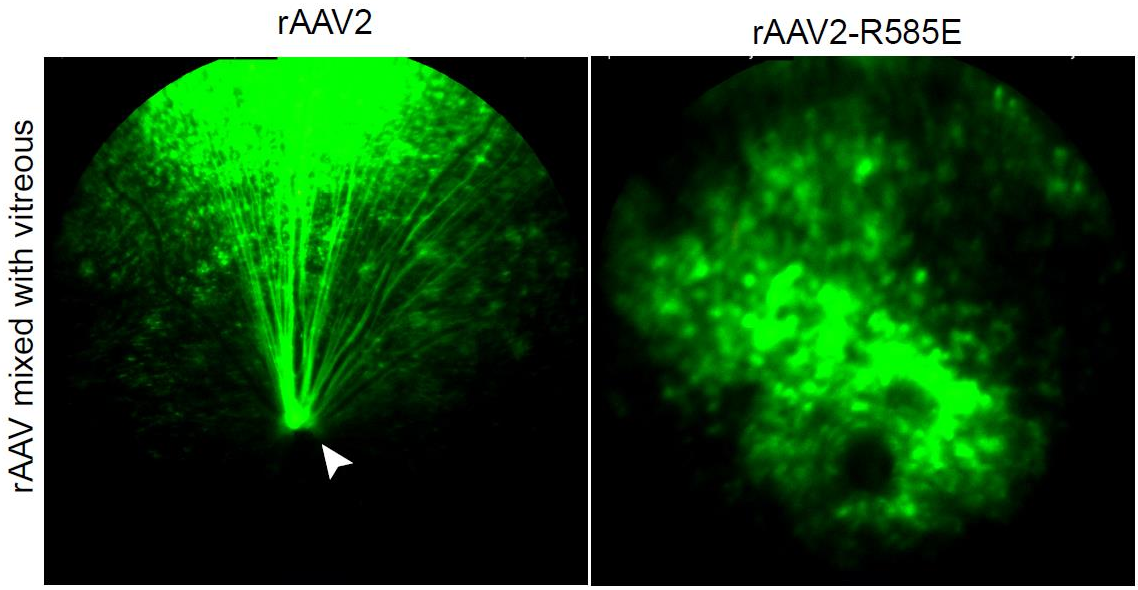

Figure 2.6 Subretinal transduction of rAAV2 capsid variants mixed with vitreous to confirm vitreous did not inhibit transduction

Vector solution was preincubated with equal volume of vitreous collected from mouse eyes for 1 hour before being injected. Transduction of RPE was seen with both rAAV2 and rAAV2-R585E, although the transduction of RGC is evident for rAAV2 by the GFP-positive axons leading to the ONH (arrowhead).

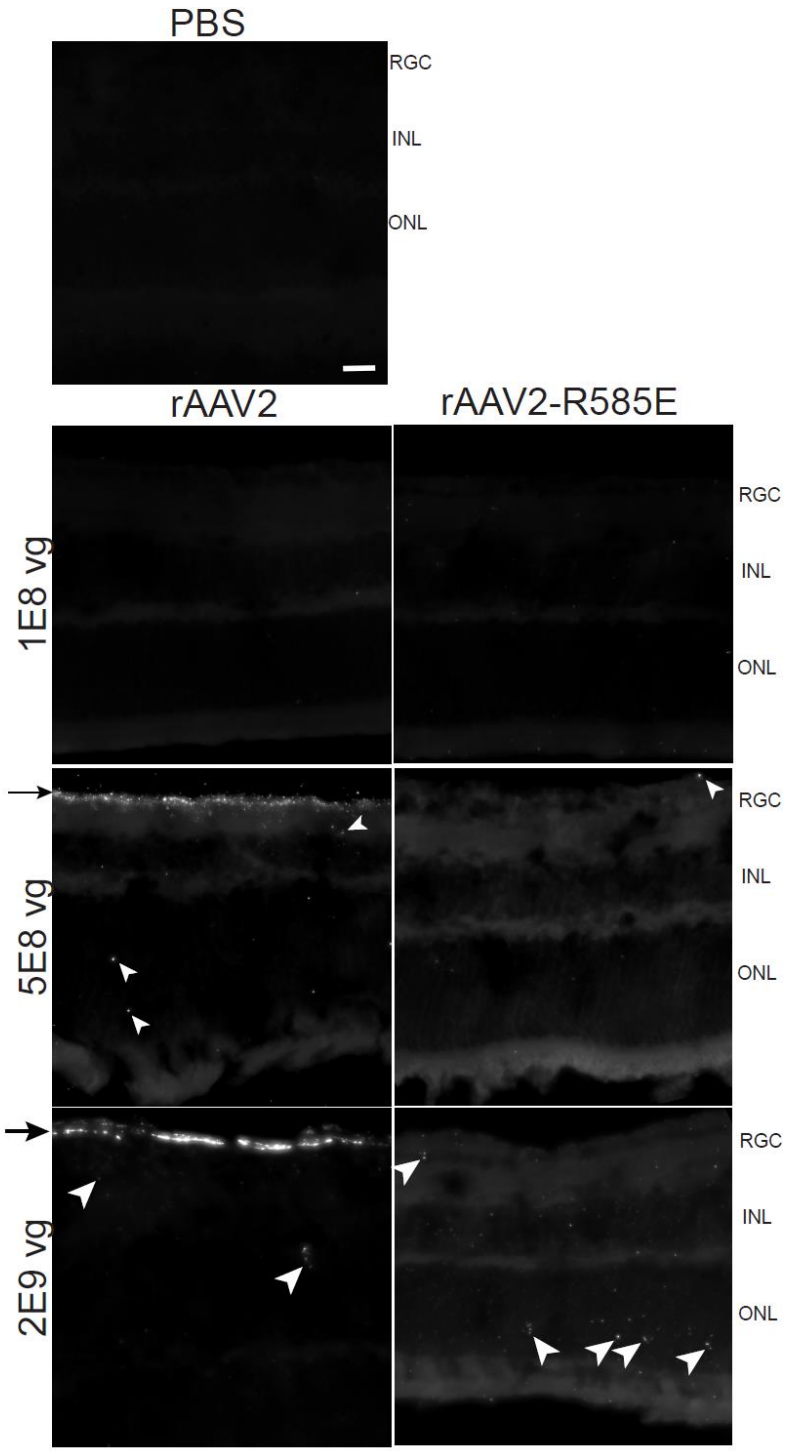

Figure 2.7 FISH of intravitreally injected eyes three days post-injection

PBS-injected eyes served as a negative control for FISH detection and had low background. Arrowheads are used to highlight FISH signal and aggregation at ILM are shown in black arrow. Scale bar = 20 μm. RGC, retinal ganglion cell layer; INL, inner nuclear layer; ONL, outer nuclear layer.

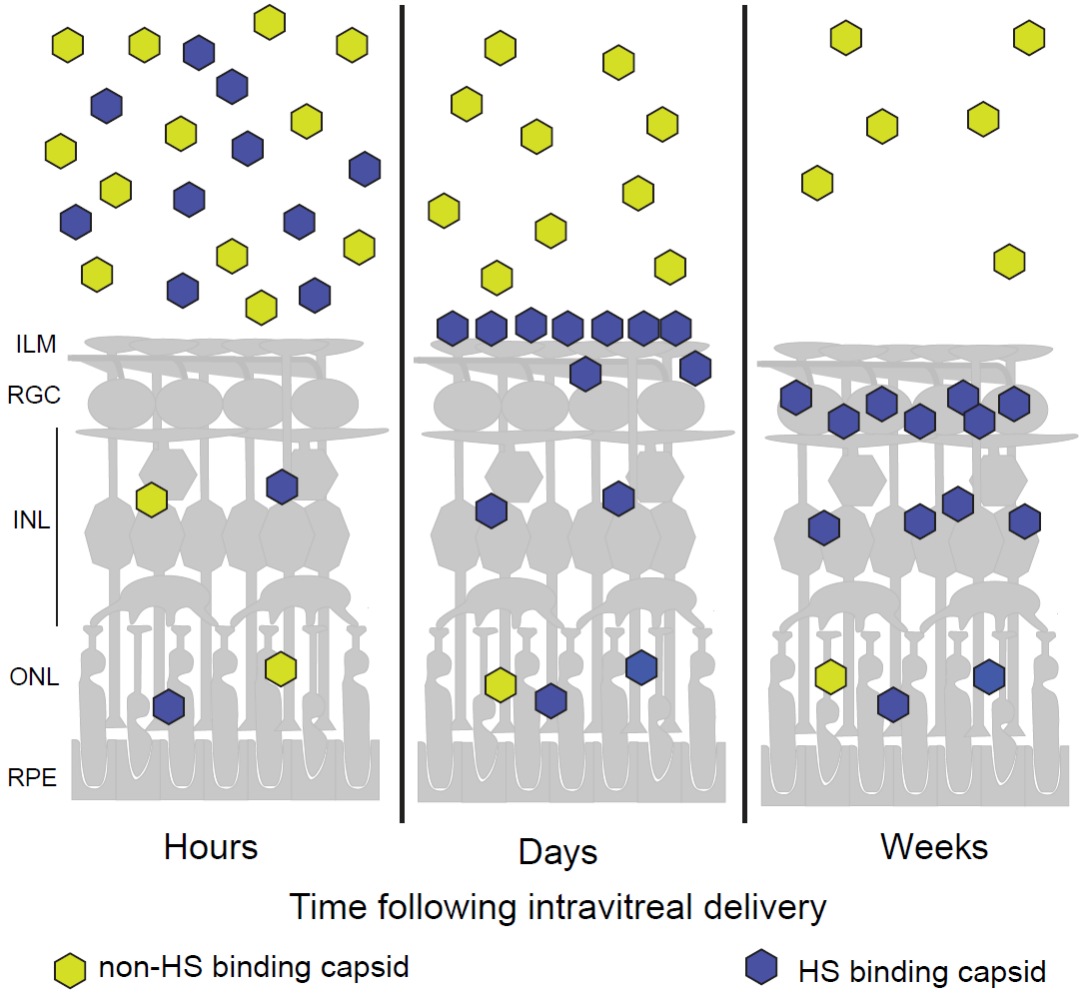

Figure 2.8 Schematic of the binding difference between capsids over time in the retina

The trafficking of IVIT-delivered AAV particles is shown on the retina (gray). Vector can be found in few numbers in the retina soon after delivery regardless of HS binding. Over time, the HS-binding vectors (blue) accumulate at the ILM to further penetrate the retina whereas non-HS-binding capsids (yellow) remain mostly in the vitreous. HS, heparan sulfate; ILM, inner limiting membrane; RGC, retinal ganglion cells; INL, inner nuclear layer; ONL, outer nuclear layer; RPE, retinal pigment epithelium.

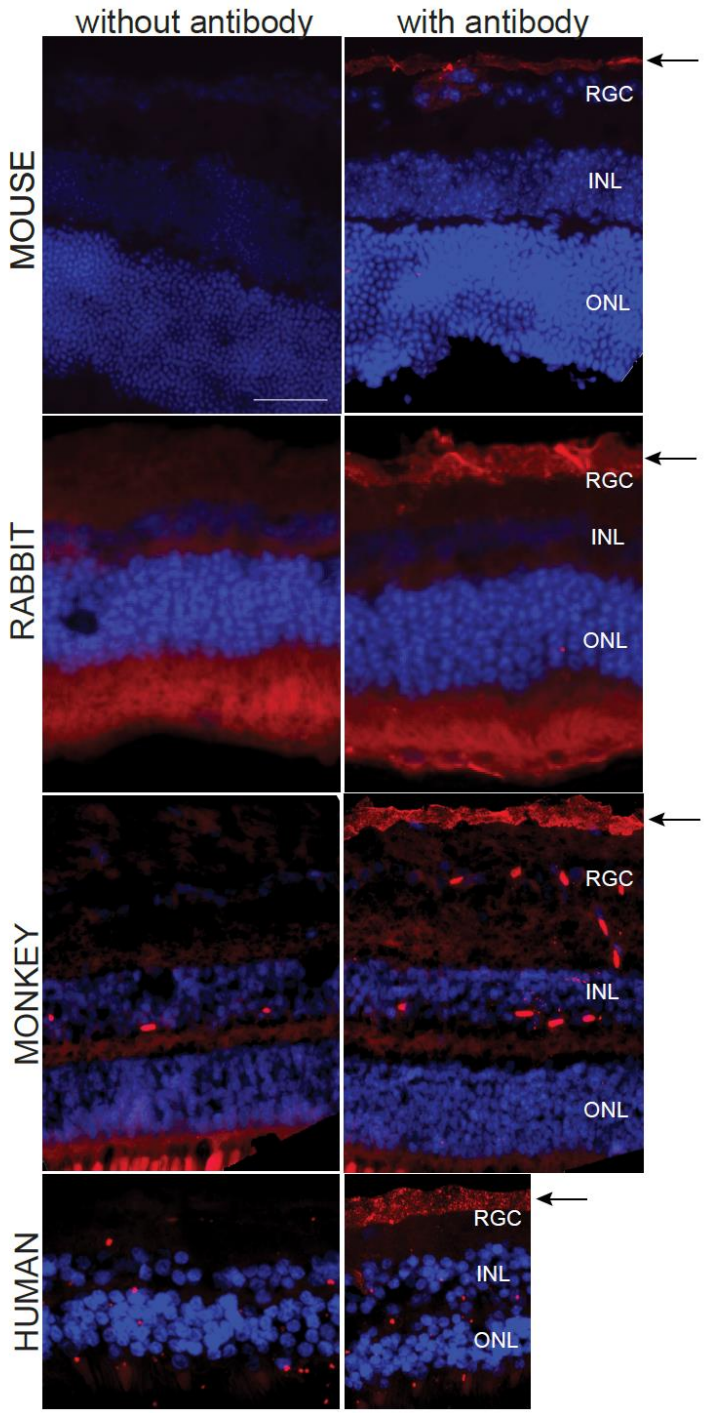

Figure 2.9 Staining of HS in the retinas of multiple animal models.

Retinas of mouse, rabbit, non-human primate, and human are shown. Each animal retina has been stained with secondary antibody only (without antibody) and with an antibody specific to HSPG (with antibody). Intense staining is seen at the ILM in all animal species and is not present in the negative control. Scale bar = 50 μm. RGC, retinal ganglion cell layer; INL, inner nuclear layer; ONL, outer nuclear layer.

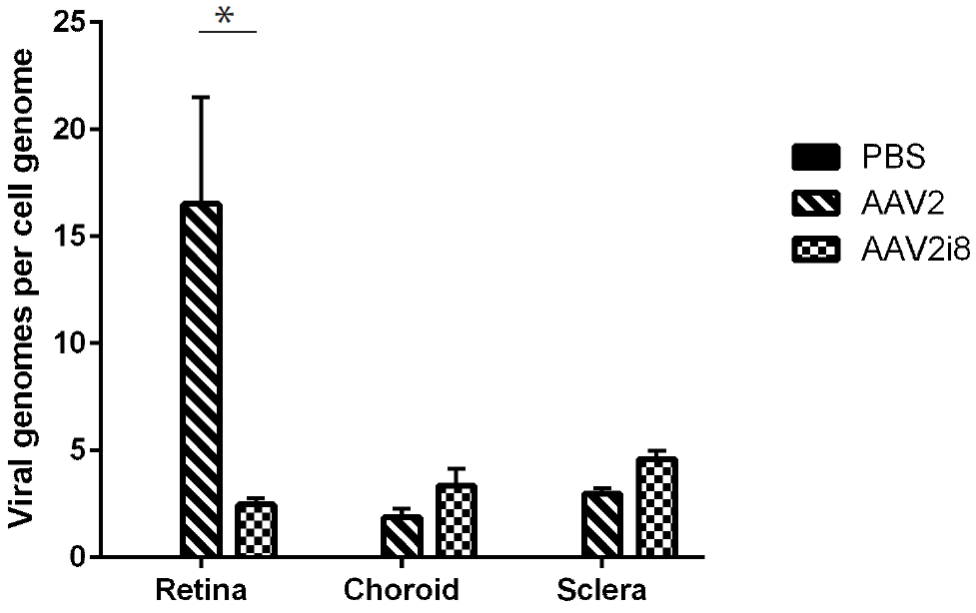

Figure 2.10 qPCR analysis of viral binding to human retinas *ex vivo.*

Results are quantified as vector genomes per cell genome. rAAV2 vector shows the greatest presence at the retina with few transgenes found elsewhere. The presence of transgenes delivered by rAAV2i8 were low in all collected tissues but showed a significant increase compared to rAAV2-delivered transgenes in both the choroid and sclera. Error bars indicated standard deviation.

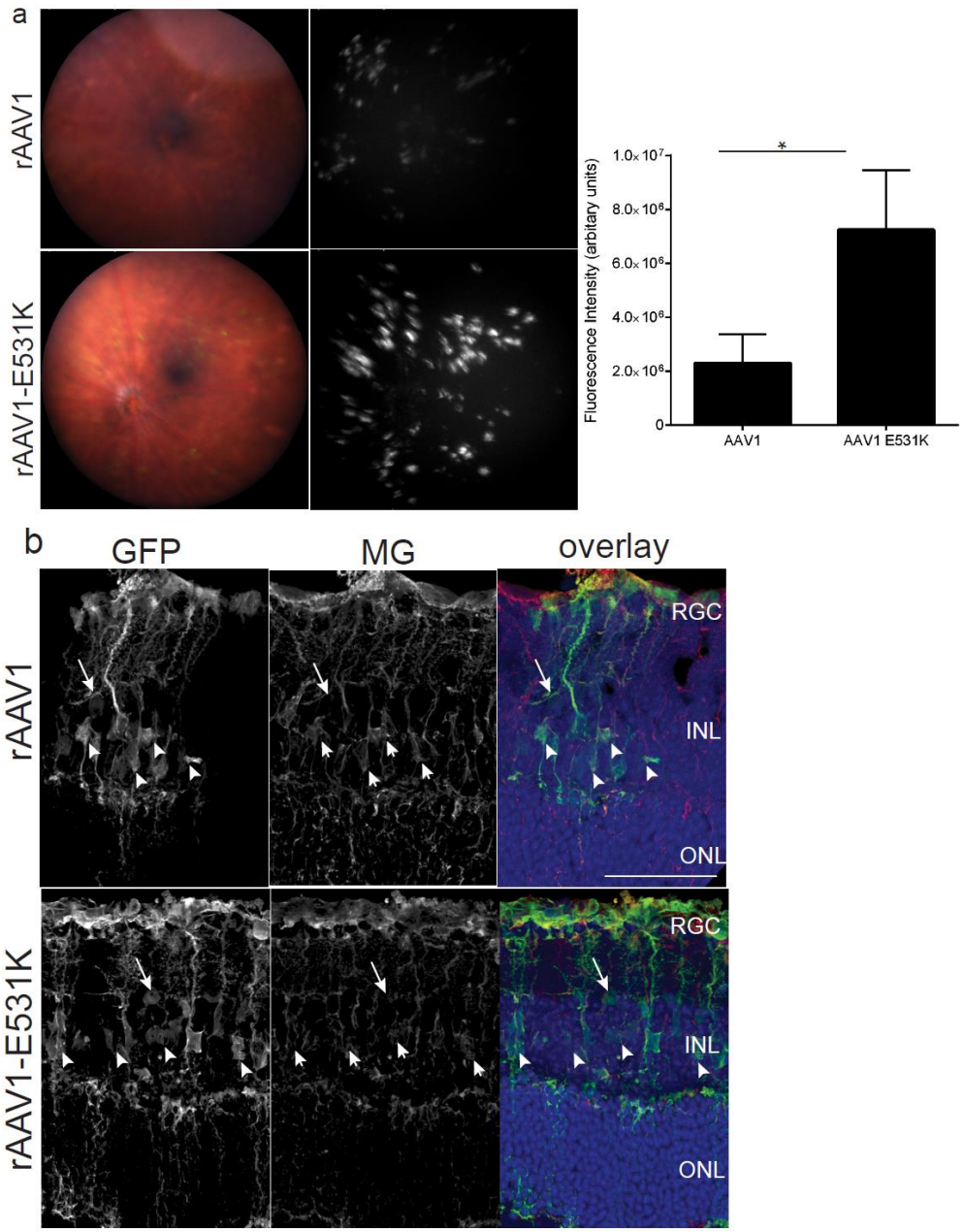

Figure 2.11 GFP fluorescence following IVIT delivery of HS-binding variants of rAAV1 eight weeks post-injection.

(a) Images show representative fundus and fluorescence of eyes treated with rAAV1 capsid or rAAV1-E531K capsid. Quantification of fundus images shows a 3-fold increase with rAAV1-E531K capsid compared to rAAV1 capsid. (b) GFP IHC of retinal sections eight weeks after injection of rAAV1 and rAAV1-E531K capsids. Images show the co-localization with Müller glia (arrowheads) and non-Müller glia (arrows). Confocal z-stack images were compressed and displayed as the maximum projection. Scale bar = 50μm. RGC, retinal ganglion cell layer; INL, inner nuclear layer; ONL, outer nuclear layer. Graph is shown with error bars indicating the SEM and significance by a non-parametric t-test (*p<0.05).

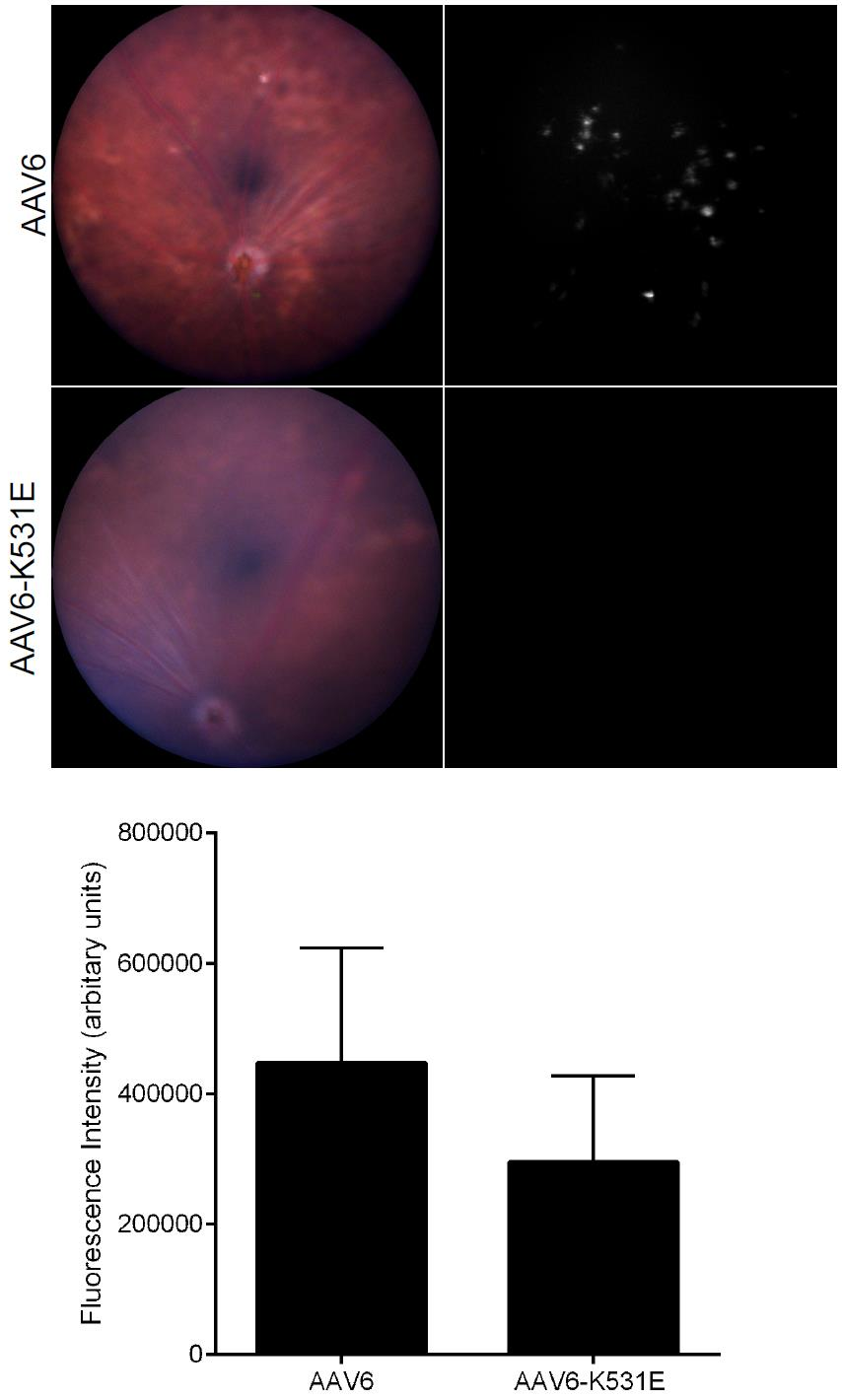

Figure 2.12 Analyses of HS-binding variants of rAAV6 eight weeks after IVIT delivery.

Images show typical fundus and fluorescence of eyes treated with rAAV6 capsid or rAAV6-K531E capsid at a low titer of $5x10^7$ vg. Punctate expression around the retinal vessels could only be seen in eyes injected with rAAV6. Quantification of fundus images did not indicate significance.

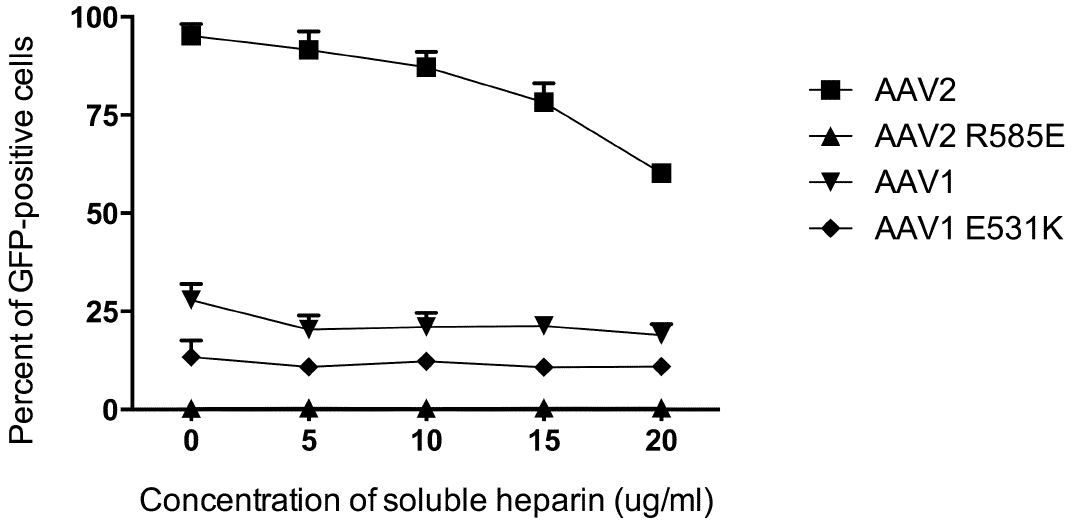

Figure 2.13 *In vitro* competition assay using soluble heparin to block the transduction of rAAV of HEK293 cells.

Viruses were incubated with increasing doses of soluble heparin and applied to cell culture at a multiplicity of infection of 10,000 vg per cell. rAAV2 displayed a dose-dependent decrease in transduction which was not observed with either rAAV1 or rAAV1-E531K. The amount of transduction of rAAV1-E531K was lower than rAAV1 in all conditions. Error bars shown as SEM.

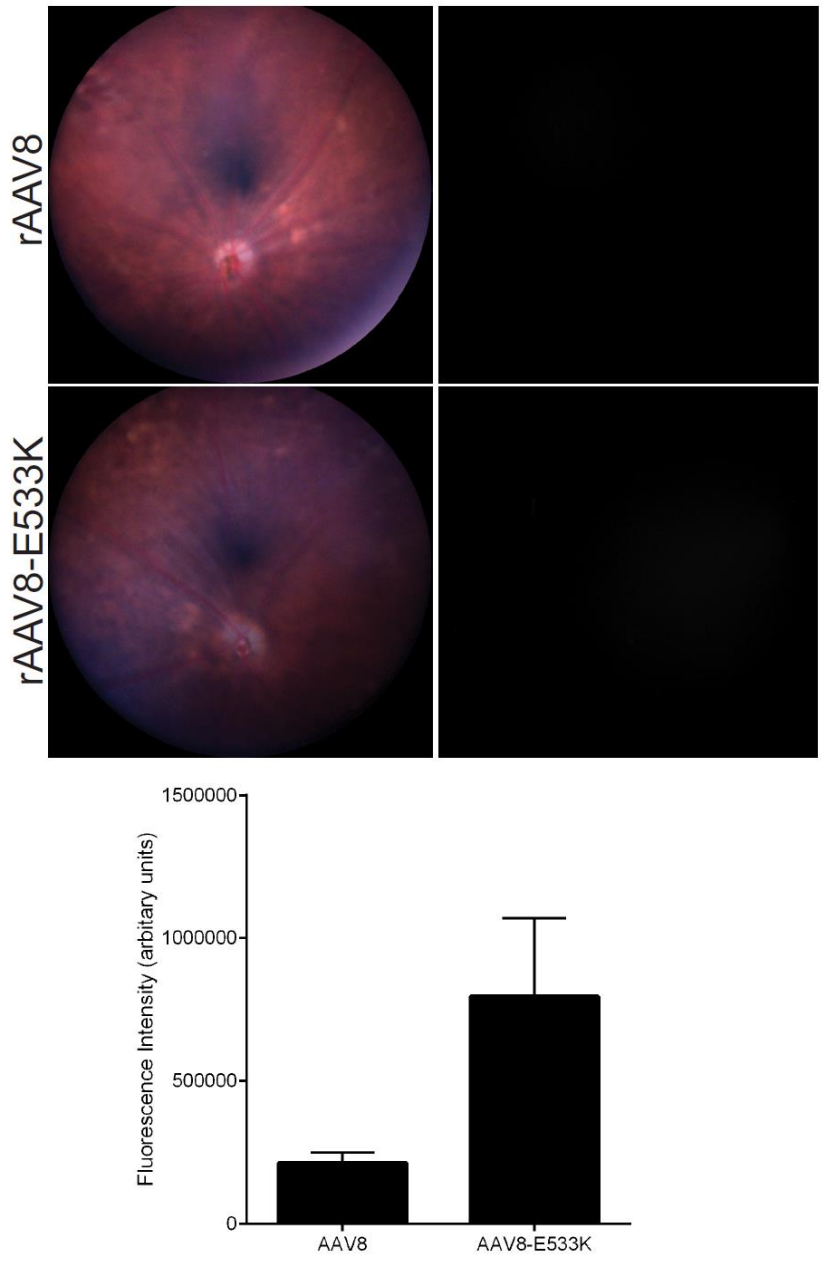

Figure 2.14 Analyses of HS-binding variants of rAAV8 eight weeks after IVIT delivery.

Images show typical fundus and fluorescence of eyes treated with rAAV8 capsid or rAAV8-E533K capsid at a titer of $1x10^8$ vg. Hazy expression could only be detected with HS-binding rAAV8-E533K capsid. Quantification of fundus images show error bars as the SEM and trend toward significance ($p<0.055$).

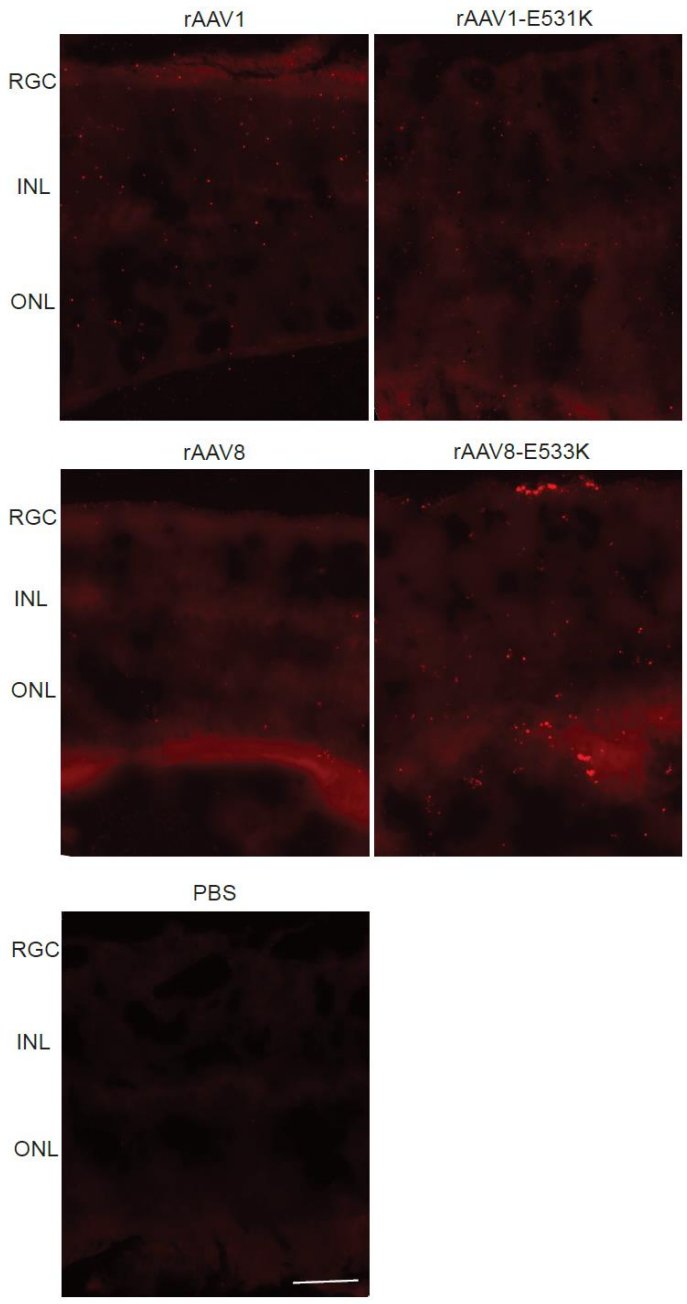

Figure 2.15 FISH detection of retinas injected with AAV serotypes and their HS-binding mutants three days after injection.

The detection reaction was carried out twice and image levels were adjusted equally to enhance weak labeling. Transgenes found in the retina were more abundant with eyes injected with the HS-binding motif compared to their natural serotypes. rAAV8-E533K capsid could be seen accumulating at the ILM in addition to its presence in the retina. PBS-injected retinas had minimal background signal. Scale bar = 20 µm. RGC, retinal ganglion cell layer; INL, inner nuclear layer; ONL, outer nuclear layer.

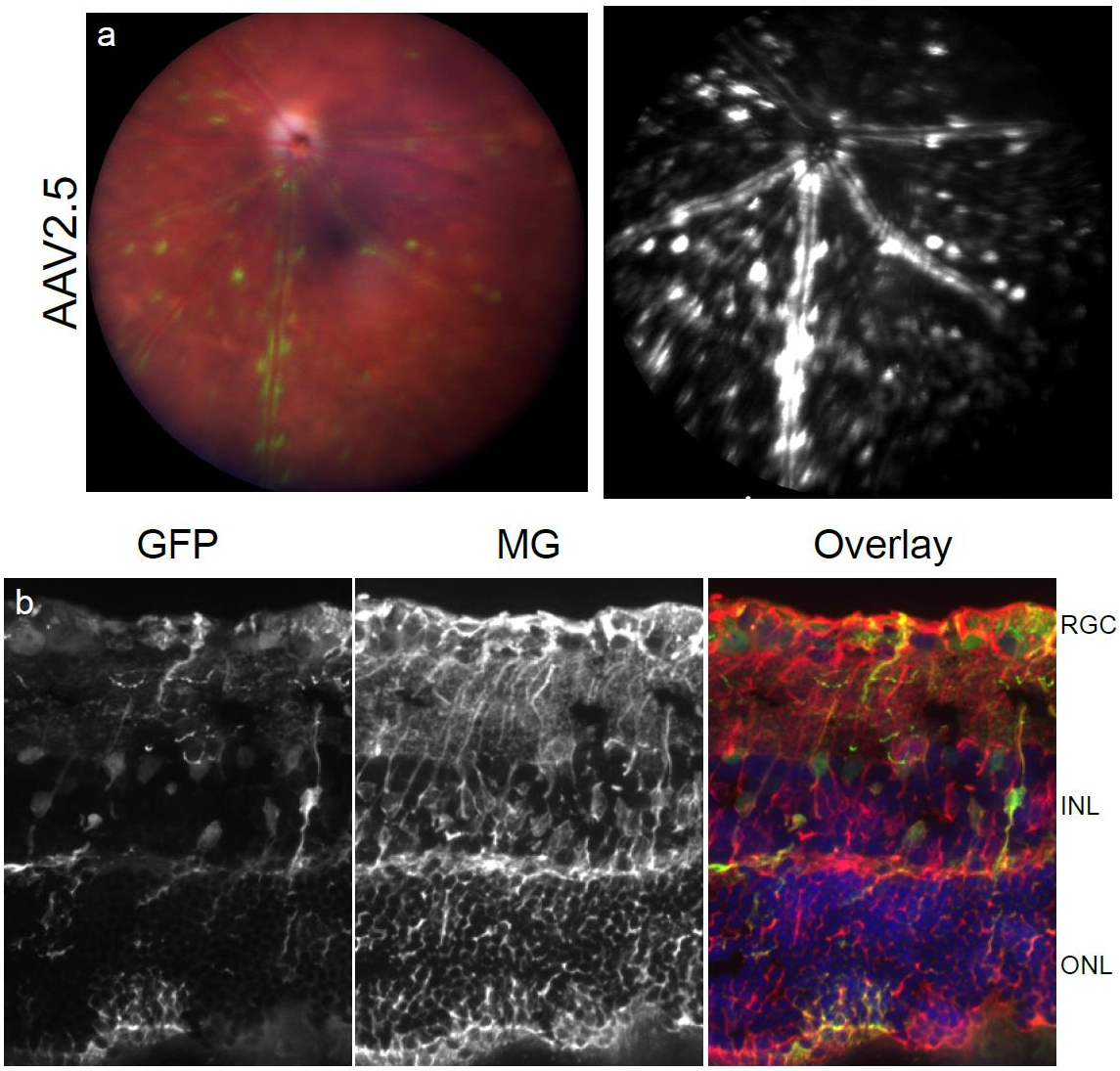

Figure 2.16 Transduction of rAAV2.5 in mouse retina

MG, Muller glia; RGC, retinal ganglion cells; INL, inner nuclear layer; ONL, outer nuclear layer.

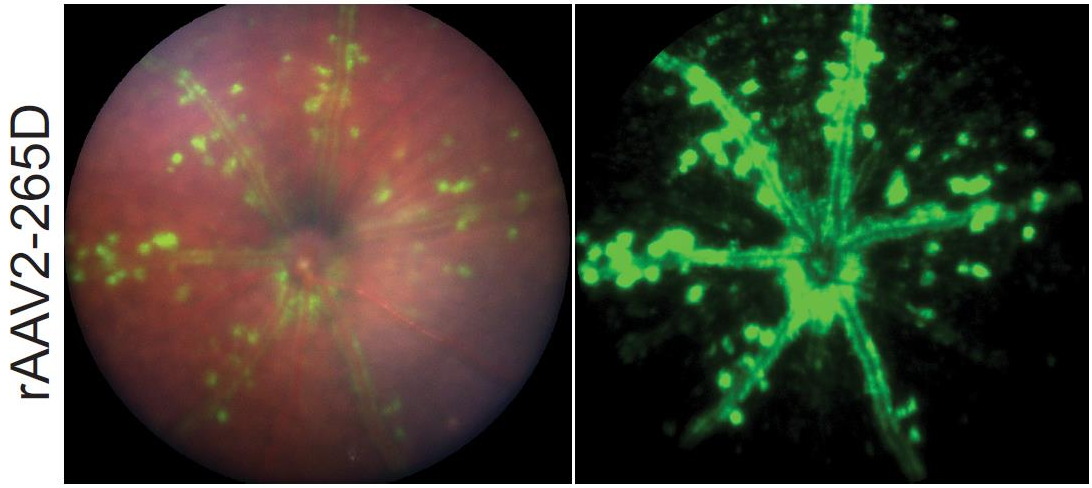

Figure 2.17 Transduction pattern of rAAV2.5 is recapitulated using a single point mutant rAAV2-265D

Fundus bright field (left) and GFP (right) are shown 8 weeks after IVIT delivery to an adult mouse. GFP fluorescence can been prominently seen around the retinal vessels with punctate spots of expression seen surrounding the vessel.

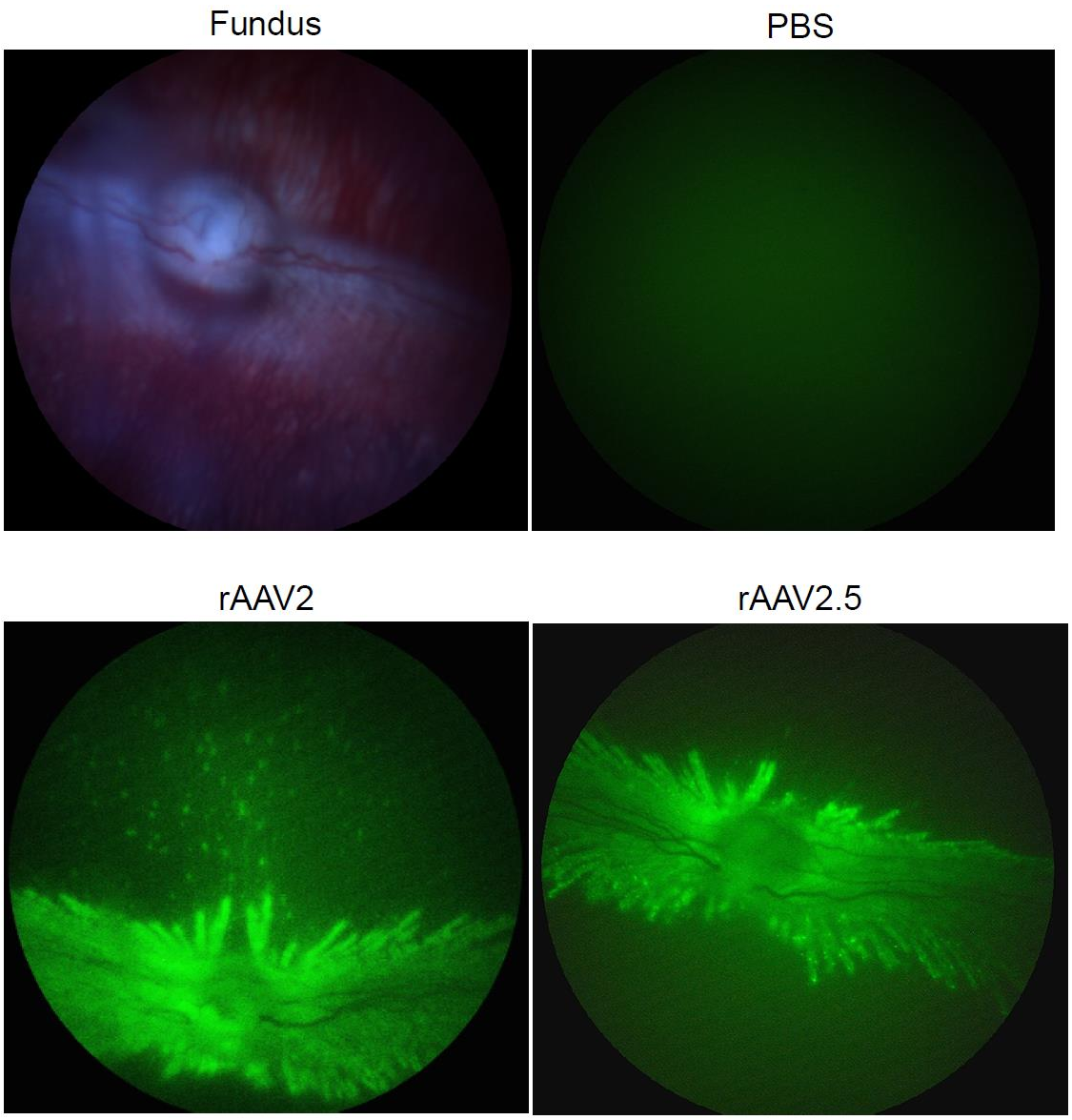

Figure 2.18 Transduction of rAAV2 and rAAV2.5 IVIT in rabbits

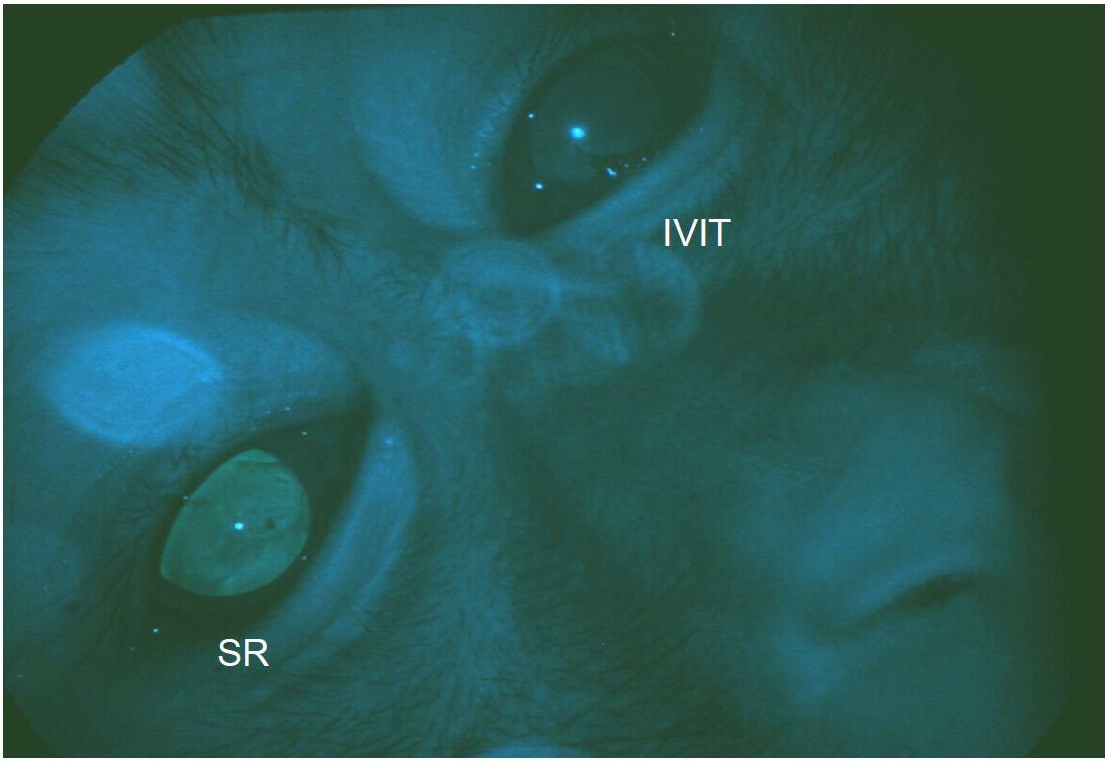

Figure 2.19 Fundoscopy of NHP eyes injected by either SR or IVIT injection of rAAV2.5

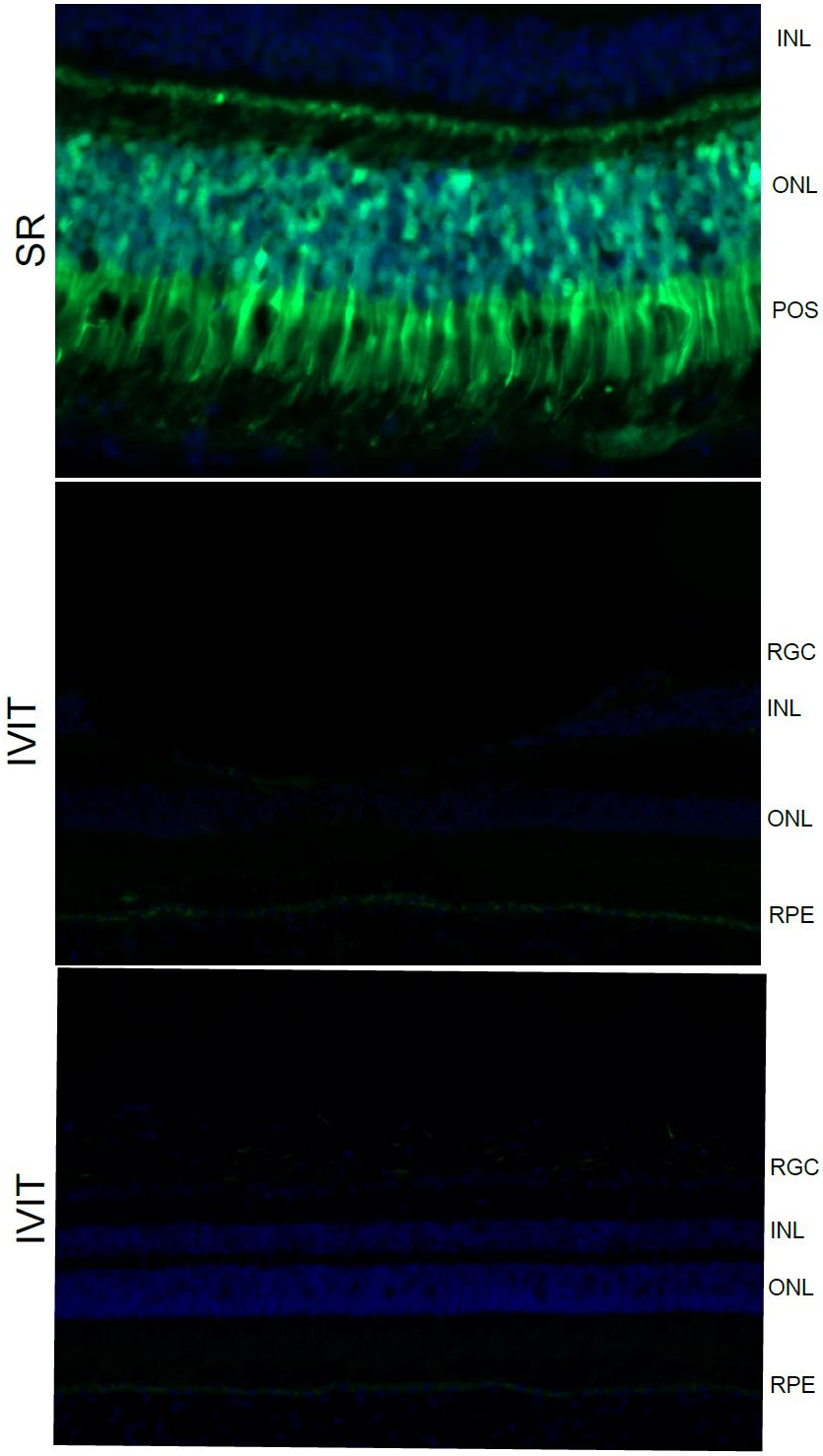

Figure 2.20 IHC of NHP retinal tissue following rAAV2.5 delivery

SR, subretinal; IVIT, intravitreal; INL, inner nuclear layer; ONL, outer nuclear layer; POS, photoreceptor outer segment; RGC, retinal ganglion cell; RPE, retinal pigment epithelium.

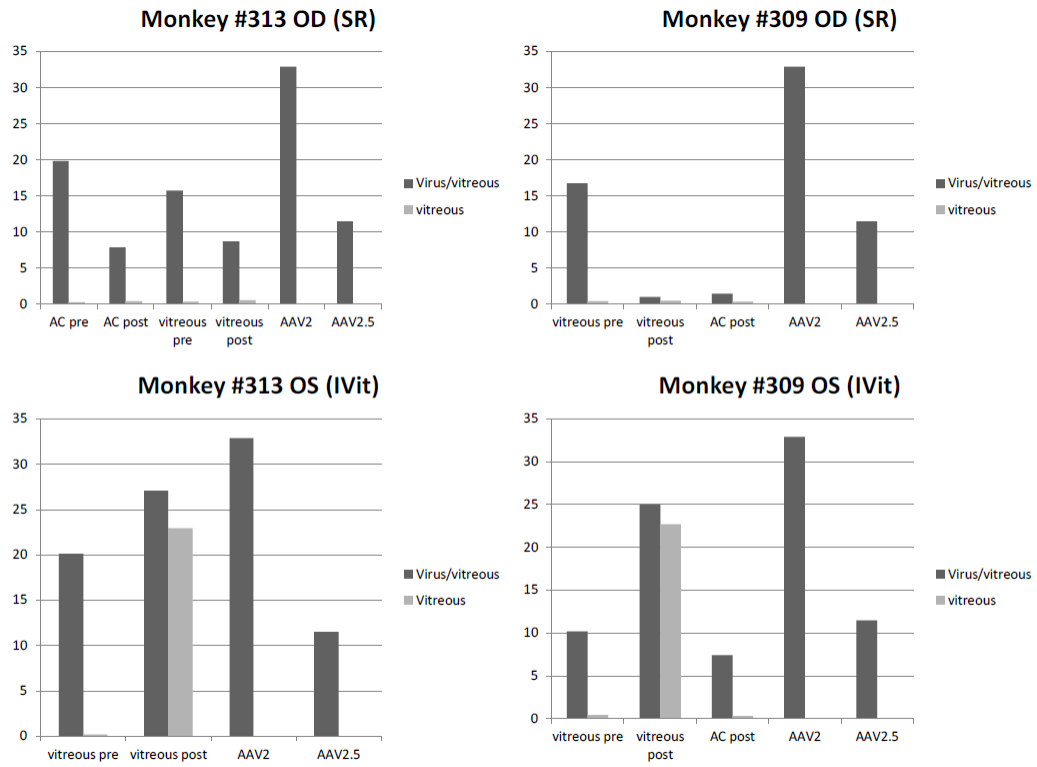

Figure 2.21 Infectious rAAV2.5 remains in the vitreous of NHP at least two months after IVIT injection

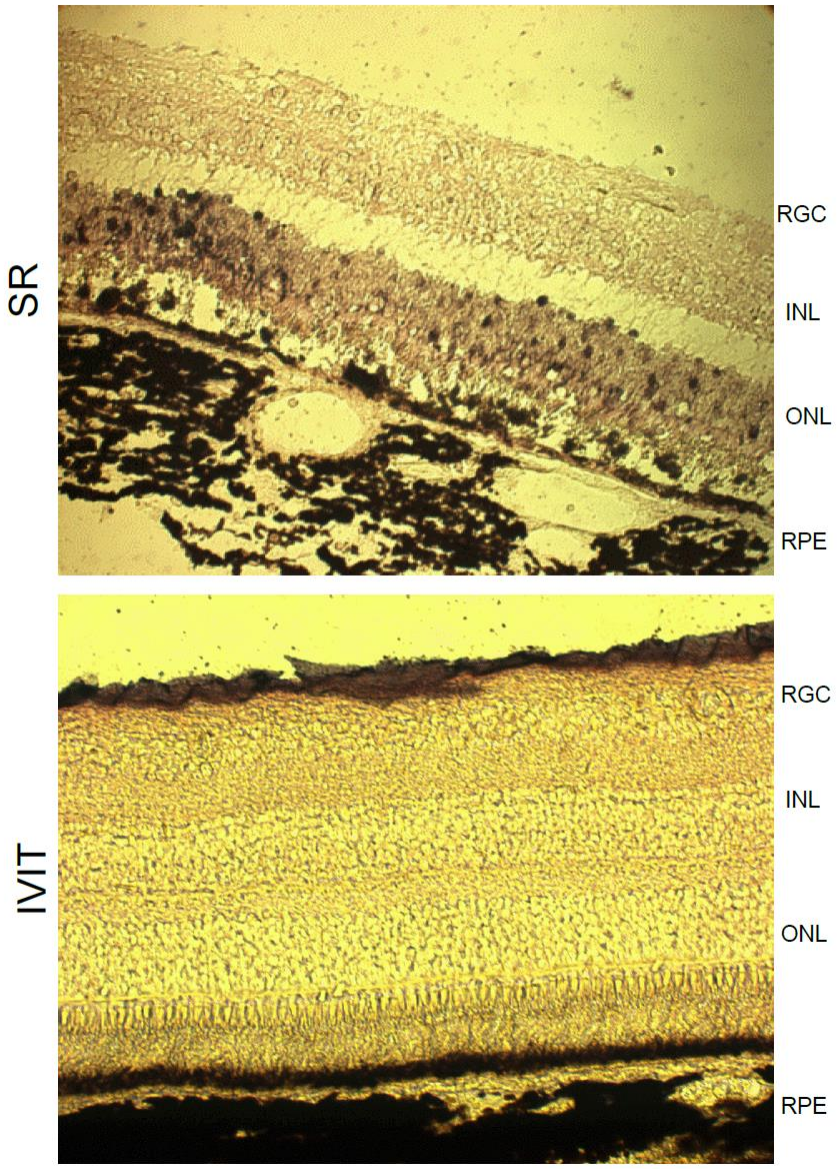

Figure 2.22 ISH on NHP retinas injected with rAAV2.5 by either SR or IVIT delivery

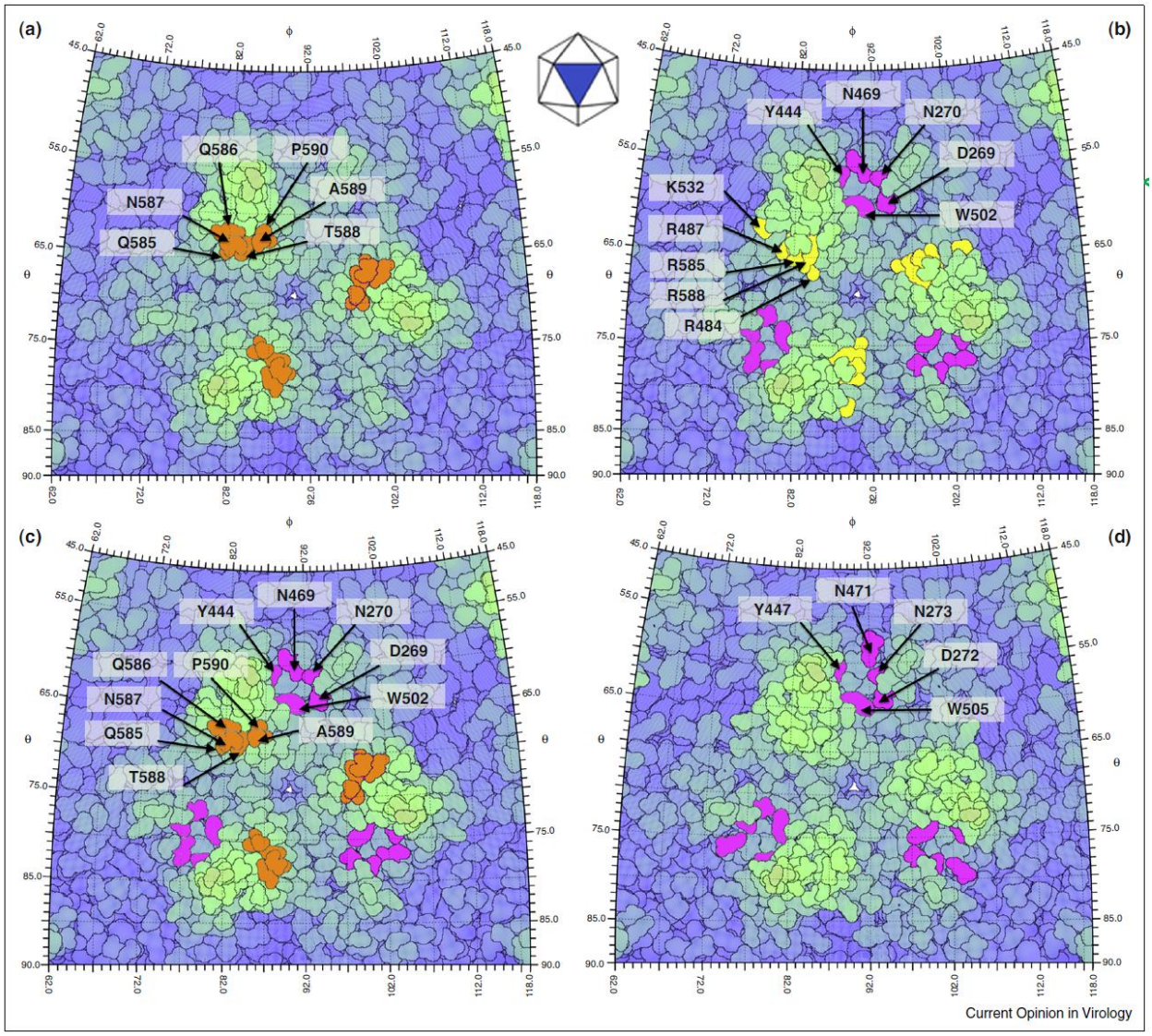

Figure 2.23 Stereographic Roadmap projections of engineered glycan receptor footprints as viewed down the threefold symmetry axis on different lab-derived, synthetic AAV strains.

The threefold symmetry axis is shown in the cartoon inset. Only surface exposed amino acids are shown, with each residue boundary depicted in black. The green regions depict the spikes on the threefold surface, while the blue regions represent the surrounding depressions. (a) Residues colored in orange depict engineered residues on AAV2i8; (b) yellow residues depict the HS footprint and pink residues depict the GAL footprint engineered on the dual glycan binding AAV2g9 strain; (c) pink residues depict the GAL footprint engineered onto AAV2i8 to generate AAV2i8g9; and (d) pink residues depict GAL footprint engineered on AAV8g9. Reprinted from *Current Opinion in Virology, Vol 18, V.J. Madigan and A. Asokan, Engineering AAV receptor footprints for gene therapy, 89-96, 2016* with permission from Elsevier.

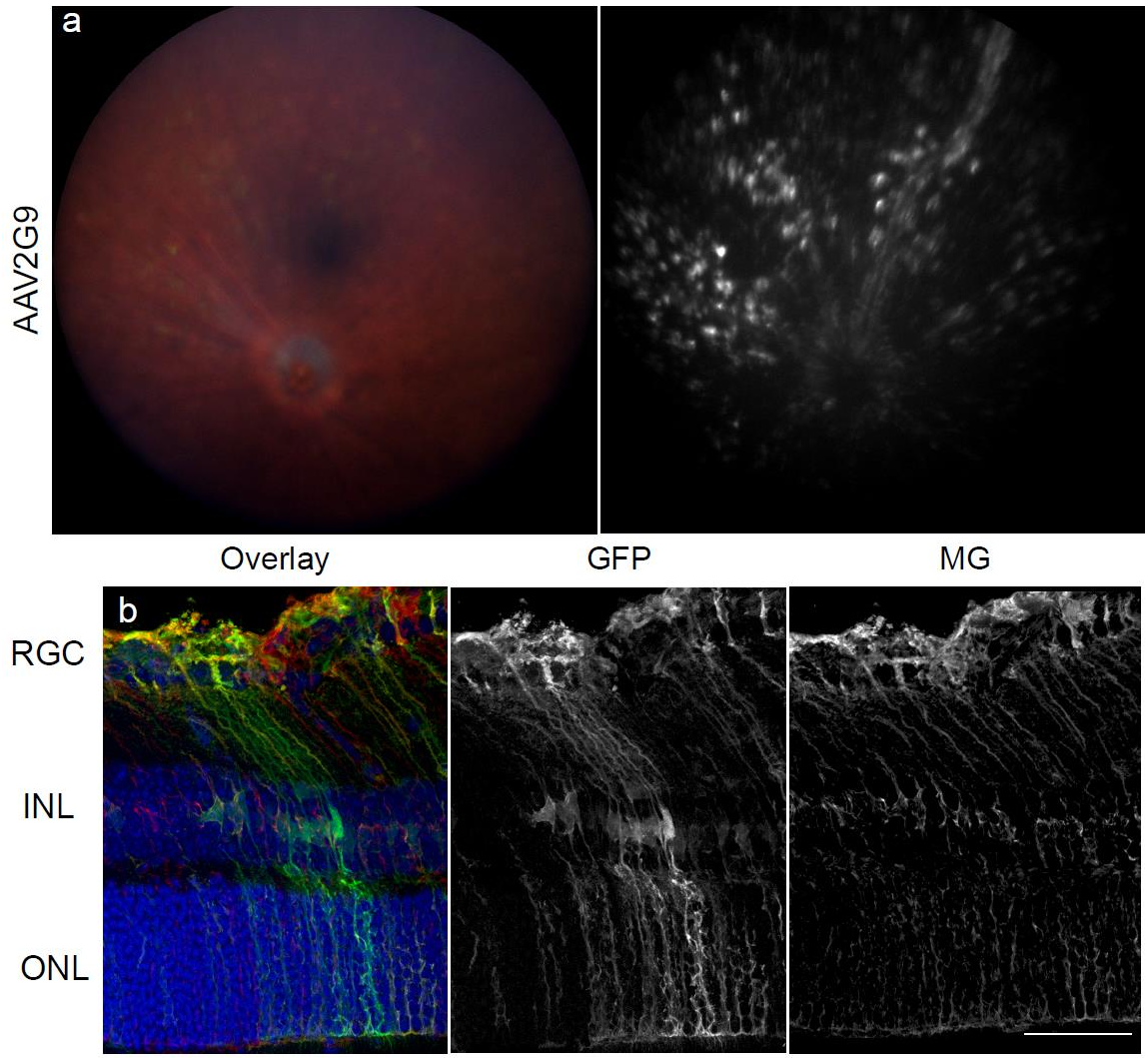

Figure 2.24 rAAV2G9 transduction of the mouse retina.

RGC, retinal ganglion cells; INL, inner nuclear layer; ONL, outer nuclear layer.

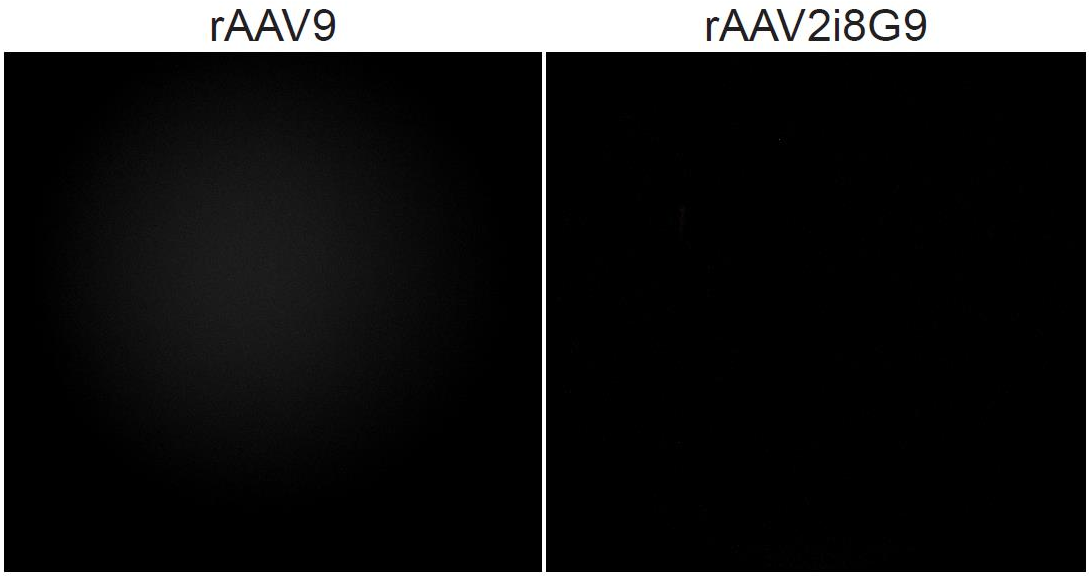

Figure 2.25 Fundus images of adult mice eight weeks after IVIT delivery of galactose-only binding capsids

GFP fluorescence is shown in grayscale.

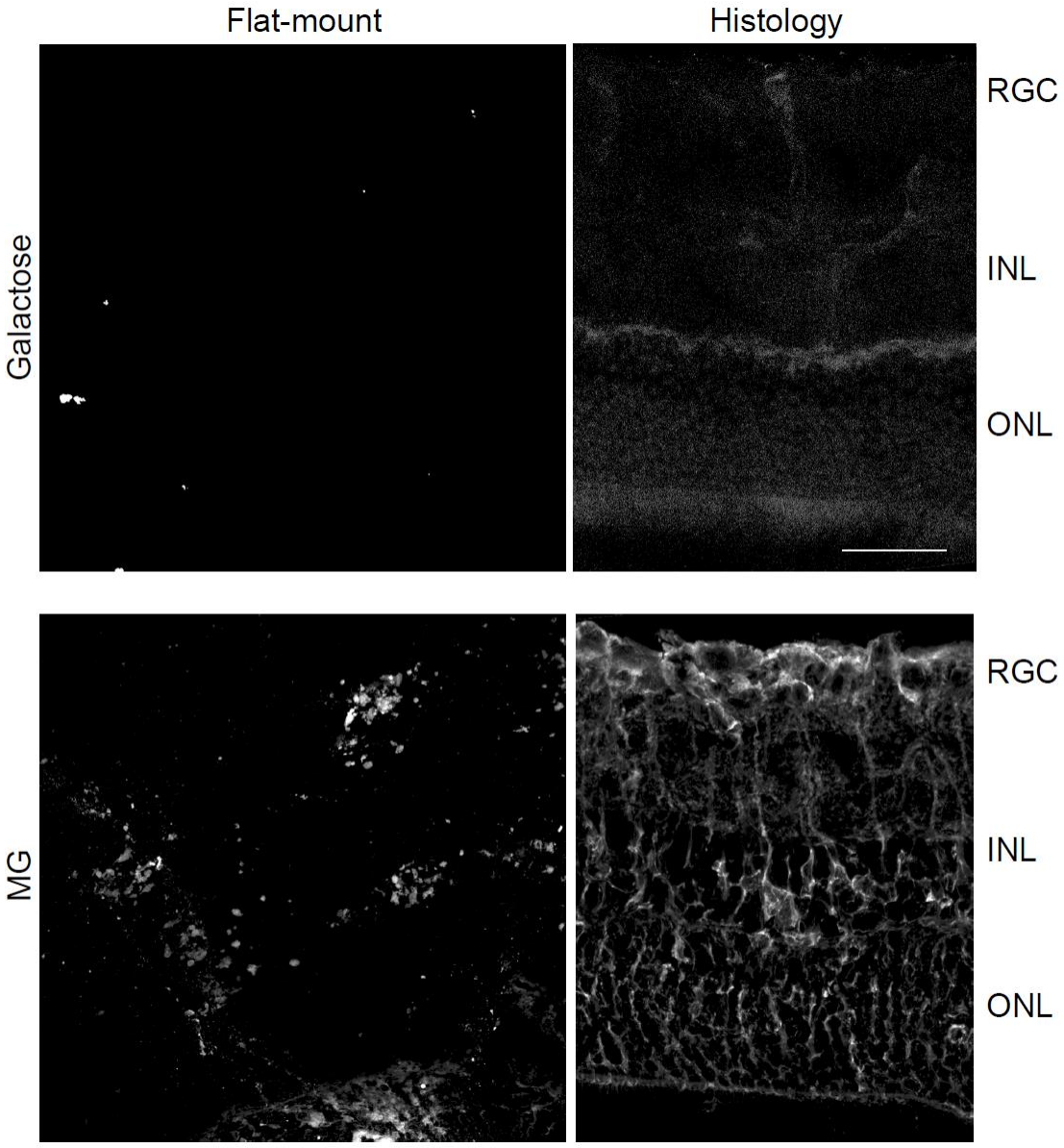

Figure 2.26 Galactose staining does not appear correlated to Müller glia

MG, Muller glia; RGC, retinal ganglion cells; INL, inner nuclear layer; ONL, outer nuclear layer.

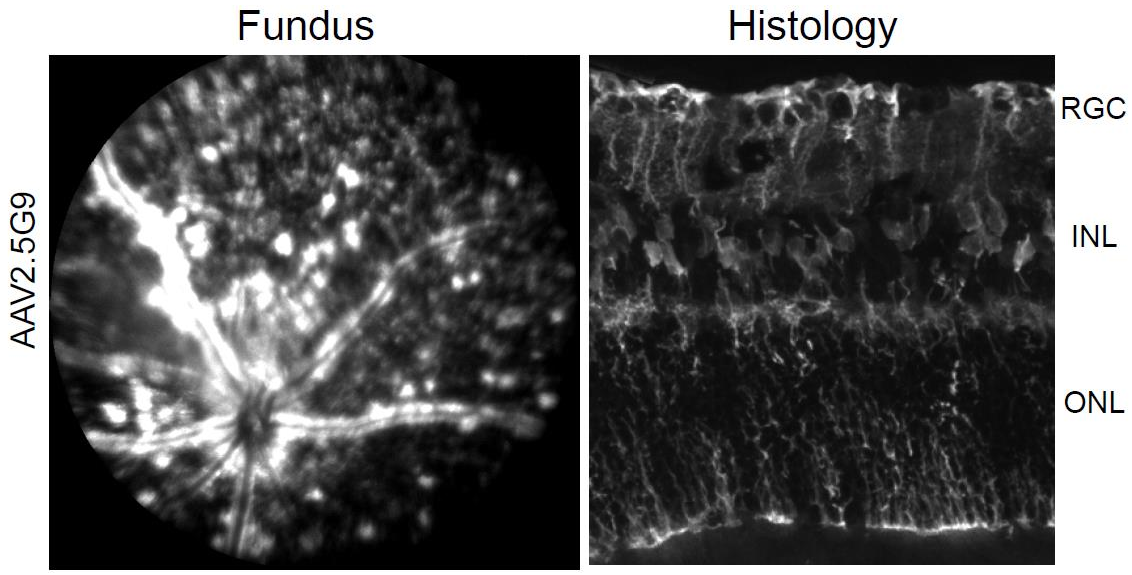

Figure 2.27 GFP fluorescence of mouse eyes eight weeks after IVIT injection with rAAV2.5G9

GFP fluorescence is shown in grayscale. Fundus images show the prominent transduction around the retinal vessels. Additional punctate fluorescence can be seen around the retina. On histology, this pattern correlated to Muller glia-specific transduction. RGC, retinal ganglion cells; INL, inner nuclear layer; ONL, outer nuclear layer.

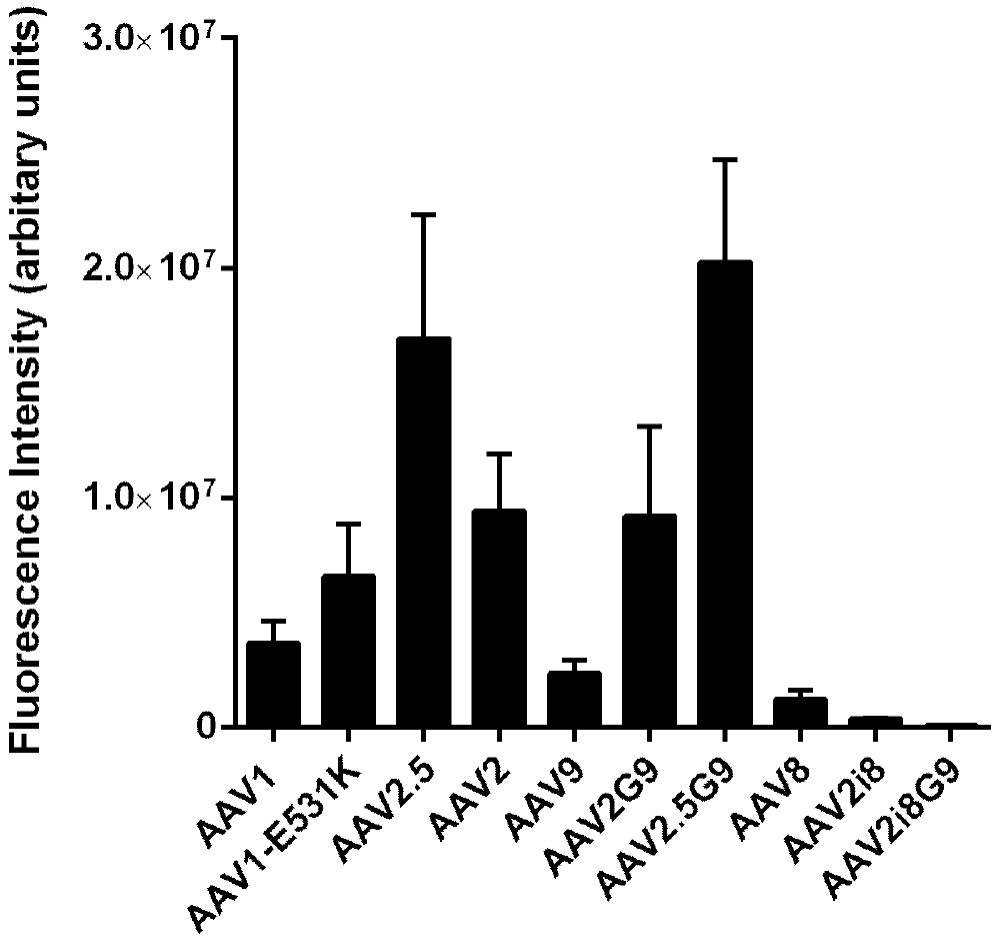

Figure 2.28 Quantification of retinal transduction following IVIT delivery of various AAV capsids

Error bars show SEM.

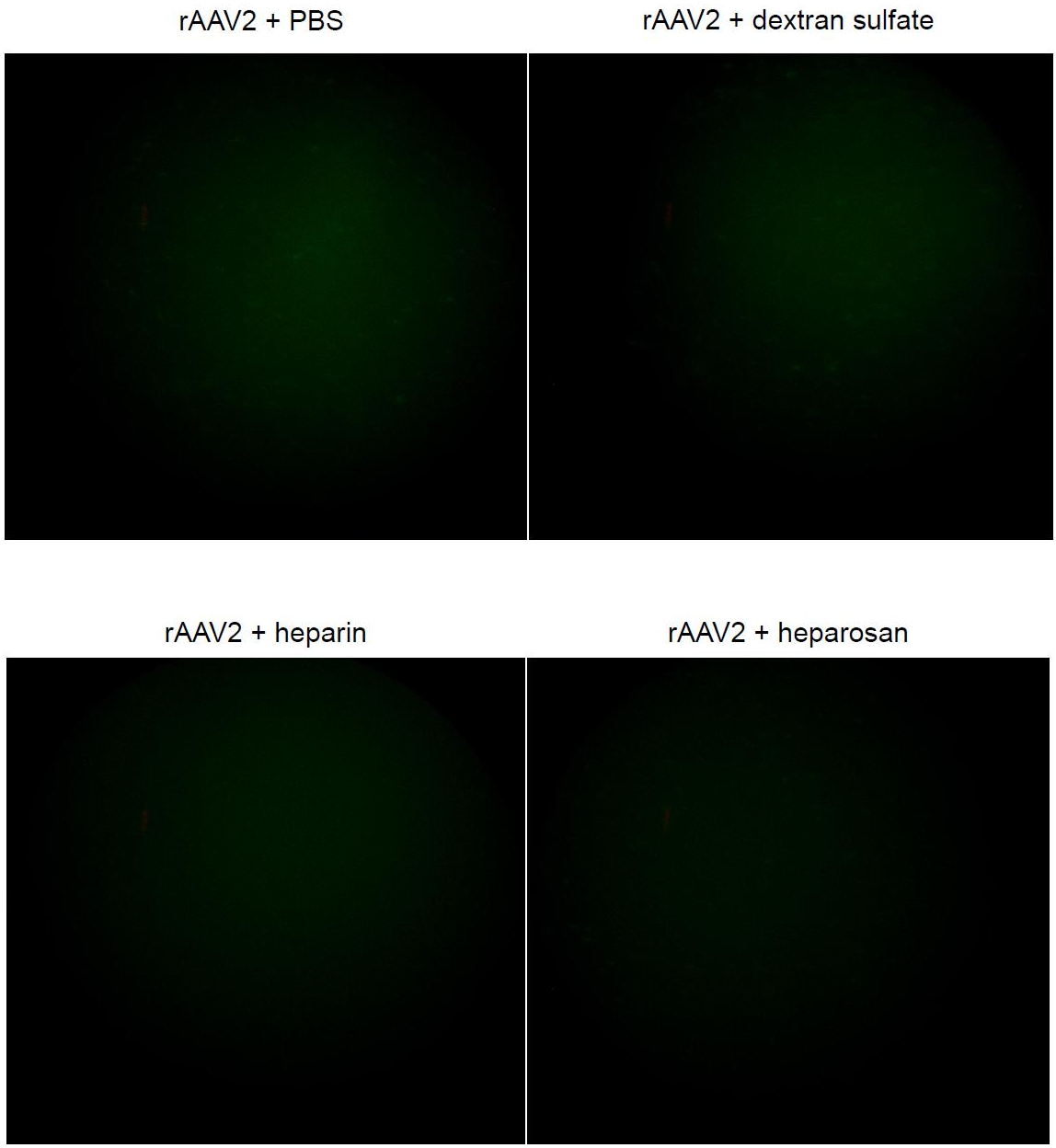

Figure 2.29 Transduction of the retina with rAAV2 mixed with soluble heparin derivatives

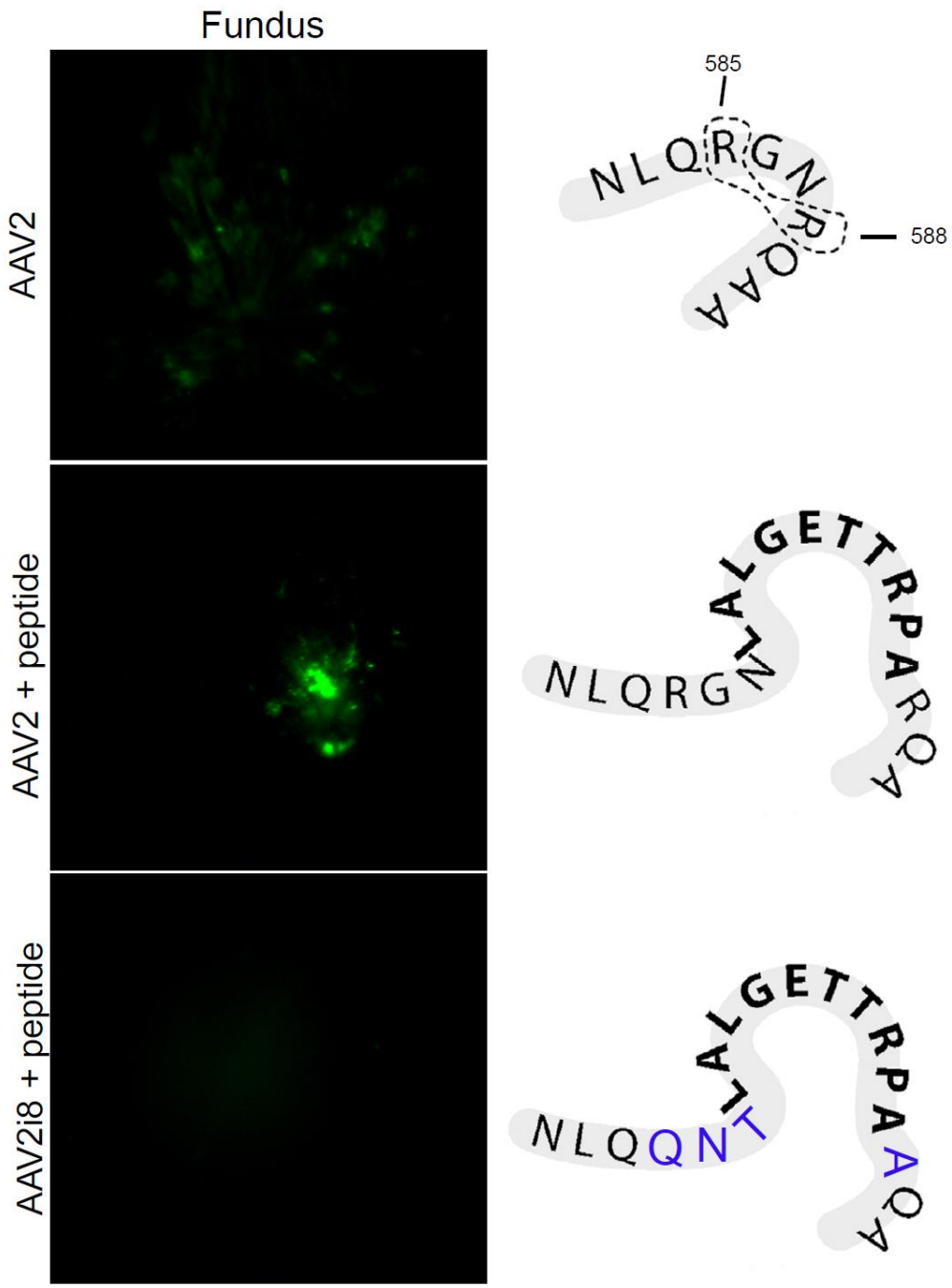

Figure 2.30 The engineered 7m8 capsid (rAAV2 + peptide) relies on HS binding for IVIT transduction

rAAV2 was compared to a 7-amino acid peptide insertion in the context of either HS binding (rAAV2 + peptide) or no HS binding (rAAV2i8 + peptide). Without HS binding, there was no transduction observed by GFP fluorescence and the peptide itself lowered the transduction of the capsid.

CHAPTER 3: Future directions

3.1 HS binding motif

The vector accumulation at the ILM is important for the ability of rAAV to transduce the retina following IVIT delivery. We showed that HS-binding motif on the rAAV1, 2, and 8 promoted the accumulation of capsid at the LIM, presumably through the HSPG found at the ILM. The addition of the HS-binding motif onto other rAAV serotypes may enhance the transduction by IVIT delivery. The lack of accumulation by several AAV serotypes could be responsible for the limited transduction of the retina by IVIT. By simply graphing the HS-binding motif onto AAV capsids, their accumulation onto the retina may increase and lead to transduction not seen by the parental capsid. First, it would be interesting to graph the HS-binding motif onto rAAV4 and rAAV5 capsids because of their tropism by SR injection. By SR delivery, rAAV4 shows restricted transduction of RPE {Weber 2003} and rAAV5 is efficiently transduced to the PRs along with RPE transduction. Although the transduction pattern by these capsids may simply be the result of the route of administration, it is more likely is that they show retinal cell-specific transduction, but cannot access these cells by IVIT delivery. This idea seems valid given the ability of IVIT rAAV5 to transduce the PRs when the ILM is altered [49, 50]. Staining for pan-SIA expression using wheat germ agglutinin indicated that SIA is abundant in the outer retina, though specific staining of either the 2,3 O-linked SIA or 2,3 N-linked SIA would help to provide a mechanism for the tropism of these serotypes. The lack of IVIT transduction by these capsids may be due to the lack of accumulation at the ILM, which would keep the vector diluted in the vitreous. By increasing the accumulation of these serotypes at the vitreoretinal junction, the capsids are no longer diluted in the vitreous and would be primed to penetrate the

retina. In addition to the accumulation out of the vitreous, the vector must be able to penetrate the retina to reach the outer retina. Given that several studies have shown the LIM to be the bottleneck to IVIT retinal transduction, we would assume that the penetration of vectors would not be an issue.

An additional capsid that would be interesting to test for enhanced transduction would the rAAV9. Within the context of neuroscience applications, rAAV9 has become the gold standard to use [80-82]. rAAV9 has been shown to cross the blood-brain barrier when delivered intravascularly in adult mice [83]. The age at which rAAV9 is delivered can change the transduction profile [84, 85]. When the vector is delivered to neonatal mice, transduction within the retina can be detected, indicating that rAAV9 may be capable of passing through the blood-retinal barrier as well [86-88]. This capability to pass through these barriers may endow it with the ability to pass through the ILM and penetrate the retina efficiently. In fact, when FISH was carried out on IVIT-delivered rAAV9, we found the presence of transgenes within the retina but did not lead to detectable transduction (data not shown). Perhaps additional mechanisms are at play and must be satisfied to promote transduction within the retina.

Many researchers have tested various AAV capsid libraries to look for a variant that would be ideal for individual applications. One way to generate a library with high diversity is by using large fragments of the *cap* gene from the various serotypes to ligate together to form a unique construct of *cap* sequence [89]. To further add diversity, capsid libraries can be subjected to error-prone DNA polymerase to introduce point mutations within the fragmented *cap* gene sequence. This approach can disrupt the motifs on the capsid needed for receptor binding and intracellular trafficking leading to new transduction patterns. Through *in vivo* selection, capsids are selected for their ability to bind to cells of interest, not necessarily for their transduction. However, this selection may exclude capsids with interesting transduction potential but had a disruption in a beneficial motif (*e.g.* HS motif for IVIT rAAV transduction). If

the accumulation at the ILM remains the bottleneck, the number of clones recovered will be reduced. Therefore, when creating the library, there should be a large proportion of vector that have HS binding. This does not mean that the library should be made and then separated based on the capsid's ability to bind to an HSPG column but rather that HS-binding motifs should be incorporated into the generation of the library to yield more viable clones that can overcome tissue barriers.

Another way to add an immense amount of diversity is to insert a peptide within the rAAV capsid that is known to lead to transduction [90-93]. So long as the peptide isn't inserted in a binding motif needed for transduction, the peptide could increase viral interaction with the cell or boost the virus trafficking in some way. Because rAAV2 can transduce cells independent of HSPG binding, peptides are often incorporated to ablate HSPG binding so that the native receptor binding does not dominate the novel transduction profile [91, 92]. The crystal structure and mutational analysis have led to a map of the rAAV2 *cap* sequence that tolerates a peptide insertion [91, 94]. This rationale was used to generate the capsid library tested for enhanced PR transduction. However, the insertions also disrupted the ability of the rAAV2 capsid to bind to HSPG [95]. From this model, we would suggest that this peptide would be best served by placing it away from the HSPG-binding motif on the base of the threefold axis of symmetry to another capsid positions [94, 96]. Large peptide ligands have been inserted into VP2 to prevent disruption of VP3 yet can still be surface exposed to alter cell surface interactions [97, 98]. By using a HSPG-binding rAAV2 capsid and placing the peptide away from this motif may yield a novel peptide that leads to transduction of a specific cell type.

3.2 Trafficking studies of all serotypes

This was the first study using ISH to detect rAAV in the retina. Previous experiments have used fluorescently-labelled capsids to detect trafficking of rAAV particles [49, 50]. The fluorescent label attaches to lysine residues on the capsid surface, where they may interfere

with native binding to receptors. The lysine is involved in enhanced transduction in rAAV1-E531K, and by covering the charged residues on rAAV1. Dalkara *et al.* (2009), did not see rAAV1 binding or transduction however we saw rAAV1 transduction in our experiments. In addition to this experimental setback, the entire set of rAAV serotypes has yet to be tested for trafficking differences in the retina. Because transduction is not indicative of trafficking, ISH studies would help the field to understand the barrier encountered by each of the serotypes. From the ISH detection of the panel of rAAV, some serotypes may show accumulation without HSPG binding which will offer additional receptors to target to further increase IVIT transduction.

To carry out these experiments, each of the rAAV serotypes could be IVIT injected into mice and eyes enucleated soon after delivery. It would be beneficial to embed the entire eye in paraffin so that vector that remains diluted in the vitreous can still be assayed. Our FISH studies conducted were carried out on cryosections with the lens removed. We tried to perform cryosections on whole-embedded eyes, but the hard structure of the lens disrupt morphology. Therefore, the lens, was removed prior to embedding which would also the vitreous. The difference in embedding would require additional protocol optimization, but would provide the most accurate picture of rAAV trafficking in the retina.

It would be important to determine trafficking studies of SR-delivered rAAV vector to parse out by what mechanism SR transduction occurs. It may be that vectors transduce the outer retina because of tropism or because the virus is concentrated proximal to cells they transduce. With some serotypes like rAAV5, there appears to be a tropism to the PRs since both IVIT and SR delivery lead to transduction of the outer retina. The bolus delivery in the SR space effectively concentrates the vector under the retina, similar to how the aggregating vectors at the ILM can transduce the retina by IVIT. To determine if a concentration effect is responsible for transduction, 1 µl of varying amount of vector could be delivered SR and assessed over time to determine the minimal amount of vector needed for transduction. From

our results in Chapter 1 of this dissertation, 1 µl of 2E9 vg can spread over the entire retina. Using ISH soon after SR injection to determine the trafficking of vectors would be similar to the ISH assessment by IVIT. With ISH, the location of vector can be determined irrespective of promoter strength and expression kinetics

Currently, to achieve the highest expression of the transgene, the vector must be delivered subretinally. Issues arise with this injection route when considering treatment for patients with extremely fragile retinas due to advanced degeneration. SR delivery is a balancing act between delivering enough vector to adequately spread and transduce a large part of the retina, but not delivering too much volume as to make the retinal detachment unable to resolve on its own. This makes it difficult to treat an entire retina by SR delivery and there is no standard protocol to determine what area of the retina to treat. ISH analysis may determine the amount of vector, rather than volume, to be the determine factor of spread. Studying the trafficking of rAAV by SR delivery will allow for the design of vectors with better spread and transduction of the retina.

Similar to the results seen with SR delivery in mice, transduction of vector is most prominent in the region of the detachment with lesser transduction outside this area. Therefore, an ideal SR AAV vector should can spread farther than the detachment. Similar to how HS binding aggregates AAV onto the ILM, capsid interaction with glycans found in the outer retina could aggregate vector and prevent the dissemination across the retina. These glycans may be more exposed during the detachment of the retina. From our experiments, we know that binding to HSPG does not influence the SR transduction of rAAV2, likely since HSPG staining did not show abundant staining in the outer retina. This would also help to explain why HS-binding rAAV8-E533K did not perform better than the rAAV8 parent capsid. In contrast, the addition of additional glycan interactions on an AAV capsid may promote the spread of vector across the outer retina. From our experiments, we found sialic acid and galactose to be abundant in the

outer retina. It would be interesting to subretinally deliver vectors that have dual glycan binding ability and observe any changes in vector spread.

Although SR delivery results in greater transduction compared to IVIT delivery, many of the issues with the SR injection can be circumvented via IVIT injection. We provided evidence to suggest that HS binding promotes the accumulation of vector out of the vitreous and onto the retina, where it can later transduce the retina with greater efficiency. Not only does the ILM serve as a barrier to retinal transduction, but the delivery of vector to the vitreous leads to a dilution of the vector and reduces its transduction potential. From our studies, we found that the small size of the mouse eye is particularly effective at increasing the interaction of AAV with the retina. However, in a large eye of a NHP, a high concentration of infectious AAV can be found in the vitreous weeks after IVIT delivery. Similar to the work done with mice, we did not identify an inhibitory molecule in the vitreous of NHP to explain the lack of transduction. It can be difficult to parse out whether the larger volume of the NHP vitreous, the increased thickness of the NHP ILM, or a combination of both are responsible for the limited transduction of IVIT AAV. Recent publication of successful AAV transduction in the NHP retina following a sub-ILM delivery indicates that at least the ILM does play an inhibitory role in the IVIT transduction of AAV. Dosage studies in the NHP also indicate that dilution is likely a factor for the limited transduction of the retina. Promoting greater interaction of AAV capsid with the retina becomes an important attribute for an ideal IVIT AAV vector. This can be carried out through glycan binding as described in the earlier chapter. A more detailed study on the kinetics of vector trafficking in the retina would help to explain the rate-limiting steps to viral transduction by either SR or IVIT delivery.

Several research groups have used a panel of AAV serotypes and characterized these capsids based on their ability to transduce the retina. However, it is becoming increasing clear that viral transduction and viral distribution are not synonymous terms. This is most evident in

the transduction differences between single-stranded and self-complementary rAAV2 by either IVIT or SR delivery. The use of various promoters can also yield results that are incongruent with previous analysis of that certain capsid serotypes were not retinal tropic. We tried to optimize the expression of GFP by using a robust promoter (CBh) in a self-complementary transgene form. Therefore, we would test the transduction of the scAAV-CBh-GFP panel, as well as carry out ISH studies.

3.3 AAV accumulation at the ILM

Another method to help reduce the dilution of delivering vector to the vitreous is to remove the vitreal fluid prior to injection. This procedure has been performed in dogs with mixed outcomes [99] but overall results seem promising [100]. This would ensure that the vector remains concentrated. The dilution in mouse vitreous would not be as much of a factor due to the small volume. Vitrectomy in NHP can lead to dramatic transduction in as little as 20 days post-injection whereas no expression is seen without vitrectomy even when observation is extended to 60 days post-injection [100]. Although performing a vitrectomy is a relatively simple procedure, it would dramatically affect the distribution of vector. Most likely, delivered vector seems to pool at the lowest point of the globe and result in intense focal transduction. Spreading the vector around the entire retina may be as simple as rotating the head in various positions and inclines for several minutes. The vitrectomy protocol may also allow for a greater volume to be delivered. Typically, up to 150 µl has been delivered to the eye for transduction, but volumes up to 1 ml have been tested and shown to be effective. While the volume of vector can be important, more likely it is the amount of vector that provides the greatest impact. Most rAAV capsids can be scaled up to produce high titered virus, but there may be capsid mutants or production issues which limit the amount of vector that can be production. It is unclear from current studies what mechanism AAV uses to traverse the retinal layers and identification of this mechanism may lead to novel AAV capsids with greater spread. Only by understanding the

small nuances of AAV retinal trafficking will we be able to exploit these mechanisms for the next generation of AAV capsids with greater IVIT transduction properties.

It may be possible that graphing an HS-binding motif may not work in all rAAV serotypes. Some capsid may bind with low affinity to HSPG and thereby reducing aggregation. Another way to achieve greater AAV presence at the retina could be through the use of microbubbles. Microbubbles are compounds that can be coupled to protein or DNA and can be loaded with rAAV particles [101]. Ultrasound destruction of microbubbles can enhance rAAV transduction [102, 103] through an increase in clathrin endocytosis [104, 105]. These microbubble-rAAV can be herded to specific regions through the use of low-frequency ultrasound [106, 107]. Once at the ILM, the change to ultrasonic frequency causes the microbubbles to burst to release rAAV. This would also temporary disrupt the ILM to increase vector penetration into the retina. When microbubbles were administered intravenously, the blood-brain barrier could be focally targeted in mouse brains [108, 109] or targeted to other tissue by redirecting ultrasound [110]. In this way, microbubbles coupled with AAV could be delivered to the vitreous, pushed to the ILM by low-frequency ultrasound, and released at the retina via high-frequency ultrasound. Because the burst of the microbubble can disrupt cell membranes to aid in the intracellular uptake of drug, the breaking of the microbubbles at the ILM may disrupt the membrane and increase the penetrance of AAV across for enhanced retinal transduction.

3.4 Further characterization of rAAV2.5G9

The specific and enhanced transduction of the rAAV2.5G9 vector was shown to be a combination of both motifs on the rAAV2 capsid. However, the exact mechanism that produced this pattern is not yet resolved. We hypothesized that staining for galactose would yield a pattern that explained the phenotype, but there was no staining on the inner retina and fain expression in the ONL. Certainly, we did not observe a co-localization with Müller glia (Figure

2.26) to explain the specific tropism of rAAV2.5G9. It would be beneficial to perform flat-mount staining of glycans to find new glycan targets. We would hypothesize that the motifs on the capsid lead the virus to accumulate on the ILM differently than the parental rAAV2.

ISH analysis on whole-mount retinas just days following injection would provide evidence to constructing a model of rAAV trafficking. By performing confocal microscopy on flat mount retinas, a 3D representation of the retinal section could be obtained. We attempted this type of analysis on whole-mount retinas at three days, one week, and two weeks post-administration; however, we found retinal curling to be the biggest issue. A methods publication of whole-mount ISH on developing mouse vasculature gene targets in the retinas has shown methanol fixation and minimal hybridization media can maintain retinal flatness [111]. We incorporated this method into our protocol, but retinal curling continued to be an issue. Therefore, additional optimization of this combined protocol is necessary to assess retinal trafficking of the chimeric rAAV2.5G9 capsid. ISH analysis over time on rAAV2.5G9-injected whole-mounts would likely show vectors found all along the inner retinal surface, but concentrated along the retinas where transduction later occurs. With a combination of FISH and IHC, it would be possible to observe the aggregation around the retinal vessels and potential retinal penetration via cellular scaffolds

It would be interesting to test the rAAV2.5G9 capsid in a large animal model to confirm the phenotype observed in mice is conserved. Often vectors which show great transduction in the mouse model fail to produce the same phenotype when translated to another animal model. Both the size of the eye and the thickness of the ILM differ substantially between small (*e.g.* mouse, rat) and large (*e.g.* rabbit, primate) animals. This lead us to do translational experiments in *ex vivo* human retinas and *in vivo* testing of rabbit and NHP eyes. The rAAV2.5 transduction surrounding retinal vessel in rabbit eyes provided evidence of a conserved tropism across animal models. Future IVIT NHP experiments would be carried out for three months or longer

similar to duration lengths in other NHP retinal studies [100, 112]. The ISH data on NHP retinas to confirm that vectors had accumulated at the ILM, but it was unclear from the experiment whether the capsid had insufficient time to penetrate through the retina or if the ILM of the NHP proved too great of a barrier.

The unique transduction of the rAAV2.5G9 motif be of benefit to disorders involving neovascularization or some vascular component. Whereas previous research using canonical rAAV2 may have resulted in sub-optimal transduction, the 265 position in the rAAV2.5 motif may provide new vectors with greater therapeutic benefit by maximizing transgene expression around vessels. We tested the ability of rAAV2.5 to deliver Nrf2 transgenes to reduce reactive oxygen species following photodamage to the retina {Liang 2016}, but did not directly compare to rAAV2 capsid.

3.5 Creation of a super capsid for retinal transduction

The AAV vectorology field has advanced rapidly, creating various capsid mutants to capitalize on specific aspects of viral trafficking. Often these mutations are to enhance various intracellular trafficking steps, alter spread, or influence tropism. However, the field has yet to bring all these mutations into a single capsid. Such a “super capsid” may provide supreme transduction that surpasses the enhancement of each mutation on its own. As stated above, rAAV transduction of a cell is a multi-step process (cell attachment, intracellular trafficking, endosomal/proteasomal escape, nuclear entry, uncoating) with additional steps added in the trafficking across the retinal tissue (ILM accumulation, retinal penetration, spread). The addition of the HS-binding motif would work to increase the amount of vector accumulating onto the ILM from IVIT delivery. Once at the retina, additional motifs to glycans in the outer retina may enhance the penetration of vector. The recent addition of the peptide in rAAV2, known as 7m8, works by increasing vector entry into the cell [72]. Once in the retinal cells, Tyr mutations in the capsid would help vectors avoid proteasomal degradation [71]. Factors like NLS may help to

further promote the vector reaching the nucleus [113]. The rAAV8 serotype is faster in uncoating than rAAV2 [87] and the ability of rAAV8 to outperform rAAV2 and rAAV5 in retinal transduction [114]. Most of these modifications are serotype independent, and because these mutations work on different mechanisms, they may synergize the transduction of the rAAV capsids.

3.6 Avoidance of rAAV neutralizing factors in the vitreous

If retinal gene therapy is to progress in its clinical relevance, it must address the avoidance of the immune system. A drawback of delivering vector to the vitreous is the potential inhibition by neutralizing antibodies [115]. Capsid or capsid mutants, like rAAV2.5, avoid interaction with neutralizing antibodies [65] and; therefore, would be a great candidate for patients with pre-existing rAAV2 neutralizing antibodies. Testing of the serum for neutralizing antibodies is indicative to the antibodies in the vitreous [115]. Development of novel capsids, like the evolutionary ancestral capsid [116]. A potentially better protocol to circumvent the neutralizing response is to supply empty capsids *en mass* to “soak up” antibodies [117]. The efforts to avoid neutralizing antibodies in the patients using novel capsid mutants that continue to show transduction of desired cells require further research.

3.7 Progress of retinal gene therapy

The future directions above have dealt with the capsid, but these novel capsids can be used to carry therapeutic transgenes to treat loss-of-function genetic diseases Gene supplementation therapy effectively treats these types of diseases like LCA; however, a more generalized therapy would ease the burden of individualized pharmacogenomics medicine. A mutant-independent strategy could augment current treatment which is reporting worsening degeneration in some patients as the disease continues to progress [118-120]. Gain-of-function or dominant negative mutations would benefit from genome editing strategy. These strategies work best before degeneration of cells and circuitry. In cases of late-stage disease progression, conversion of retinal cells to PRs or repopulation of PRs are the best option.

3.7.1 Delivery of neurotrophic factor

Several neurotrophic factors have been studied for retinal preservation in genetic rodent retinal degenerative models. For example, GDNF has prevented the loss of retinal cells in both an rd mouse model and RP rat model [121-123]. The use of the rAAV2.5G9 capsid to deliver GDNF transgenes to Müller glial cells superior transduction to the Müller glia-specific rAAV6 mutant known as rAAVShH10. Comparing rAAV2.5G9 transduction to rAAVShH10 in an rd mouse model may indicate the new vector is capable of rescue at lower vector titers. Either way, the ability to use two serologically independent capsids with identical tropism will be beneficial in the treatment of both eyes for patients. Benefits have been observed using BDNF as well [124-128]. However, not all neurotropic factors are therapeutic. The delivery of the neurtin neurotropic factor was unable to functionally rescue the PR-degenerative rd mouse model [96] and CNTF has had varying therapeutic effects [129-133].

3.7.2 Induction of retinal regeneration

Another strategy to deal with the loss of PRs is to repopulate the retina with stem cells [134-137]. One way of doing this is through the SR delivering of RPC to the outer retina. However, Müller glia retain stem cell properties [138] and are great cell target to convert into RPC because the Müller glia are not degenerated in diseases. Retinal development may lead insight into another approach that could be used to reconstruct the retina. During development, RPC rise to the numerous cell types that exist in the retina before terminally differentiating into the Müller glia. By coaxing the Müller glia back into its undifferentiated state, these cells may repopulate the retina in areas of major PR death. Once the retina has been repopulated, that these induced cells would continue their natural lineage back to Müller glia. Because Müller glia span the entire thickness of the retina, they are easily targeted by IVIT delivery of rAAV2.5G9, further eliminating the disruption of the retina by SR delivery. However, the disruption of OLM could help integration stem cells similar to OLM disruption but other means [139, 140]. Stem cell

integration into the retina still requires further optimization [132] and the use of neurotropic factors can improve integration and survival [141]. The use of patient-derived stem cells would avoid possible immune-related issues to stem cell transplants [142, 143]. The four transcript factors needed to induce pluripotency (Oct4, Sox2, Klf4, c-myc) in differentiated cells [144] may be used to generate the *in vivo* stem cells from Müller glia. Transgenes for these transcription factors are not likely to fit into the small space of a single AAV vector; however, vectors packaging each of the factors could then be combined during injection to convert Müller glia. By inducing stem cells in an intact retina, the correct environment for differentiation should be satisfied rather than using Matrigel [145, 146]. Several labs are currently working on converting patient-derived fibroblast into iPSC and then coaxing these cells to devolve into a retinal state using media and Matrigel. Because SR-delivered stem cells are capable of migrating and establishing connections on their own, it is likely that iPSC will also be able to migrate to the ONL and establish connections with the bipolar cells.

.

REFERENCES

1. Venkatesh, A., et al., *Retinal gene delivery by rAAV and DNA electroporation.* Curr Protoc Microbiol, 2013. **Chapter 14**: p. Unit 14D 4.

2. Morgenstern, J.P. and H. Land, *Advanced mammalian gene transfer: high titre retroviral vectors with multiple drug selection markers and a complementary helper-free packaging cell line.* Nucleic Acids Res, 1990. **18**(12): p. 3587-96.

3. Alba, R., A. Bosch, and M. Chillon, *Gutless adenovirus: last-generation adenovirus for gene therapy.* Gene Ther, 2005. **12 Suppl 1**: p. S18-27.

4. Fallaux, F.J., et al., *New helper cells and matched early region 1-deleted adenovirus vectors prevent generation of replication-competent adenoviruses.* Hum Gene Ther, 1998. **9**(13): p. 1909-17.

5. Samulski, R.J., et al., *Targeted integration of adeno-associated virus (AAV) into human chromosome 19.* EMBO J, 1991. **10**(12): p. 3941-3950.

6. Berns, K.I., et al., *Detection of adeno-associated virus (AAV)-specific nucleotide sequences in DNA isolated from latently infected Detroit 6 cells.* Virology, 1975. **68**(2): p. 556-60.

7. Boutin, S., et al., *Prevalence of serum IgG and neutralizing factors against adeno-associated virus (AAV) types 1, 2, 5, 6, 8, and 9 in the healthy population: implications for gene therapy using AAV vectors.* Hum Gene Ther, 2010. **21**(6): p. 704-12.

8. Georg-Fries, B., et al., *Analysis of proteins, helper dependence, and seroepidemiology of a new human parvovirus.* Virology, 1984. **134**(1): p. 64-71.

9. Atchison, R.W., B.C. Casto, and W.M. Hammon, *Adenovirus-Associated Defective Virus Particles.* Science, 1965. **149**(3685): p. 754-6.

10. Xiao, P.J. and R.J. Samulski, *Cytoplasmic trafficking, endosomal escape, and perinuclear accumulation of adeno-associated virus type 2 particles are facilitated by microtubule network.* J Virol, 2012. **86**(19): p. 10462-73.

11. Rabinowitz, J.E. and R.J. Samulski, *Building a better vector: the manipulation of AAV virions.* Virology, 2000. **278**(2): p. 301-8.

12. Xiao, P.J., et al., *Disruption of Microtubules Post-Virus Entry Enhances Adeno-Associated Virus Vector Transduction.* Hum Gene Ther, 2016. **27**(4): p. 309-24.

13. Nicolson, S.C. and R.J. Samulski, *Recombinant adeno-associated virus utilizes host cell nuclear import machinery to enter the nucleus.* J Virol, 2014. **88**(8): p. 4132-44.

14. Johnson, J.S. and R.J. Samulski, *Enhancement of adeno-associated virus infection by mobilizing capsids into and out of the nucleolus.* J Virol, 2009. **83**(6): p. 2632-44.

15. Srivastava, A., E.W. Lusby, and K.I. Berns, *Nucleotide Sequence and Organization of the AdenoAssociated Virus 2 Genome.* J Virol, 1983. **45**(2): p. 555-564.

16. King, J.A., et al., *DNA helicase-mediated packaging of adeno-associated virus type 2 genomes into preformed capsids.* EMBO J, 2001. **20**(12): p. 3282-91.

17. Kronenberg, S., J.A. Kleinschmidt, and B. Bottcher, *Electron cryo-microscopy and image reconstruction of adeno-associated virus type 2 empty capsids.* EMBO Rep, 2001. **2**(11): p. 997-1002.

18. Summerford, C. and R.J. Samulski, *Membrane-Associated Heparan Sulfate Proteoglycan Is a Receptor for Adeno-Associated Virus Type 2 Virions.* Journal of Virology, 1998. **72**(2): p. 1438-1445.

19. Wu, Z., et al., *Single amino acid changes can influence titer, heparin binding, and tissue tropism in different adeno-associated virus serotypes.* J Virol, 2006. **80**(22): p. 11393-7.

20. Kaludov, N., et al., *Adeno-associated virus serotype 4 (AAV4) and AAV5 both require sialic acid binding for hemagglutination and efficient transduction but differ in sialic acid linkage specificity.* J Virol, 2001. **75**(15): p. 6884-93.

21. Shen, S., et al., *Terminal N-linked galactose is the primary receptor for adeno-associated virus 9.* J Biol Chem, 2011. **286**(15): p. 13532-40.

22. Asokan, A., et al., *Reengineering a receptor footprint of adeno-associated virus enables selective and systemic gene transfer to muscle.* Nat Biotechnol, 2010. **28**(1): p. 79-82.

23. Qing, K., et al., *Human fibroblast growth factor receptor 1 is a co-receptor for infection by adeno-associated virus 2.* Nature Medicine, 1999. **5**(1): p. 71-77.

24. Akache, B., et al., *The 37/67-kilodalton laminin receptor is a receptor for adeno-associated virus serotypes 8, 2, 3, and 9.* J Virol, 2006. **80**(19): p. 9831-6.

25. Grieger, J.C., V.W. Choi, and R.J. Samulski, *Production and characterization of adeno-associated viral vectors.* Nat Protoc, 2006. **1**(3): p. 1412-28.

26. Rabinowitz, J.E., et al., *Cross-Packaging of a Single Adeno-Associated Virus (AAV) Type 2 Vector Genome into Multiple AAV Serotypes Enables Transduction with Broad Specificity.* Journal of Virology, 2002. **76**(2): p. 791-801.

27. Xiao, X., J. Li, and R.J. Samulski, *Production of high-titer recombinant adeno-associated virus vectors in the absence of helper adenovirus.* J Virol, 1998. **72**(3): p. 2224-32.

28. Ferrari, F.K., et al., *Second-strand synthesis is a rate-limiting step for efficient transduction by recombinant adeno-associated virus vectors.* J Virol, 1996. **70**(5): p. 3227-3234.

29. McCarty, D.M., P.E. Monahan, and R.J. Samulski, *Self-complementary recombinant adeno-associated virus (scAAV) vectors promote efficient transduction independently of DNA synthesis.* Gene Ther, 2001. **8**(16): p. 1248-54.

30. McCarty, D.M., et al., *Adeno-associated virus terminal repeat (TR) mutant generates self-complementary vectors to overcome the rate-limiting step to transduction in vivo.* Gene Ther, 2003. **10**(26): p. 2112-8.

31. Ren, C., et al., *Genomic stability of self-complementary adeno-associated virus 2 during early stages of transduction in mouse muscle in vivo.* Hum Gene Ther, 2005. **16**(9): p. 1047-57.

32. Wang, Z., et al., *Rapid and highly efficient transduction by double-stranded adeno-associated virus vectors in vitro and in vivo.* Gene Ther, 2003. **10**(26): p. 2105-11.

33. Yokoi, K., et al., *Ocular gene transfer with self-complementary AAV vectors.* Invest Ophthalmol Vis Sci, 2007. **48**(7): p. 3324-8.

34. Gray, S.J., K.T. Woodard, and R.J. Samulski, *Viral vectors and delivery strategies for CNS gene therapy.* Ther Deliv, 2010. **1**(4): p. 517-34.

35. Murlidharan, G., R.J. Samulski, and A. Asokan, *Biology of adeno-associated viral vectors in the central nervous system.* Front Mol Neurosci, 2014. **7**: p. 76.

36. Hauswirth, W.W., et al., *Treatment of leber congenital amaurosis due to RPE65 mutations by ocular subretinal injection of adeno-associated virus gene vector: short-term results of a phase I trial.* Hum Gene Ther, 2008. **19**(10): p. 979-90.

37. Maguire, A.M., et al., *Safety and efficacy of gene transfer for Leber's congenital amaurosis.* N Engl J Med, 2008. **358**(21): p. 2240-8.

38. Maguire, A.M., et al., *Age-dependent effects of RPE65 gene therapy for Leber's congenital amaurosis: a phase 1 dose-escalation trial.* The Lancet, 2009. **374**(9701): p. 1597-1605.

39. Bainbridge, J.W., et al., *Effect of gene therapy on visual function in Leber's congenital amaurosis.* N Engl J Med, 2008. **358**(21): p. 2231-9.

40. Acland, G.M., et al., *Gene therapy restores vision in a canine model of childhood blindness.* Nat Genet, 2001. **28**(1): p. 92-5.

41. Acland, G.M., et al., *Long-term restoration of rod and cone vision by single dose rAAV-mediated gene transfer to the retina in a canine model of childhood blindness.* Mol Ther, 2005. **12**(6): p. 1072-82.

42. Bennicelli, J., et al., *Reversal of blindness in animal models of leber congenital amaurosis using optimized AAV2-mediated gene transfer.* Mol Ther, 2008. **16**(3): p. 458-65.

43. Cideciyan, A.V., et al., *Human RPE65 gene therapy for Leber congenital amaurosis: persistence of early visual improvements and safety at 1 year.* Hum Gene Ther, 2009. **20**(9): p. 999-1004.

44. Simonelli, F., et al., *Gene therapy for Leber's congenital amaurosis is safe and effective through 1.5 years after vector administration.* Mol Ther, 2010. **18**(3): p. 643-50.

45. Bennett, J., et al., *Safety and durability of effect of contralateral-eye administration of AAV2 gene therapy in patients with childhood-onset blindness caused by RPE65 mutations: a follow-on phase 1 trial.* The Lancet, 2016. **388**(10045): p. 661-672.

46. Chiang, B., et al., *Circumferential flow of particles in the suprachoroidal space is impeded by the posterior ciliary arteries.* Exp Eye Res, 2016. **145**: p. 424-31.

47. Bogner, B., et al., *Capsid Mutated Adeno-Associated Virus Delivered to the Anterior Chamber Results in Efficient Transduction of Trabecular Meshwork in Mouse and Rat.* PLoS One, 2015. **10**(6): p. e0128759.

48. Giove, T.J., M. Sena-Esteves, and W.D. Eldred, *Transduction of the inner mouse retina using AAVrh8 and AAVrh10 via intravitreal injection.* Exp Eye Res, 2010. **91**(5): p. 652-9.

49. Dalkara, D., et al., *Inner limiting membrane barriers to AAV-mediated retinal transduction from the vitreous.* Mol Ther, 2009. **17**(12): p. 2096-102.

50. Kolstad, K.D., et al., *Changes in adeno-associated virus-mediated gene delivery in retinal degeneration.* Hum Gene Ther, 2010. **21**(5): p. 571-8.

51. Yin, L., et al., *Intravitreal injection of AAV2 transduces macaque inner retina.* Invest Ophthalmol Vis Sci, 2011. **52**(5): p. 2775-83.

52. Ivanova, E., et al., *Evaluation of AAV-mediated expression of Chop2-GFP in the marmoset retina.* Invest Ophthalmol Vis Sci, 2010. **51**(10): p. 5288-96.

53. Pellissier, L.P., et al., *Specific tools for targeting and expression in Muller glial cells.* Mol Ther Methods Clin Dev, 2014. **1**: p. 14009.

54. Aartsen, W.M., et al., *GFAP-driven GFP expression in activated mouse Muller glial cells aligning retinal blood vessels following intravitreal injection of AAV2/6 vectors.* PLoS One, 2010. **5**(8): p. e12387.

55. Hellstrom, M., et al., *Cellular tropism and transduction properties of seven adeno-associated viral vector serotypes in adult retina after intravitreal injection.* Gene Ther, 2009. **16**(4): p. 521-32.

56. Halfter, W., et al., *Origin and turnover of ECM proteins from the inner limiting membrane and vitreous body.* Eye (Lond), 2008. **22**(10): p. 1207-13.

57. Candiello, J., et al., *Biomechanical properties of native basement membranes.* FEBS J, 2007. **274**(11): p. 2897-908.

58. Cehajic-Kapetanovic, J., et al., *Glycosidic enzymes enhance retinal transduction following intravitreal delivery of AAV2.* Mol Vis, 2011. **17**: p. 1771-83.

59. Kern, A., et al., *Identification of a Heparin-Binding Motif on Adeno-Associated Virus Type 2 Capsids.* Journal of Virology, 2003. **77**(20): p. 11072-11081.

60. Gray, S.J., et al., *Global CNS gene delivery and evasion of anti-AAV-neutralizing antibodies by intrathecal AAV administration in non-human primates.* Gene Ther, 2013. **20**(4): p. 450-9.

61. Natkunarajah, M., et al., *Assessment of ocular transduction using single-stranded and self-complementary recombinant adeno-associated virus serotype 2/8.* Gene Ther, 2008. **15**(6): p. 463-7.

62. Kong, F., et al., *Self-complementary AAV5 vector facilitates quicker transgene expression in photoreceptor and retinal pigment epithelial cells of normal mouse.* Exp Eye Res, 2010. **90**(5): p. 546-54.

63. Arnett, A.L., et al., *Heparin-binding correlates with increased efficiency of AAV1- and AAV6-mediated transduction of striated muscle, but negatively impacts CNS transduction.* Gene Ther, 2013. **20**(5): p. 497-503.

64. Bowles, D.E., et al., *Phase 1 gene therapy for Duchenne muscular dystrophy using a translational optimized AAV vector.* Mol Ther, 2012. **20**(2): p. 443-55.

65. Li, C., et al., *Single amino acid modification of adeno-associated virus capsid changes transduction and humoral immune profiles.* J Virol, 2012. **86**(15): p. 7752-9.

66. Shen, S., et al., *Engraftment of a galactose receptor footprint onto adeno-associated viral capsids improves transduction efficiency.* J Biol Chem, 2013. **288**(40): p. 28814-23.

67. Murlidharan, G., et al., *CNS-restricted Transduction and CRISPR/Cas9-mediated Gene Deletion with an Engineered AAV Vector.* Mol Ther Nucleic Acids, 2016. **5**(7): p. e338.

68. Boye, S.E., et al., *Highly Efficient Delivery of AAV vectors to the Primate Retina.* Hum Gene Ther, 2016.

69. Messina, E.L., et al., *Adeno-associated viral vectors based on serotype 3b use components of the fibroblast growth factor receptor signaling complex for efficient transduction.* Hum Gene Ther, 2012. **23**(10): p. 1031-42.

70. Klimczak, R.R., et al., *A novel adeno-associated viral variant for efficient and selective intravitreal transduction of rat Muller cells.* PLoS One, 2009. **4**(10): p. e7467.

71. Boye, S.L., et al., *Impact of Heparan Sulfate Binding on Transduction of Retina by Recombinant Adeno-Associated Virus Vectors.* J Virol, 2016. **90**(8): p. 4215-31.

72. Khabou, H., et al., *Insight into the mechanisms of enhanced retinal transduction by the engineered AAV2 capsid variant -7m8.* Biotechnol Bioeng, 2016.

73. Charbel Issa, P., et al., *Assessment of tropism and effectiveness of new primate-derived hybrid recombinant AAV serotypes in the mouse and primate retina.* PLoS One, 2013. **8**(4): p. e60361.

74. Kay, C.N., et al., *Targeting photoreceptors via intravitreal delivery using novel, capsid-mutated AAV vectors.* PLoS One, 2013. **8**(4): p. e62097.

75. Petrs-Silva, H., et al., *Novel properties of tyrosine-mutant AAV2 vectors in the mouse retina.* Mol Ther, 2011. **19**(2): p. 293-301.

76. Lompre, A.M., et al., *Efficient transduction of vascular smooth muscle cells with a translational AAV2.5 vector: a new perspective for in-stent restenosis gene therapy.* Gene Ther, 2013. **20**(9): p. 901-12.

77. Petrs-Silva, H., et al., *High-efficiency transduction of the mouse retina by tyrosine-mutant AAV serotype vectors.* Mol Ther, 2009. **17**(3): p. 463-71.

78. Gray, S.J., et al., *Optimizing promoters for recombinant adeno-associated virus-mediated gene expression in the peripheral and central nervous system using self-complementary vectors.* Hum Gene Ther, 2011. **22**(9): p. 1143-53.

79. Ogata, N., et al., *Expression of basic fibroblast growth factor mRNA in developing choroidal neovascularization.* Current Eye Research, 2009. **15**(10): p. 1008-1018.

80. Gadalla, K.K., et al., *Improved survival and reduced phenotypic severity following AAV9/MECP2 gene transfer to neonatal and juvenile male Mecp2 knockout mice.* Mol Ther, 2013. **21**(1): p. 18-30.

81. Jackson, K.L., R.D. Dayton, and R.L. Klein, *AAV9 supports wide-scale transduction of the CNS and TDP-43 disease modeling in adult rats.* Mol Ther Methods Clin Dev, 2015. **2**: p. 15036.

82. Donsante, A., et al., *Intracerebroventricular delivery of self-complementary adeno-associated virus serotype 9 to the adult rat brain.* Gene Ther, 2016. **23**(5): p. 401-7.

83. McLean, J.R., et al., *Widespread neuron-specific transgene expression in brain and spinal cord following synapsin promoter-driven AAV9 neonatal intracerebroventricular injection.* Neurosci Lett, 2014. **576**: p. 73-8.

84. Bostick, B., et al., *Systemic AAV-9 transduction in mice is influenced by animal age but not by the route of administration.* Gene Ther, 2007. **14**(22): p. 1605-9.

85. Foust, K.D., et al., *Intravascular AAV9 preferentially targets neonatal neurons and adult astrocytes.* Nat Biotechnol, 2009. **27**(1): p. 59-65.

86. Dalkara, D., et al., *Enhanced gene delivery to the neonatal retina through systemic administration of tyrosine-mutated AAV9.* Gene Ther, 2012. **19**(2): p. 176-81.

87. Bemelmans, A.P., et al., *A single intravenous AAV9 injection mediates bilateral gene transfer to the adult mouse retina.* PLoS One, 2013. **8**(4): p. e61618.

88. Byrne, L.C., et al., *The expression pattern of systemically injected AAV9 in the developing mouse retina is determined by age.* Mol Ther, 2015. **23**(2): p. 290-6.

89. Li, W., et al., *Engineering and selection of shuffled AAV genomes: a new strategy for producing targeted biological nanoparticles.* Mol Ther, 2008. **16**(7): p. 1252-60.

90. Michelfelder, S., et al., *Peptide ligands incorporated into the threefold spike capsid domain to re-direct gene transduction of AAV8 and AAV9 in vivo.* PLoS One, 2011. **6**(8): p. e23101.

91. Shi, W., G.S. Arnold, and J.S. Bartlett, *Insertional mutagenesis of the adeno-associated virus type 2 (AAV2) capsid gene and generation of AAV2 vectors targeted to alternative cell-surface receptors.* Hum Gene Ther, 2001. **12**(14): p. 1697-711.

92. Shi, X., et al., *Insertional mutagenesis at positions 520 and 584 of adeno-associated virus type 2 (AAV2) capsid gene and generation of AAV2 vectors with eliminated heparin-binding ability and introduced novel tropism.* Hum Gene Ther, 2006. **17**(3): p. 353-61.

93. Buchholz, C.J., T. Friedel, and H. Buning, *Surface-Engineered Viral Vectors for Selective and Cell Type-Specific Gene Delivery.* Trends Biotechnol, 2015. **33**(12): p. 777-90.

94. Naumer, M., et al., *Development and validation of novel AAV2 random libraries displaying peptides of diverse lengths and at diverse capsid positions.* Hum Gene Ther, 2012. **23**(5): p. 492-507.

95. Dalkara, D., et al., *In vivo-directed evolution of a new adeno-associated virus for therapeutic outer retinal gene delivery from the vitreous.* Sci Transl Med, 2013. **5**(189): p. 189ra76.

96. Jomary, C., et al., *Epitope-tagged recombinant AAV vectors for expressing neurturin and its receptor in retinal cells.* Mol Vis, 2001. **7**: p. 36-41.

97. Warrington, K.H., Jr., et al., *Adeno-associated virus type 2 VP2 capsid protein is nonessential and can tolerate large peptide insertions at its N terminus.* J Virol, 2004. **78**(12): p. 6595-609.

98. Lux, K., et al., *Green fluorescent protein-tagged adeno-associated virus particles allow the study of cytosolic and nuclear trafficking.* J Virol, 2005. **79**(18): p. 11776-87.

99. Boyd, R.F., et al., *Reduced retinal transduction and enhanced transgene-directed immunogenicity with intravitreal delivery of rAAV following posterior vitrectomy in dogs.* Gene Ther, 2016. **23**(6): p. 548-56.

100. Tshilenge, K.T., et al., *Vitrectomy Before Intravitreal Injection of AAV2/2 Vector Promotes Efficient Transduction of Retinal Ganglion Cells in Dogs and Nonhuman Primates.* Hum Gene Ther Methods, 2016. **27**(3): p. 122-34.

101. Muller, O.J., et al., *Augmentation of AAV-mediated cardiac gene transfer after systemic administration in adult rats.* Gene Ther, 2008. **15**(23): p. 1558-65.

102. Li, H.L., et al., *Ultrasound-targeted microbubble destruction enhances AAV-mediated gene transfection in human RPE cells in vitro and rat retina in vivo.* Gene Ther, 2009. **16**(9): p. 1146-53.

103. Xie, W., et al., *Ultrasound microbubbles enhance recombinant adeno-associated virus vector delivery to retinal ganglion cells in vivo.* Acad Radiol, 2010. **17**(10): p. 1242-8.

104. Geers, B., et al., *Elucidating the mechanisms behind sonoporation with adeno-associated virus-loaded microbubbles.* Mol Pharm, 2011. **8**(6): p. 2244-51.

105. Jin, L.F., et al., *Ultrasound targeted microbubble destruction stimulates cellular endocytosis in facilitation of adeno-associated virus delivery.* Int J Mol Sci, 2013. **14**(5): p. 9737-50.

106. Dermitzakis, A., et al., *The polydisperse acoustic signature of rigid microbubbles.* Conf Proc IEEE Eng Med Biol Soc, 2015. **2015**: p. 133-6.

107. Pouliopoulos, A.N. and J.J. Choi, *Superharmonic microbubble Doppler effect in ultrasound therapy.* Phys Med Biol, 2016. **61**(16): p. 6154-71.

108. Hsu, P.H., et al., *Noninvasive and targeted gene delivery into the brain using microbubble-facilitated focused ultrasound.* PLoS One, 2013. **8**(2): p. e57682.

109. Poon, C., D. McMahon, and K. Hynynen, *Noninvasive and targeted delivery of therapeutics to the brain using focused ultrasound.* Neuropharmacology, 2016.

110. Schlegel, P., et al., *Locally Targeted Cardiac Gene Delivery by AAV Microbubble Destruction in a Large Animal Model.* Hum Gene Ther Methods, 2016. **27**(2): p. 71-8.

111. Powner, M.B., et al., *Visualization of gene expression in whole mouse retina by in situ hybridization.* Nat Protoc, 2012. **7**(6): p. 1086-96.

112. Ye, G.J., et al., *Safety and Biodistribution Evaluation in Cynomolgus Macaques of rAAV2tYF-CB-hRS1, a Recombinant Adeno-Associated Virus Vector Expressing Retinoschisin.* Hum Gene Ther Clin Dev, 2015. **26**(3): p. 165-76.

113. Bremner, K.H., L.W. Seymour, and C.W. Pouton, *Harnessing nuclear localization pathways for transgene delivery.* Curr Opin Mol Ther, 2001. **3**(2): p. 170-7.

114. Lebherz, C., et al., *Novel AAV serotypes for improved ocular gene transfer.* J Gene Med, 2008. **10**(4): p. 375-82.

115. Kotterman, M.A., et al., *Antibody neutralization poses a barrier to intravitreal adeno-associated viral vector gene delivery to non-human primates.* Gene Ther, 2015. **22**(2): p. 116-26.

116. Zinn, E., et al., *In Silico Reconstruction of the Viral Evolutionary Lineage Yields a Potent Gene Therapy Vector.* Cell Rep, 2015. **12**(6): p. 1056-68.

117. Mingozzi, F., et al., *Overcoming preexisting humoral immunity to AAV using capsid decoys.* Sci Transl Med, 2013. **5**(194): p. 194ra92.

118. Weleber, R.G., et al., *Results at 2 Years after Gene Therapy for RPE65-Deficient Leber Congenital Amaurosis and Severe Early-Childhood-Onset Retinal Dystrophy.* Ophthalmology, 2016. **123**(7): p. 1606-20.

119. Jacobson, S.G., et al., *Improvement and decline in vision with gene therapy in childhood blindness.* N Engl J Med, 2015. **372**(20): p. 1920-6.

120. Bainbridge, J.W., et al., *Long-term effect of gene therapy on Leber's congenital amaurosis.* N Engl J Med, 2015. **372**(20): p. 1887-97.

121. Frasson, M., et al., *Glial cell line-derived neurotrophic factor induces histologic and functional protection of rod photoreceptors in the rd/rd mouse.* Invest Ophthalmol Vis Sci, 1999. **40**(11): p. 2724-34.

122. Dalkara, D., et al., *AAV mediated GDNF secretion from retinal glia slows down retinal degeneration in a rat model of retinitis pigmentosa.* Mol Ther, 2011. **19**(9): p. 1602-8.

123. Buch, P.K., et al., *In contrast to AAV-mediated Cntf expression, AAV-mediated Gdnf expression enhances gene replacement therapy in rodent models of retinal degeneration.* Mol Ther, 2006. **14**(5): p. 700-9.

124. Martin, K.R.G., et al., *Gene Therapy with Brain-Derived Neurotrophic Factor As a Protection: Retinal Ganglion Cells in a Rat Glaucoma Model.* Investigative Opthalmology & Visual Science, 2003. **44**(10): p. 4357.

125. Hojo, M., et al., *Photoreceptor protection by iris pigment epithelial transplantation transduced with AAV-mediated brain-derived neurotrophic factor gene.* Invest Ophthalmol Vis Sci, 2004. **45**(10): p. 3721-6.

126. Schuettauf, F., et al., *Adeno-associated viruses containing bFGF or BDNF are neuroprotective against excitotoxicity.* Curr Eye Res, 2004. **29**(6): p. 379-86.

127. Saito, T., et al., *TrkB-T1 receptors on Muller cells play critical role in brain-derived neurotrophic factor-mediated photoreceptor protection against phototoxicity.* Curr Eye Res, 2009. **34**(7): p. 580-8.

128. Ren, R., et al., *Long-term rescue of rat retinal ganglion cells and visual function by AAV-mediated BDNF expression after acute elevation of intraocular pressure.* Invest Ophthalmol Vis Sci, 2012. **53**(2): p. 1003-11.

129. Liang, F.Q., et al., *AAV-mediated delivery of ciliary neurotrophic factor prolongs photoreceptor survival in the rhodopsin knockout mouse.* Mol Ther, 2001. **3**(2): p. 241-8.

130. Schlichtenbrede, F.C., et al., *Intraocular gene delivery of ciliary neurotrophic factor results in significant loss of retinal function in normal mice and in the Prph2Rd2/Rd2 model of retinal degeneration.* Gene Ther, 2003. **10**(6): p. 523-7.

131. Leaver, S.G., et al., *AAV-mediated expression of CNTF promotes long-term survival and regeneration of adult rat retinal ganglion cells.* Gene Ther, 2006. **13**(18): p. 1328-41.

132. West, E.L., et al., *Defining the integration capacity of embryonic stem cell-derived photoreceptor precursors.* Stem Cells, 2012. **30**(7): p. 1424-35.

133. Lipinski, D.M., et al., *CNTF Gene Therapy Confers Lifelong Neuroprotection in a Mouse Model of Human Retinitis Pigmentosa.* Mol Ther, 2015. **23**(8): p. 1308-19.

134. MacLaren, R.E., et al., *Retinal repair by transplantation of photoreceptor precursors.* Nature, 2006. **444**(7116): p. 203-7.

135. Pearson, R.A., et al., *Restoration of vision after transplantation of photoreceptors.* Nature, 2012. **485**(7396): p. 99-103.

136. Barber, A.C., et al., *Repair of the degenerate retina by photoreceptor transplantation.* Proc Natl Acad Sci U S A, 2013. **110**(1): p. 354-9.

137. Warre-Cornish, K., et al., *Migration, integration and maturation of photoreceptor precursors following transplantation in the mouse retina.* Stem Cells Dev, 2014. **23**(9): p. 941-54.

138. Bachleda, A.R., L.H. Pevny, and E.R. Weiss, *Sox2-Deficient Muller Glia Disrupt the Structural and Functional Maturation of the Mammalian Retina.* Invest Ophthalmol Vis Sci, 2016. **57**(3): p. 1488-99.

139. West, E.L., et al., *Pharmacological disruption of the outer limiting membrane leads to increased retinal integration of transplanted photoreceptor precursors.* Exp Eye Res, 2008. **86**(4): p. 601-11.

140. Pearson, R.A., et al., *Targeted disruption of outer limiting membrane junctional proteins (Crb1 and ZO-1) increases integration of transplanted photoreceptor precursors into the adult wild-type and degenerating retina.* Cell Transplant, 2010. **19**(4): p. 487-503.

141. West, E.L., et al., *Manipulation of the recipient retinal environment by ectopic expression of neurotrophic growth factors can improve transplanted photoreceptor integration and survival.* Cell Transplant, 2012. **21**(5): p. 871-87.

142. West, E.L., et al., *Long-term survival of photoreceptors transplanted into the adult murine neural retina requires immune modulation.* Stem Cells, 2010. **28**(11): p. 1997-2007.

143. Lakowski, J., et al., *Effective transplantation of photoreceptor precursor cells selected via cell surface antigen expression.* Stem Cells, 2011. **29**(9): p. 1391-404.

144. Takahashi, K. and S. Yamanaka, *Induction of pluripotent stem cells from mouse embryonic and adult fibroblast cultures by defined factors.* Cell, 2006. **126**(4): p. 663-76.

145. Boucherie, C., et al., *Brief report: self-organizing neuroepithelium from human pluripotent stem cells facilitates derivation of photoreceptors.* Stem Cells, 2013. **31**(2): p. 408-14.

146. Gonzalez-Cordero, A., et al., *Photoreceptor precursors derived from three-dimensional embryonic stem cell cultures integrate and mature within adult degenerate retina.* Nat Biotechnol, 2013. **31**(8): p. 741-7.